



BEST AVAILABLE COPY

**Certificate of Mailing**

I hereby certify that this correspondence is being deposited with the United States Postal Service with sufficient postage as first class mail in an envelope addressed to: Mail Stop Amendment, Commissioner for Patents, P.O. Box 1450, Alexandria, VA 22313-1450 on August 15, 2005.

Rhonda A. Etienne 8/15/05  
Rhonda A. Etienne Date

**PATENT**

**IN THE UNITED STATES PATENT AND TRADEMARK OFFICE**

Applicant: Fein  
Serial No.: 09/919,102  
Filed: July 31, 2001  
Group Art Unit: 1653  
Confirmation No: 2446  
Examiner: Witz  
Title: **SELECTIVE ENZYME TREATMENT OF SKIN CONDITIONS**  
Our Ref. No.: HOFE-02

Cincinnati, Ohio 45202

August 15, 2005

Commissioner for Patents  
P.O. Box 1450  
Alexandria, VA 22313-1450

**DECLARATION OF HOWARD FEIN, M.D.**  
**PURSUANT TO 37 C.F.R. §1.132**

I, HOWARD FEIN M.D., declare as follows:

1. I am a named inventor in the above-identified patent application.
2. I hold a Doctor of Medicine from the University of Southern California School of Medicine. I have six years of experience in dermatology and treatment of skin conditions, which is the subject of the application. I have read the Advisory Action of

BEST AVAILABLE COPY

May 27, 2005, and the Office Action of December 10, 2004, and understand the position of the Examiner.

3. My invention regulates removing a layer of skin for treating a patient having a condition affecting that layer in two ways. The first way is in the choice of the particular enzyme. The enzyme is chosen for its substrate selectivity, the substrate being present in a particular layer of skin containing the lesion to be removed. The second way is the choice of conditions under which the enzyme is applied (e.g., its concentration, duration of treatment, etc.). Because none of the SU1685448, deFaire, or Freeman references disclose a method by which a particular enzyme is chosen for its function in the selective layer of skin containing the lesion to be removed, and in which the condition (time, concentration, etc.) for applying the enzyme is chosen for the patient's particular situation, I disagree with the Examiner that each of these discloses my invention.

4. I acknowledge that the Examiner has restricted my claims, and that my elected claims are directed to a hydrolase to treat seborrheic keratosis.

5. A hydrolase, and all other enzymes, have a particular affinity for the material or substrate on which it can act; that is, enzyme-substrate affinity. Hydrolases are a heterogeneous group of catabolic enzymes that break apart the bonds of macromolecules such as proteins, lipids, and sugars through the addition of water molecules. Proteases are a subset of the larger hydrolase class of enzymes, which are responsible for the catabolism or dissolution of proteins. During the process of

catabolysis, the protease must physically bind and interact with the substrate protein before it can be degraded. Each protease is limited in its ability to bind protein substrates. Certain enzymes are highly specific and can cleave only one substrate protein, while other proteases are highly non-specific and can cleave a multitude of protein substrates.

6. By way of example, the outermost layer of the epidermis (the stratum corneum) contains an abundance of the protein keratin. A keratinase enzyme, which specifically degrades keratin, can therefore be used to selectively degrade the stratum corneum. Keratinocytes, cells that comprise the bulk of the epidermis, are held in place by protein adhesions called desmosomes. An enzyme such as trypsin that degrades the desmosomes can be used to degrade the middle layers of the epidermis. Finally, the epidermis rests on a structure called the basement membrane that is rich in type IV collagen protein. Using an enzyme specific for type IV collagen, i.e. a type IV collagenase such as dispase, the entire epidermis can be separated from the dermis and deeper tissue layers.

7. Using an enzyme to regulate removal of a particular layer of skin results from the fact that each protease is capable of degrading only a certain subset of proteins. Enzyme selectivity is not related to variables such as temperature, concentration, method of application, or other variables, but is biologically predetermined. The inventive method selectively regulates removal of skin by the choice of enzyme to degrade particular protein targets that are present within the various layers of skin.

8. Selectivity due to the choice of enzyme, in this case a protease, is based upon capability of a protease to degrade only a certain subset of proteins that are present within the various layers of skin. This capability, to cause selective epidermal separation, is due in part to the ability of a protease to digest desmosomal proteins. Proteolytic enzymes act at specific sites on a protein molecule. The epidermal layer has a predominance of substrates for trypsin, dispase, etc. Thus, these enzymes are selective for a layer of skin (one or all of the epidermal layers), and hence regulate removal of this layer of skin when the enzyme is applied topically or is injected. This is contrasted with the action or selectivity of another enzyme such as, e.g., collagenase being selective for a layer of skin where there is a predominance of collagen.

9. The extent of the regulation within that layer of skin is determined by factors related to the selectivity of the method. For example, the depth of tissue damage is determined by multiple factors, including the duration and method of application.

10. My method combines the selectivity in the choice of a particular enzyme with the selectivity of conditions under which the enzyme is applied to regulate removal of a layer of skin, as the claims require. When I exposed skin to topical protease solutions according to my claimed method, it regulated removal of the epidermis. There were reproducible, differential patterns of ablation for subcorneal, intraepidermal, and subepidermal layers. The dermis, however, was not affected.

11. In my method, the enzyme is the sole active agent. I understand the Examiner believes that SU1685448 discloses my method because the four other components, theophylline, lanoline, sunflower oil, and DMSO, would not materially affect the enzyme. I assert that the Examiner is incorrect, as I subsequently explain.

12. SU1685448 discloses DMSO at concentrations ranging from 22.5% to 32%. I assert that DMSO at these concentrations does exert material effects on an enzyme's activity. Thus, SU1685448 does not disclose my invention, because its non-enzyme components would indeed affect the enzyme's activity.

To reinforce my assertion, I further provide copies of each of the following references demonstrating that 22.5% to 32% DMSO has material effects on an enzyme:

(a) Middleton (1970, Proc. Soc. Exp. Biol. Med. 134:1096, 1099 and 1101-1102) discloses that DMSO in concentrations above 10% interfered with the action of proteolytic enzymes (e.g., elastase, trypsin) on dog skin. This effect was pronounced in concentrations above 25%. Middleton concluded that changes "in protein configuration may be partially responsible for the effects of DMSO on the enzymes".

(b) Henderson (1975, Ann. NY Acad. Sci. 27:38) discloses that DMSO at a concentration of 20% or less reversibly inactivated glutamate dehydrogenase, forming an inactive monomer. At a DMSO concentration of 20% or more, the inactivation was irreversible.

(c) Anigbogu (1995, Int. J. Pharmaceutics 125:265) demonstrated spectroscopic changes between "the penetration enhancer" DMSO and the protein components of human stratum corneum with a concentration of DMSO as low as 10% (e.g., Fig. 7).

Thus, each of Middleton and Henderson demonstrated that DMSO as used in SU1685448 has a material effect at least on an enzyme's activity. Anigbogu demonstrated that DMSO as used in SU1685448 has a material effect at least on the enzyme's substrate and/or the enzyme itself.

13. These references further supplement the known classification of DMSO as a penetration enhancer (see title of Anigbogu referring to “the penetration enhancer dimethylsulfoxide”), and its known toxicity to the dermis (Block, L., “Medicated Topicals” in Remington: The Science and Practice of Pharmacy, 2000, p. 842 attached). DMSO exerts its effect by extracting soluble components of the stratum corneum, delaminating the horny layer, and denaturing the proteins (Purdon et al., 2004, pp. 99-100; Kurihara-Bergstrom, T. et al., 1987, pp. 274-280; Kurihara-Bergstrom, T. et al., 1986, pp. 479-486, each attached). Hence, DMSO is an active that denatures the proteins in the skin and provides additional potential substrates for a hydrolase if the hydrolase itself is unaltered.

14. My invention also does not require lanolin as is required in SU1685448. As known to one skilled in the art, lanolin is an allergen, resulting in inflammation. (Block, L. “Medicated Topicals” in Remington: The Science and Practice of Pharmacy, 2000, p. 846). To counteract the inflammatory effect of lanolin, SU1685448 also adds an anti-inflammatory agent. In contrast, my method uses an enzyme alone to regulate removal of a layer of skin. It does not have DMSO which alters skin penetration. It does not

have lanolin, which causes inflammation. It does not have an anti-inflammatory agent to counteract inflammation.

15. I therefore disagree that SU1685448 discloses each element of my invention.

16. In my method, the enzyme regulates removal of a layer of skin because its activity is known and is biologically predictable. deFaire discloses a multifunctional enzyme (see at least title). By definition, a multifunctional enzyme is a protein that contains at least two distinct enzymatic activities. Applying a multifunctional enzyme to the skin cannot regulate removal of a layer of skin unless its other activities were selectively inhibited.

17. A protein with two distinct enzymatic activities (i.e., a multifunctional enzyme), even if it could be used in the claimed method (e.g., by treating it to inhibit other than the desired enzymatic activity) does not anticipate my invention where the activity of my enzyme is predictable and is the basis for regulated removal of a layer of skin.

18. In addition, the combination of enzymatic activities in a multifunctional enzyme may alter distinct and predictable properties of the separate enzymes, rendering any method using a multifunctional enzyme at least less able to regulate removal of a layer of skin. The depth of skin affected depends upon the duration and timing of treatment intervals in addition the concentrations and types of enzyme and formulations.

19. My claimed method applies the enzyme to the skin either topically or by injection. I understand the Examiner believes that Freeman discloses my method. As one skilled in this art, I emphatically disagree as I subsequently explain. Should the Examiner maintain Freeman's stripping flow is the same as my method, I respectfully request citation to a reference or an affidavit stating the facts supporting this position.

20. Freeman discloses a device. Using this device, Freeman achieves "A synergistic effect of proteolytic digestion of the intracellular matrix and 'stripping' flow" by a "controlled, continuous stream of proteolytic enzyme solution, causing gentle but effective tissue erosion". Freeman therefore uses enzyme action in combination with "stripping" flow, provided in a "streaming" action (Freeman ¶¶ 20-22).

21. Freeman does not disclose my invention because Freeman requires two actions: a mechanical action resulting from use of his device, and an enzyme action. My method uses only enzyme action. Further, one skilled in art readily appreciates that Freeman's mechanical stripping inherently does not regulate removal of a skin layer because it uses an additional mechanical means, whereas my method is naturally regulated by the action of the enzyme alone.



22. As an example, I topically applied 2.5% trypsin to a seborrheic keratosis lesion. After 15 minutes, erosion was present. There was rapid intraepidermal acanthosis, and after 24 hours there was complete epidermal dissolution. There was slight erythema one month post-treatment. There was no evidence of scar formation three months post-treatment. Thus, my method used enzyme alone to result in scar-free ablation of the lesion.

23. In contrast, mechanical stripping results in potentially unlimited depths of tissue damage. This is not regulated removal of a layer of skin, as the claims require. The ability to regulate removal of a particular skin layer with my method using a topically applied protease confines damage to specific epidermal zones.

24. Therefore, as it relates to the treatment of skin conditions, Freeman does not disclose my method because Freeman does not rely only on a biologically predictable and regulated removal of a layer of skin.

25. All claims are amended to clarify the regulated removal of a layer of skin using my method. For example, independent claim 1 recites

1. A method for treating a patient having a condition affecting at least one layer of skin comprising administering in situ by topical application or injection a physiologically acceptable formulation consisting essentially of at least one hydrolase in an amount and for a duration effective to regulate removal of said layer and treat said condition.

Independent claim 24 recites

24. A method to treat skin comprising topically applying to an outermost layer of skin a composition consisting essentially of a protease in a biologically acceptable formulation in an amount to selectively regulate removal of at least one epidermal layer containing a skin condition to thereby treat said skin.

Independent claim 30 recites

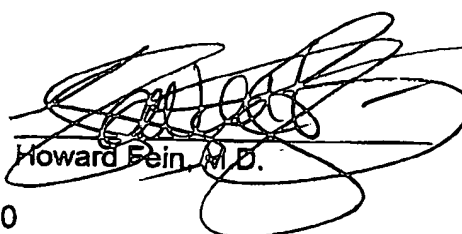
30. A method to target skin treatment of an affected area comprising providing to said affected area by topical application or injection a composition consisting essentially of at least one hydrolase in an amount and formulation effective to selectively regulate skin removal in said affected area.

Independent claim 34 recites

34. A method for treating a condition affecting skin comprising applying by topical application or injection a composition to the affected skin, the composition containing at least one hydrolase at a concentration selective for regulating depth of skin treatment and applied to an area selective for regulating a radial surface of skin treatment.

I hereby declare that all statements made herein of my own knowledge are true and that all statements made on information and belief are believed to be true; and further that these statements were made with the knowledge that willful false statements and the like so made are punishable by fine or imprisonment or both, under Section 1001 of Title 18 of the United States Code and that such willful false statements may jeopardize the validity of the subject application or any patent issued thereon.

8/13/2005  
Date

  
Howard Fein, M.D.

## Effects of Dimethylsulfoxide on Normal and Burned Dog Skin (34951)

CHARLES J. MIDDLETON, EDWARD L. HOWES, AND MARY F. MAZENS

*Surgical Research Laboratories and Department of Surgery, Hartford Hospital,  
Hartford, Connecticut 06115*

Dimethylsulfoxide (DMSO), an alkyl sulfide, is a powerful solvent derived from a waste product of paper manufacture. Its properties and the clinical problems for which it has been tried have been described in a comprehensive review (1).

Experimentally and clinically DMSO has been reported to penetrate skin rapidly and to cause no permanent tissue damage even in high concentrations (2). Effects on the collagen of the dermis have been claimed in the treatment of several dermatoses—psoriasis, scleroderma, keloids, radiation fibrosis, and eczema (3-5)—suggesting that at least abnormal collagen is affected by DMSO.

Burn therapy with DMSO has received only limited attention. DMSO alone and combined with Sulfamylon was applied intermittently in the treatment of partial and full-thickness burns in rats (6). Penetration of the eschar by DMSO was theoretically demonstrated by the addition of methylene blue. There was no increase in survival rates nor decrease in *Pseudomonas* organisms (7). Rabbit skin placed in DMSO for 24 hr produced skin that could be penetrated easily with a finger, indicating destruction (8). Tensile strength of rat tail tendons treated for 24 hr with varied concentrations of DMSO decreased when a concentration of 95% or higher was used. It was concluded DMSO changed the physical properties of collagen by causing lysis of its intermolecular bonds.

With this background and because dried collagen from tendon swelled markedly in DMSO, we wondered if DMSO could alter the susceptibility of collagen to digestion by proteolytic enzymes that ordinarily did not attack it. By definition, only collagenase digests sclerocollagen while trypsin and similar pro-

teolytic enzymes can digest collagen only after it is denatured. Here we have investigated the effect of DMSO on the tensile strength of normal and burned dog skin and on the capacity of proteolytic enzymes other than collagenase to digest both. Partially denatured beef tendon collagen is also used.

**Methods and Materials.** Large swatches of fresh skin were excised from the abdomen of a dead dog and were mechanically defatted. Several 12 × 6 cm. pieces were cut and burned to full thickness by passing them through a bunsen burner flame for 15 sec with the keratin side toward the flame. Sections of both burned and normal skin were then totally immersed in 50% and 100% DMSO at room temperature for 24 hr. All skin was then fashioned into 8 × 1-cm strips with small triangles cut from the middle of the long sides to leave a central isthmus of 3 mm. Their tensile strengths were tested on a Scott Tester, Model X-3,<sup>1</sup> with special clamps for holding the skin. To correlate anatomical changes, specimens of normal and normal treated, and burned untreated and treated were examined for microscopic differences after coloring with hematoxylin and eosin stain.

The enzyme study was initiated by determining the effect of varied concentrations of DMSO on the activity of elastase and trypsin against substrates that they do attack. One milligram of elastase (Worthington) in 0.1% concentration was incubated with 13 mg. of elastin orcein (9), while 0.1% trypsin (Princeton) was incubated with 10 mg. of azocol (10). One milliliter of different concentrations (1.0%, 5%, 10%, 25%, 50%, and 100%) of DMSO were added while the same

<sup>1</sup>Scott Testers, Inc., Providence, Rhode Island 02901.

TABLE 1. Tensile Strengths of Normal and Burned Dog Skin After Treatment with DMSO for 24 hr at Room Temperature.

Type of skin	Tensile strength (lb)					Average	% Loss
Normal (control)	15.0	13.0	13.0	17.0	14.0	14.4	—
Normal and 50% DMSO	13.5	13.0	15.0	12.5	12.0	13.2	8
Normal and 100% DMSO	12.0	12.5	9.0	11.0	10.5	11.0	24
Burned (control)	4.0	4.0	5.0	3.5	6.0	4.5	69
Burned and 50% DMSO	1.5	2.0	2.5	3.0	4.0	2.6	82
Burned and 100% DMSO	2.5	1.5	0.5	0.5	1.0	1.2	91

amount of distilled water was added to the controls. They were incubated for 24 hr at 37°.

Next, enzymatic digestion of normal and burned dog skin was studied before and after pretreatment with DMSO. The dog skin was cut into 1 × 0.5-cm pieces and some pieces were treated with 6 cc 100% DMSO for 8 and 24 hr. After washing three times in distilled water, they were incubated in 0.2% concentrations of trypsin, elastase, protease, and collagenase. To each tube 5 mg of neomycin sulfate was added to inhibit bacterial

growth. Cultures were taken after incubation for 24 hr at 37° to be certain of sterility. If contaminated, the tube was discarded. Lysis was judged on a 1-4+ scale. The ease with which the tissue disintegrated on probing was noted. Complete lysis was unattainable because no enzyme was used to dissolve fat.

The effect of DMSO pretreatment on the susceptibility of partially denatured collagen to attack by proteolytic enzymes was studied by putting 15-mg pieces of shredded defatted beef tendon in 1 ml of Tris buffer with 0.5% trypsin (Princeton), elastase (Worthington),



FIG. 1. Darkly stained, compact, uniform collagenous bundles in normal dog skin. H & E stain. 160X.

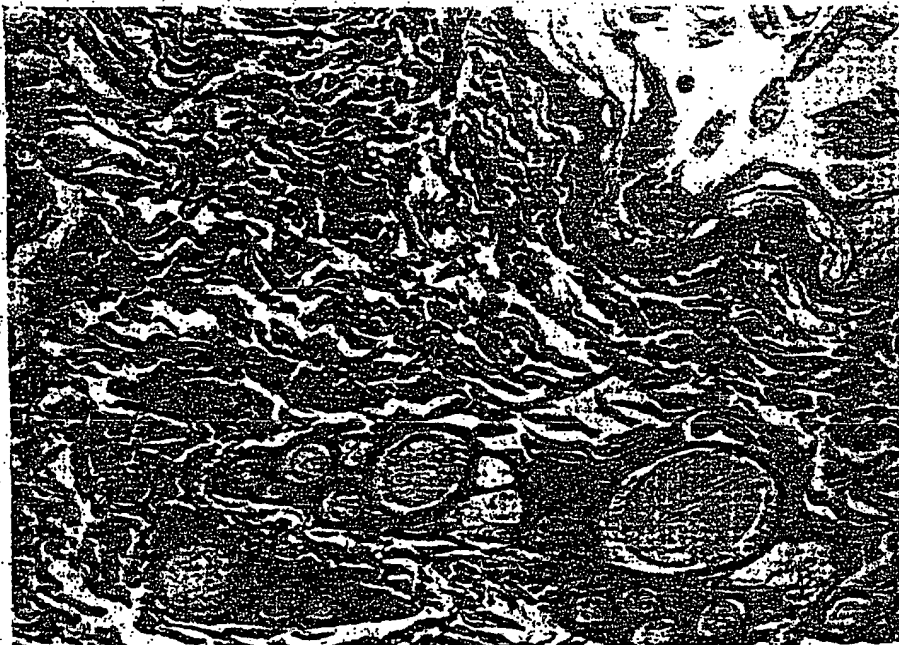


FIG. 2. Swollen and separated collagenous bundles of normal dog skin after soaking in 100% DMSO. H & E stain. 160X.

protease (S.E.A.B.), and collagenase (Worthington). They were incubated for 24 hr at 37°. The collagen was then dried for 21 days and weighed to determine the amount lost. Using a second batch of collagen, 1 ml 100% DMSO was substituted for Tris buffer. In a third experiment pieces of beef tendon collagen were pretreated with 100% DMSO for 24 hr at 37°. Tris buffer, pH 7.2, water, and acetic acid, 3%, were used for controls. This collagen was then washed three times with distilled water and dried for 10 days. At this time, 0.5% concentrations of the same enzymes were added to known amounts which were incubated, dried, and weighed as above to determine if any of the collagen had been made soluble. All samples were subsequently incubated again at 37° for 24 hr in 1 ml of distilled water, rewashed with distilled water, dried for 2 weeks, and weighed.

**Results.** Normal untreated skin had the greatest tensile strength, average 14.4 lb (Table I). Burned skin treated with 100%

DMSO had the least tensile strength, 1.2 lb average. Normal skin pretreated with 50% DMSO had 8% less tensile strength than the average normal skin, whereas with treatment with 100% DMSO there was 24% less strength. Burned normal skin had 69% less tensile strength. Burned skin treated with 50% DMSO had 82% less tensile strength, while that treated with 100% DMSO had 91% less strength than the average normal skin. The data show that burning lowers tensile strength of skin suggesting destruction of contained collagen. DMSO lowers somewhat the strength of normal skin, but not as much as that of burned skin. The amount of lowering is dependent on the strength of the DMSO used and one suspects on the duration of contact.

Microscopic changes in collagen of the dermis are shown in Figs. 1 through 4. The darkly stained, compact, uniform collagenous bundles in normal dog skin are seen in Fig. 1. They become swollen and separate after



FIG. 3. Collagenous bundles of burned dog skin. Coagulated bundles, loss of identity of fibers, and poor staining. H & E stain. 160X.

soaking in 100% DMSO (Fig. 2). Burning of normal dog skin (Fig. 3) causes coagulation, swelling, and loss of identity of fibers with poor staining characteristics. In addition to these changes, soaking in 100% DMSO results in cleft formation (Fig. 4).

Elastin orcein was completely digested by elastase, while there was 79% digestion in the presence of 10% DMSO. With increased concentrations, elastase activity was totally inhibited. Trypsin digested 83% of azocol without DMSO, but the percentage fell from 78% to 25% as the DMSO concentration was increased from 10% to 100%. Under the circumstances of the experiment, elastase is more affected by DMSO than trypsin.

None of the proteolytic enzymes (Table II) digested normal dog skin except collagenase. All digested, however, a limited amount of burned dog skin. Eight hours of pretreatment of burned skin with 100% DMSO caused no appreciable difference, but

after 24 hr of pretreatment there was a marked increase in digestion by elastase, collagenase, and protease, but no change in the action of trypsin. Free DMSO had been removed in these experiments by washing.

Table III shows the effect of DMSO on the proteolytic digestion of partially denatured beef tendon collagen. Five milligrams of trypsin, elastase, protease, and collagenase in 1 ml of Tris buffer digested 75%, 79%, 85%, and 100% of the collagen, respectively. Dissolved in 1 ml of 100% DMSO all the enzymes were completely inhibited except for an insignificant 2% digestion by trypsin. The DMSO control lost 11%. After 100% DMSO pretreatment of this collagen and washing out, all the enzymes caused complete digestion. Interestingly, DMSO-pretreated collagen incubated in Tris buffer (pH 7.2) yielded a loss of 53% on washing, suggesting that the DMSO had caused part of this collagen to become soluble in Tris buffer. With Tris buffer alone only 9% was lost.

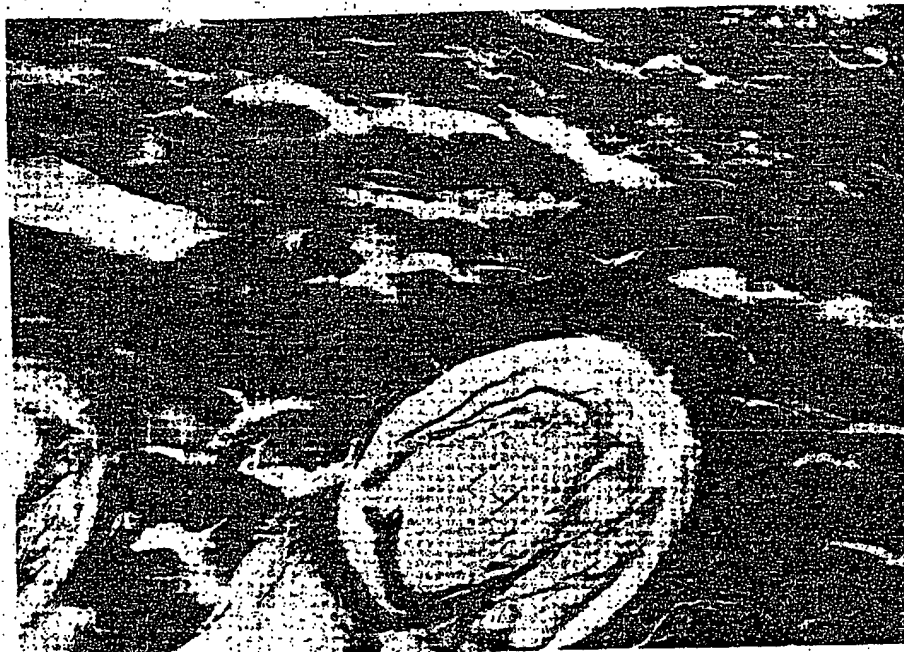


FIG. 4. Collagenous bundles of burned dog skin after soaking in 100% DMSO for 24 hr. Coagulated bundles, loss of identity of fibers, poor staining, swollen hair follicles, and many clefts. H & E stain. 160X.

Incubation of beef tendon collagen in 100% DMSO and 3% acetic acid for 24 hr caused marked swelling and increases in weight (Table IV). At 37° the acetic acid-treated material resisted drying more than the DMSO-treated. When incubated again with water, washed, dried, and weighed, the DMSO-treated sample lost 96% of its weight, while the acetic acid-treated material still weighed three times its original weight. The

distilled water-treated sample lost 13%, Tris buffer 15%, and no solution 25%. Thus, while both DMSO and acetic acid caused swelling of partially denatured collagen, the former readily lost its absorbed water on drying at room temperature, while the latter did not, and the secondary solubility of the DMSO-treated collagen in water indicates a chemical change has occurred.

*Discussion.* DMSO swelled normal and

TABLE II. Effect of DMSO (100%) Pretreatment on Proteolytic Digestion (1-4+) of Washed Normal and Burned Dog Skin.

Enzyme (0.2%) in distilled water	No treatment		Treated 8 hr		Treated 24 hr	
	Normal skin	Burned skin	Normal skin	Burned skin	Normal skin	Burned skin
Trypsin	0	1+	1+	1+	1+	4+
Elastase	0	1+	1+	1+	1+	3+
Protease	0	1+	1+	1+	2+	4+
Collagenase	2+	2+	2+	2+	3+	4+

TABLE III. Influence of DMSO and DMSO Pretreatment on Digestion by Proteolytic Enzymes of Partially Denatured Beef Tendon Collagen (15 mg).

Enzyme (0.5%)	Enzyme in Tris buffer pH 7.2 (% digested)	Enzyme in 100% DMSO (% digested)	In Tris buffer but collagen pretreatment with DMSO (% digested)
Trypsin	75	2	100
Elastase	79	0	98
Protease	85	0	100
Collagenase	100	0	100
Control			
Tris buffer (no enzyme)	9	—	53
Control			
100% DMSO (no enzyme)	—	11	—

burned skin, changed the microscopic appearance of the dermis, and reduced their tensile strengths, particularly burned skin. DMSO pretreatment made skin, particularly burned skin, more susceptible to the action of proteolytic enzymes and to enzymes that ordinarily do not attack collagen. Partially denatured beef tendon collagen not only became greatly swollen with DMSO and more susceptible to the action of enzymes, but it became water and Tris buffer soluble. Lower concentrations of DMSO were required to attack partially denatured collagen or burned skin than was required to attack normal skin.

DMSO in concentrations above 10% interfered with the action of proteolytic enzymes, especially above 25%.

These results find some parallel in the works of others (5). Patients with scleroderma treated topically with high concentrations of DMSO had increased amounts of acid muco-

polysaccharides in involved areas, presumably from a breakdown of collagen. But mucopolysaccharides increase locally anyway during healing (11). Postirradiated subcutaneous plaques treated with topical 90% DMSO underwent involution that correlated microscopically with a reduction of both soluble and insoluble fractions of collagen, while mucopolysaccharides remained constant (4). A shift toward degradation in the balance between synthesis and degradation rather than an actual breakdown of collagen was suspected. A reduction in the collagenous fraction extractable with neutral salt solution, but not in insoluble collagen was found when rabbit skin was treated *in vitro* with pure DMSO (8). In *in vivo* studies of rabbit's skin both synthesis and catabolism of collagen were believed to be diminished simultaneously after DMSO treatment because no significant change occurred in the amount of insoluble

TABLE IV. Weight Change of 15 mg of Partially Denatured Beef Tendon Collagen Incubated at 37° for 24 hr in Various Solutions.

Incubating solutions	After 1 week of drying (mg)	After 2 weeks of drying (mg)	After incubating again in distilled water and drying for 2 weeks	% Change in weight after washing and second drying
100% DMSO	62.89	14.72	0.56	-96
3% Acetic acid	656.18	342.33	371.09	+30X
Distilled water	16.89	14.69	13.10	-18
Tris buffer pH 7.2	13.91	13.62	12.79	-15
Control				
distilled water not incubated	16.32	14.41	11.27	-25



collagen present. No change occurred in the tensile strength of rat tail tendon until a concentration of 95% DMSO was used (8).

Because DMSO inhibited the action of proteolytic enzymes, this inhibition might be expected to occur against naturally occurring enzymes, as white blood cells, as well as in those added externally. In these experiments however, there was a prolonged contact between the DMSO and the enzyme that may not occur *in vivo*. If external enzymes were used after DMSO it should be washed away. A small but constant amount of DMSO has been found still fixed to various tissues after 24 hr of dialysis (12). Others have reported effects of DMSO on enzymes. Increased trypsin-catalyzed hydrolysis of *p*-toluene sulfonyl-L-arginine methyl ester has been found with up to 20% concentration of DMSO, but above 30% there was precipitation of the buffer or substrate (13). With a different substrate, an almost linear decline in trypsin activity was found with increasing concentrations of DMSO starting at 5% (12). Changes in protein configuration may be partially responsible for the effects of DMSO on enzymes. DMSO inhibition of pancreatic DNAase has been demonstrated at pH 6, but at higher pH the action of DNAase was enhanced (14). The marked enhancement of digestion of shredded beef tendon collagen we found with trypsin, elastase, and protease after pretreatment with 100% DMSO and washing away illustrates how the attack on the substrate may be regarded as enhancement of the activity of an enzyme rather than a change to different solubilities. Cutting, tearing, pretreatment with acids, bases, some salts, and heating have been found to make collagen more vulnerable to attack by trypsin (15). DMSO must now be added to this list. Indeed, properly applied, DMSO treatment alone might be all that is needed for the lysis of burned collagen. The effect becomes apparent, however, only after exposure in excess of 8 hr and at high concentrations.

In treating burns in rats it has been suggested that 90% DMSO applied in a spray twice a day might have been more valuable if applied continuously (6). On the other

hand, because of water evaporation on application, a concentration of 67% might be most efficacious for topical use because the heat of hydration on application in higher concentrations might increase diffusion rates across the epidermis (16). DMSO hydrate contains 2 moles of water. The absorption of DMSO from the local area must decrease its concentration and affect the duration of action of a higher concentration. The toxicity of a maintained high concentration in the burned individual must be studied separately. DMSO has been shown to be bacteriostatic against *Staphylococcus* and *Pseudomonas* (17).

**Summary.** 1. Dimethylsulfoxide swells collagen in the dermis and decreases the tensile strength of both normal and full-thickness burned dog skin, especially the latter. These effects are more pronounced with 100% than with 50% DMSO.

2. The digestion of burned dog skin *in vitro* by elastase, collagenase, and protease is increased by pretreatment for 24 hr with 100% DMSO.

3. Pretreatment for 24 hr with 100% DMSO not only increases the degree of digestion of partially denatured beef tendon collagen by enzymes, but also partially converts it to a form soluble in water and Tris buffer at pH 7.2.

4. DMSO appears to be a denaturant of collagen, more active against burned and partially denatured collagen than against sclerocollagen.

5. A continuous application of DMSO at 90%–100% concentrations for at least 24 hr might render full-thickness burn eschar more readily removed by solutes and might increase its susceptibility to enzymatic digestion.

1. Jacob, S. W., and Wood, D. C., *Amer. J. Surg.* 114, 414 (1967).

2. Kligman, A. M., *J. Amer. Med. Ass.* 193, 796 (1965).

3. Engel, M. F., *Ann. N. Y. Acad. Sci.* 141, 638 (1967).

4. Frommhold, W., Bublitz, G., and Gries, G., *Ann. N. Y. Acad. Sci.* 141, 603 (1967).


5. Scherbel, A. L., McCormack, L. J., and Layle, J. K., *Ann. N. Y. Acad. Sci.* 141, 615 (1967).

6. Krizek, T. J., Davis, J. H., Desprez, J. D., and

Tobin, C.  
7. Krizek, T. J., and Davis, J. H., *J. Surg. Res.* 19, 100 (1955).  
8. Gruber, R. A., and Acacia, E. J., *J. Surg. Res.* 19, 100 (1955).  
9. Sankel, H. (1955).  
10. C. (1955).  
11. L. (1959).  
12. L. (1959).

- Kiehn, C. L., *Plast. Reconst. Surg.* 39, 248 (1967).
7. Krizek, T. J., and Davis, J. H., *J. Trauma* 7, 433 (1967).
8. Gries, G., Bublitz, G., and Lindner, J., *Ann. N. Y. Acad. Sci.* 141, 630 (1967).
9. Sachai, L. A., Winter, K. K., Sicher, N., and Frankel, S., *Proc. Soc. Exp. Biol. Med.* 90, 323 (1955).
10. Oakley, C. L., Warrick, G. H., and VanHeyn- ingh, W. E., *J. Pathol. Bacteriol.* 58, 229 (1946).
11. Howes, E. L., Mandl, I., Zaffuto, S., and Ackermann, W., *Surg. Gynec. Obstet.* 109, 177 (1959).
12. Gerhards, E., and Gibian, H., *Ann. N. Y. Acad. Sci.* 141, 65 (1967).
13. Rammier, D. H., *Ann. N. Y. Acad. Sci.* 141, 219 (1967).
14. Monder, C., *Ann. N. Y. Acad. Sci.* 141, 300 (1967).
15. Marriott, R. H., *J. Int. Soc. Leather Trades Chem.* 16, 6 (1932).
16. Rammier, D. H., and Zaffaroni, A., *Ann. N. Y. Acad. Sci.* 141, 13 (1967).
17. Krizek, T. J., and Davis, J. H., *Clin. Res.* 12, 349 (1964).

Received Jan. 23, 1970. P.S.E.B.M., 1970, Vol. 134.


**PubMed** National Library of Medicine 

PubMed Nucleotide Protein Genome Structure OMIM PMC Journals Books

for

Limits Preview/Index History Clipboard Details

Display   20

All: 1 Review: 0 

☐ 1: Proc Soc Exp Biol Med. 1970 Sep;134(4):1096-103.

[Related Articles, Links](#)

**Effects of dimethylsulfoxide on normal and burned dog skin.**

Middleton CJ, Howes EL, Mazens MF.

PMID: 4318661 [PubMed - indexed for MEDLINE]

er  
ar

Display   20

[Write to the Help Desk](#)  
[NCBI](#) | [NLM](#) | [NIH](#)  
[Department of Health & Human Services](#)  
[Privacy Statement](#) | [Freedom of Information Act](#) | [Disclaimer](#)

# EFFECTS OF DIMETHYL SULFOXIDE ON SUBUNIT PROTEINS\*

Thomas R. Henderson and Rogene F. Henderson  
*Inhalation Toxicology Research Institute*  
*Lovelace Foundation for Medical Education and Research*  
*Albuquerque, New Mexico 87108*

J. Lyndal York

*Biochemistry Department*  
*University of Arkansas School of Medicine*  
*Little Rock, Arkansas 72201*

Studies of subunit proteins have suggested that the association of subunits is often stabilized not only by hydrogen bonding and hydrophobic bonding, but also by bound water and water bridges between proton-donor and proton-acceptor groups on a surface of the proteins.<sup>1-3</sup> That bound water and water bridges play a significant role in the maintenance of the structure of a given biopolymer has been detected through observation of the alterations in the properties of a polymer when it is dissolved in D<sub>2</sub>O. Increased stabilization is often observed because deuterium has a higher bonding strength than hydrogen (it is calculated to be 0.24 kcal/mol greater<sup>4</sup>). The increased strength of heavy-water bridges is a credible explanation for many of the effects of D<sub>2</sub>O that have been observed on genetic control mechanisms *in vivo* and on allosteric, subunit proteins *in vitro*.<sup>5,6</sup>

The solvent, dimethyl sulfoxide (DMSO), resembles D<sub>2</sub>O in that it forms stronger hydrogen bonds with proton-donor groups of biopolymers than does water.<sup>7</sup> The effects of DMSO are also thought to be due in part to the formation of hydrate structures in which the hydrogen bonds between DMSO and water or other proton-donor groups are stronger than the hydrogen bonds between water molecules. Thus we might expect the effects brought about by the replacement of water bridges by heavy-water bridges, and if both heavy water and DMSO were added to a biopolymer, the effects of the two solvents could be additive in nature.

DMSO affects hydrophobic bonding, and at higher concentrations it may also affect hydrophobic bonding in proteins. Herakovits<sup>8</sup> has reported that methylated solvents such as DMSO appear to be more effective denaturants of biopolymers than the parent, unsubstituted compounds, apparently because of the activity of methylated compounds in breaking hydrophobic bonds.

In order to distinguish between the effects of DMSO on hydrophobic and hydrophobic bonding in proteins, one may compare the effects either over a range of temperatures or over a range of solvent concentrations. Hydrogen bonds become weaker and hydrophobic bonding becomes somewhat stronger as the temperature is raised from 0 to 40°C.<sup>9</sup> By working at lower temperatures, one can study the protein under conditions such that hydrogen bonding and bound water make a maximal contribution to the stability of the protein, and the contribution of hydrophobic bonding is minimized. While methyl-substituted compounds such as DMSO are

\*This work was supported in part by grants from the National Institutes of Health, and by National Science Foundation grant 30742X.

considered to be very effective in disrupting hydrophobic bonding, the concentrations employed for this are 50-70%;<sup>10</sup> thus one can also minimize the effects of DMSO on hydrophobic bonding by working at low solvent concentrations.

This paper summarizes the changes in the properties of several model subunit proteins provoked by the partial replacement of solvent water by DMSO, and discusses how these may be related to certain of the *in vivo* responses to DMSO.

## METHODS

The preparation and assay of glutamate dehydrogenase were as described elsewhere.<sup>9</sup> The assay mixture contained  $4 \times 10^{-4}$  M NAD<sup>+</sup>,  $2 \times 10^{-3}$  M NaCl, 0.05 M Tris-chloride buffer (pH 8.0), 0.15 M L-glutamate, and 0.1 mg protein, in a final volume of 3 ml. For DMSO solutions, DMSO was added to Tris base and the pH was adjusted to 8.0 with HCl, in order to correct for the effects of DMSO on the pH meter reading. For D<sub>2</sub>O solutions of DMSO, the pD = the pH meter reading + 0.4.<sup>11</sup> All percentage solutions of DMSO refer to v/v%.

Spectrophotometric measurements were performed in 1 cm cells on a Zeiss PMQ II equipped with a Sargent SRL recorder. For absorption measurements below 200 nm, sensitivity and amplification were set at maximum, with minimum resolving time, in order to obtain measurements with an accuracy of  $\pm 1\%$  and a band width of less than 0.3 nm. All measurements were made in air.

Type B-3  $\beta$ -glucuronidase ( $1.5 \times 10^6$  units/g) and the substrate, phenolphthalein  $\beta$ -D-glucuronide (sodium salt) were obtained from Sigma Chemical Co., St. Louis, Missouri. (One unit of enzyme activity is defined as the activity that liberates 1  $\mu$ g/hr phenolphthalein at 37°C in 1 ml assay mixture.<sup>12,13</sup>) The phenolphthalein liberated was measured by adding four volumes of 0.2 M glycine-sodium carbonate buffer (pH 10.4); where DMSO additions affected the final pH; extra Na<sub>2</sub>CO<sub>3</sub> was added to ensure that the final pH was 10.2-10.4. The phenolphthalein concentration was determined at 540 nm, from standards similarly diluted. The acetate buffer used in an assay by Fishman<sup>14</sup> was not suitable for assays performed in the presence of DMSO, because it has a pH of 5.0 and is not sensitive to moderate amounts of DMSO; because the pH was shifted. We therefore used 0.01 M K<sub>2</sub>HPO<sub>4</sub> in the assay medium, because it has a pH of 5.0 and is not sensitive to moderate amounts of DMSO.

A purified form of B-3 glucuronidase was prepared by a modification of the method of Fishman:<sup>11</sup> a 20 mg/ml solution of enzyme was made in 0.15 M sodium citrate buffer (pH 5.0) and cooled to 0°C, and cold absolute methanol (-20°C) was added. The mixture was gradually cooled to -20°C, and the fraction precipitated by 20% methanol (v/v) was removed by centrifugation and discarded. The fraction precipitated by 30% methanol was collected, as it contained more than 80% of the  $\beta$ -glucuronidase activity.

The DMSO used in these experiments was reagent grade or the highest grade available from Sigma Chemical Co., Pierce Chemical Co., and Mallinckrodt Chemical Co. No differences were noted in the properties of DMSO from these three sources.

The rate of thrombin-induced fibrinogen clotting was measured by noting the rate of increase in opacity at 600 nm (clotting rate). All assays were performed with bovine fibrinogen (Sigma fraction I, obtained from Calbiochem) and bovine thrombin (Parke-Davis), which were further purified before use, as described elsewhere.<sup>15,16</sup> The system was free of Ca<sup>++</sup> and cross-linking enzymes. The assay medium consisted of 0.02 M sodium phosphate buffer, 0.02 M sodium borate, and 0.15 M NaCl. The pH was adjusted to the indicated values after the addition of

DMSO to the medium. Fibrinogen in 0.15 M KCl was added to a final concentration of 2.75 mg/ml in all experiments. In order to make the initial rate data comparable, the  $\Delta A_{400\text{ nm}}/\text{min}$  were normalized to an  $A_{400}$  of 1.0, because the  $A_{400}$  varies with the pH, temperature, and DMSO concentration. In the presence of DMSO, a lag period or subthreshold phase was noted, and was defined as the time until the initial increase in opacity after the addition of thrombin. Fibrin monomers were prepared by dissolving a synthesized clot in cold 1 M KBr, which contained 0.05 M sodium phosphate (pH 5.3). The rate of polymerization of fibrin monomers was measured by the increase in opacity at 350 nm after the addition of 2 vols 0.05 M phosphate buffer (pH 7.5). The final pH of the medium was 6.6, and the fibrin concentration was 1.67 mg/ml.

## RESULTS

The first subunit protein assayed in the presence of DMSO was bovine liver glutamate dehydrogenase [GDH—L-glutamate-NAD(P) oxidoreductase (deaminating) EC 1.4.1.3]. Rammler<sup>13</sup> had speculated that DMSO might induce changes in GDH protein similar to those caused by allosteric modifiers, and it was of interest to test this hypothesis. This enzyme is composed of enzymatically inactive subunits, with a molecular weight of ca. 50,000,<sup>13-15</sup> which associate to form an enzymatically active hexamer of approximately 300,000 molecular weight.<sup>16-18</sup> This hexamer is usually referred to as the monomeric form, and appears to exist as

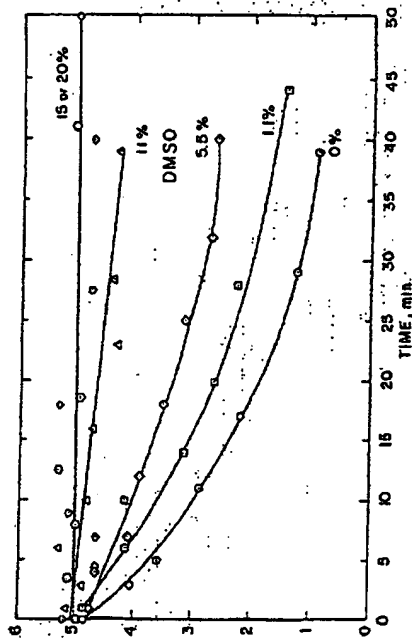


FIGURE 1. Stabilization of GDH by DMSO at low ionic strength. Enzyme solutions of 4 mg/ml in 0.01 M Tris-HCl buffer (pH 8.0) were prepared at 5°C and diluted at zero time to 0.4 mg/ml in the same buffer, containing the indicated amount of DMSO. While the temperature was maintained at 5°C, 0.1 ml aliquots were removed at regular time intervals for measurement of GDH activity by the routine assay, in which 2.9 ml assay mixture, which contained 1.2  $\mu\text{mol}$  NAD<sup>+</sup>, 6  $\mu\text{mol}$  NaCl, 150  $\mu\text{mol}$  Tris buffer (pH 8.0), and 450  $\mu\text{mol}$  L-glutamate, were mixed with the test solution and the initial rate of absorbance change at 340 nm was determined. The assay was performed at 25°C;  $v = \Delta A_{400\text{ nm}}/\text{min}/\text{mg}$  protein.

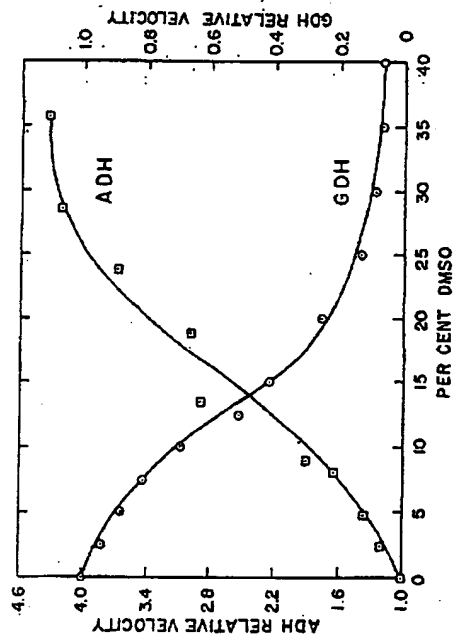


FIGURE 2. Reciprocal effects of DMSO on glutamate and alanine dehydrogenase activities. The GDH assay was as described in the legend for FIGURE 1; the alanine dehydrogenase (ADH) assay mixture was similar, but contained 150  $\mu\text{mol}$  L-alanine instead of glutamate. GDH and ADH activities in the absence of DMSO were arbitrarily set at 1.0, and other values were calculated relative to this. ADH activity in the absence of DMSO was approximately 2% of the GDH activity.

an equilibrium between an active and inactive conformation. The active monomer appears to associate linearly to form rods of indefinite length. The strong stabilizing effects of D<sub>2</sub>O on the polymeric form and the stabilization of GDH against denaturation by dilution suggest that bound water plays a significant role in maintaining the structure of this enzyme and in facilitating conformational-type changes.<sup>19</sup>

The effects of DMSO that we have detected on this enzyme include dissociation of the polymeric forms, shifting of the equilibrium between the active and inactive monomers (to favor the inactive monomer), and either stabilization or denaturation of the enzyme, depending on the DMSO concentration and temperature.<sup>20</sup> The effect of DMSO on GDH that was detectable at the lowest DMSO levels was protection of the enzyme from inactivation by dilution at low temperatures. FIGURE 1 shows that GDH was appreciably stabilized at 5°C in dilute solutions, even by 5% DMSO. These effects result primarily from the effects of DMSO on the hydrophilic groups of GDH and bound water, since hydrophobic bonding is minimized at low temperatures. Independent evidence for this interpretation was shown by the similar stabilization of GDH against inactivation by dilution in a D<sub>2</sub>O environment.<sup>21</sup>

When DMSO was added to the medium during GDH assay, the GDH activity diminished as the DMSO concentration was increased (FIGURE 2). The sigmoid shape of the curve suggests that this was due to a cooperative type of inhibition, such as is often seen with allosteric modifiers. The increase in alanine dehydrogenase activity also suggests that there were conformational changes, since the alanine dehydrogenase activity is considered to be associated with the inactive rather than the active monomer.

When the effects of DMSO on the inhibition of GDH activity in  $H_2O$  and  $D_2O$  were compared,  $D_2O$  appeared to exert a synergistic effect with DMSO in inhibiting GDH (Figure 3). This can be interpreted as an apparent increase in the concentration of the inactive monomer.  $D_2O$  facilitates the reaction of the enzyme with DMSO, but does not change the maximal slope of 2.7; this indicates that the inactive monomer may have more exchangeable groups on the surface of the protein than can form hydrogen bonds with DMSO or  $D_2O$  than does the active monomer.

The effects of DMSO in inhibiting GDH were reversible by the allosteric effector ADP, in a competitive manner (Figure 4). This further suggests that DMSO shifts the equilibrium between monomers, thus stabilizing the inactive form. ADP supposedly affects GDH by stabilizing the active monomer, and thus shifting the active-inactive monomer equilibrium in the opposite direction from DMSO.

Although the effects of DMSO on GDH are reversible, at DMSO levels above ca. 30%, denaturation-type effects occur that are no longer reversed by dilution of the DMSO or addition of ADP. This is evidence that when it is present in higher concentrations, DMSO may denature subunit proteins by rupturing both hydrophilic and hydrophobic bonding.

In order to study the effects of DMSO on the maintenance of an active conformation in a nonallosteric-type subunit protein, we have used as a model the lysosomal enzyme  $\beta$ -glucuronidase ( $\beta$ -D-glucuronohydrolase, EC 3.2.1.31). This enzyme is widely distributed in animal tissues, and can readily be assayed by measurement of the rate of hydrolysis of phenolphthalein  $\beta$ -glucuronide.<sup>10</sup> Under ordinary conditions this is a relatively stable enzyme, but it has been reported<sup>10,12</sup> that highly purified  $\beta$ -glucuronidase can be dissociated by dilution into inactive subunits, which can be reassociated and reactivated nonspecifically by incubation with polycations.<sup>10,12</sup>

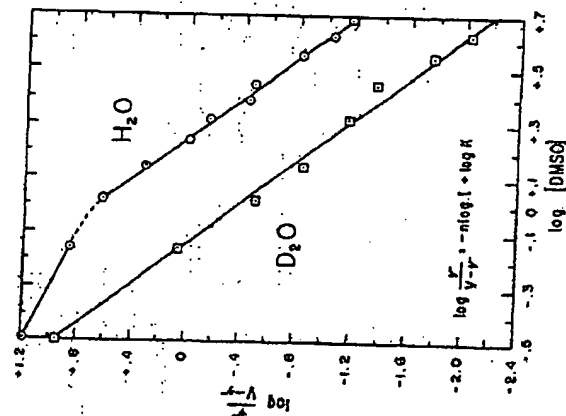


FIGURE 3. Comparison of the inhibitory effects of DMSO on GDH in  $H_2O$  and  $D_2O$ . The assay conditions were as described in the legend for Figure 1, except that the assay was done in both  $D_2O$  and  $H_2O$ , and the data were plotted in a Hill plot.

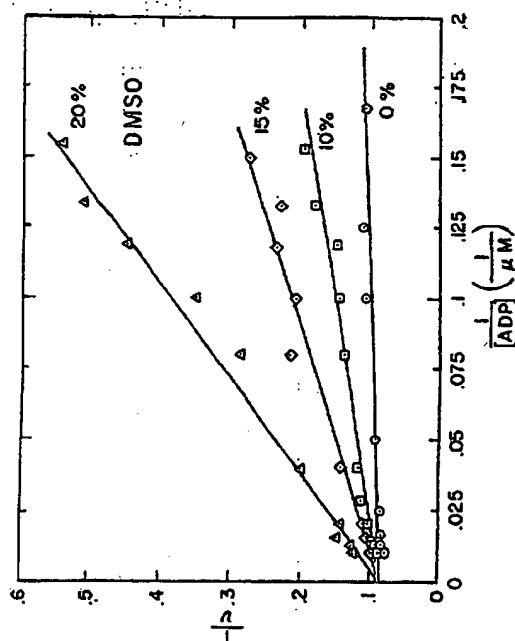


FIGURE 4. Reversal of DMSO inhibition by ADP. Routine assays of GDH were performed as described in the legend for Figure 1, with the addition of the indicated amounts of ADP.

One of the more striking effects of DMSO on  $\beta$ -glucuronidase activity was a lowering of the temperature of inactivation when the enzyme was incubated in the absence of substrate (Figure 5). In the absence of DMSO, the enzyme activity in 0.01 M  $KH_2PO_4$  was stable at 37°C, and a 30-min heating period at 56°C was necessary for 90% inactivation. In the presence of 20% DMSO, the rate of inactivation of  $\beta$ -glucuronidase was slow at 25°C, but it proceeded at a faster rate at 37°C. Replacement of  $H_2O$  by  $D_2O$  in the incubation medium had only a minimal effect. The rapid inactivation of  $\beta$ -glucuronidase by DMSO could also be readily demonstrated in tissue slices or homogenates, if the DMSO concentrations were 50% or higher.

The inactivation of  $\beta$ -glucuronidase by DMSO was greatly influenced by the pH, salt concentration, and DMSO concentration. It required almost twice as much DMSO to inactivate the enzyme (at comparable rates) at 25°C as at 37°C. The enzyme was most stable at pHs between 4.5 and 5.2, and at 37°C the stability of the enzyme in 20% DMSO was markedly reduced at pHs above and below these values. The enzyme was most stable in 0.04 M  $KH_2PO_4$  in the presence of 20–40% DMSO, and its stability diminished as the  $KH_2PO_4$  concentration was elevated.

No method has been found that will reverse the inactivation of  $\beta$ -glucuronidase by DMSO. Neither overnight dialysis at 5°C nor dilution of the enzyme when dissolved in DMSO solutions resulted in any appreciable reactivation. The addition to the assay mixture of 1 mg/ml DNA or serum albumin, which has been reported to reactivate the inactive form<sup>10</sup> of the enzyme,<sup>10,12</sup> had no effect. Thus the available evidence suggests that the major effect of exposure of  $\beta$ -glucuronidase to DMSO in the absence of substrate was an irreversible denaturation of the enzyme.

In the presence of substrate, moderate levels of DMSO inhibited  $\beta$ -glucuronidase in a reversible manner (Figure 6). Since the kinetics of inhibition became it-

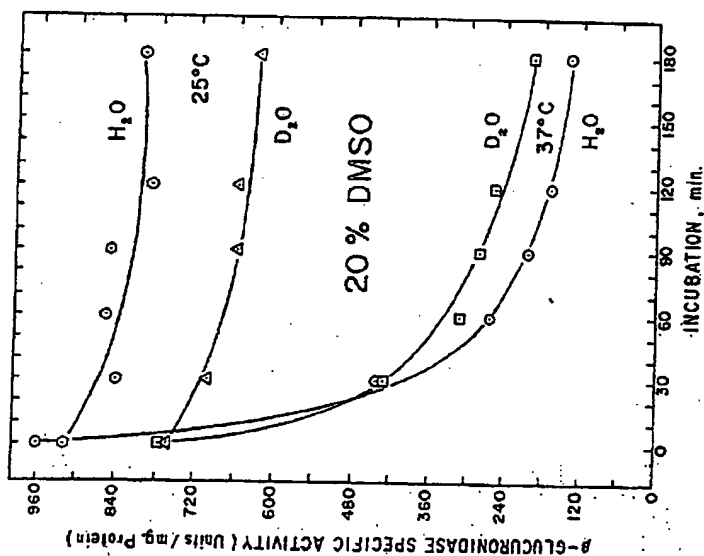


FIGURE 5. The stability of  $\beta$ -glucuronidase in DMSO solutions as a function of temperature. Solutions of  $\beta$ -glucuronidase were prepared in  $H_2O$  or  $D_2O$ , which contained 1 mg/ml protein, 20% DMSO, and 0.01 M  $KH_2PO_4$  at  $5^\circ C$ . The solutions were then incubated at either  $25^\circ C$  or  $37^\circ C$ . At the indicated time intervals, 0.1 ml aliquots were removed and assayed for  $\beta$ -glucuronidase activity by addition of 0.9 ml  $H_2O$  or  $D_2O$ , which contained 10  $\mu$ mol  $KH_2PO_4$  and 1  $\mu$ mol phenolphthalein glucuronide. The reaction mixture was incubated for 15 min at  $37^\circ C$ , then 4 ml 0.2 M glycine- $Na_2CO_3$  buffer (pH 10.4) were added and the absorbance of the liberated phenolphthalein at 540 m $\mu$  in 1 cm cells measured. One unit of enzyme activity corresponds to the liberation of 1  $\mu$ g phenolphthalein/hr at  $37^\circ C$ .

regular at substrate levels higher than 5  $\mu$ moles/ml, this region was investigated in further detail. At ultrahigh substrate levels the purified  $\beta$ -glucuronidase appeared to be subject to substrate inhibition, but this was reversed by DMSO (Figure 7). These results show how DMSO can affect the same enzyme in completely different ways, depending on the conditions of exposure and the presence or absence of substrates.

Studies of the effects of DMSO on the clotting of fibrinogen were undertaken because of previous reports that DMSO inhibited blood clotting under some conditions.<sup>21</sup> The effects of DMSO on purified fibrinogen and thrombin were investigated to determine what types of mechanism might be involved in the interactions between the two subunit proteins and DMSO. Initial studies showed that the thrombin-in-

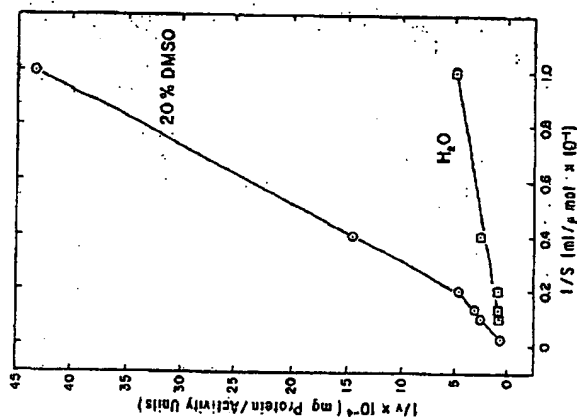


FIGURE 6. Reversal of DMSO inhibition of  $\beta$ -glucuronidase by substrate. Purified  $\beta$ -glucuronidase was assayed as described in the legend for Figure 5 over a range of substrate concentrations from 0.1 to 10  $\mu$ mol phenolphthalein  $\beta$ -glucuronide, in the presence and absence of DMSO.

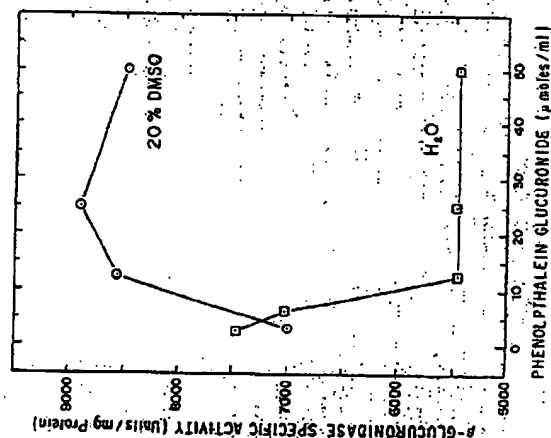


FIGURE 7. Protection of  $\beta$ -glucuronidase from substrate inhibition by DMSO. Assay methods were as described in the legend for Figure 6, but the substrate range was 5-25  $\mu$ mol, in a total volume of 0.5 ml.

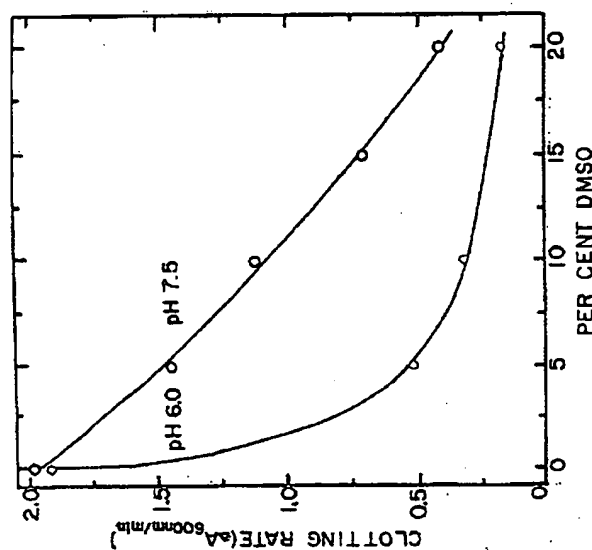


FIGURE 8. Inhibition of fibrinogen clotting by DMSO. Buffer solutions of 0.02 M phosphate, 0.02 M borate, and 0.15 M NaCl were prepared with the indicated amount of DMSO and adjusted to pH 6.0 (○—○) or pH 7.5 (○—○). Fibrinogen was added to a final concentration of 2.75 mg/ml. Ten units of thrombin were added at time 0, and the  $\Delta A_{600\text{nm}}$  was measured in 1 cm cuvettes. All assays were performed at 25°C.

duced clotting of fibrinogen was quite sensitive to DMSO, but the extent of inhibition at a given DMSO level was appreciably sensitive to the pH of the assay medium (FIGURE 8). This system was much more sensitive to low levels of DMSO at pH 6.0 than at pH 7.5.

Further studies of the effects of pH on the inhibition of clotting by DMSO are shown in FIGURE 9. The thrombin-induced gelling of fibrinogen over the pH range of this study shows no marked sensitivity to pH in the absence of DMSO. In the presence of 20% DMSO the rate of clotting was maximally inhibited at pH 6.0, and the degree of inhibition diminished linearly between pH 6.5 and 8.0. The lag time (or subthreshold time) before clotting commenced was also maximal at pH 6.0. This suggests that DMSO may have a particular affinity for proton-donor groups whose ionization state changes in the pH range of 6.0-8.0, such as free amino groups. The data also suggest that DMSO binds with the un-ionized species, since it required a fourfold higher concentration of DMSO to produce the same amount of inhibition at pH 7.5 as at pH 6.0. The similar inhibition by 20% glycerol at pH 6.0 suggests that at this acidity the inhibition may be nonspecific, in that other solvents with hydrogen-bonding substituents may produce similar effects. On the other hand, the interaction of substances such as glycerol with an un-ionized binding site could also be enhanced at pH 6.0.

The comparison of DMSO with glycerol was initially performed to determine whether the effect of DMSO was simply the result of a change in the dielectric constant of the clotting medium. Since glycerol and DMSO have similar dielectric constants, but have quite different effects on clotting rates at pH values over 7.0, it is unlikely that the effect of DMSO on clotting results from a change in the dielectric constant of the assay medium.

Since the clotting phenomenon, as measured by opacity increase, is the end result of an initial proteolysis of fibrinogen by thrombin, followed by polymerization of the released fibrin monomers to small linear polymers and then to larger polymers, it was of interest to determine which phase(s) of the clotting reactions were most sensitive to DMSO.

The time course of opacity development after the addition of thrombin to fibrinogen in the presence and absence of DMSO is shown in FIGURE 10. In the presence of DMSO, a significant lag phase (subthreshold phase) preceded the first-order rate of opacity development. The subthreshold phase increased in length as the temperature and DMSO concentration were increased. The subthreshold phase has been interpreted as the time required for thrombin to generate a critical concentration of fibrin monomers. Once the concentration of fibrin monomers had become high enough, polymerization would occur. This lag phase was therefore taken as a measure of the rate of formation of thrombin-catalyzed fibrin from fibrinogen. The rate of thrombin action in attaining a critical concentration of fibrin monomers was taken to be the reciprocal of the subthreshold time.

To test this hypothesis, hirudin, a potent inhibitor of thrombin, was added to the system just after the end of the subthreshold phase, when the opacity had increased to only 10% of its final value. The opacity continued to increase at the same rate as the control, but the final opacity was only 46% of that in the uninhibited reaction.

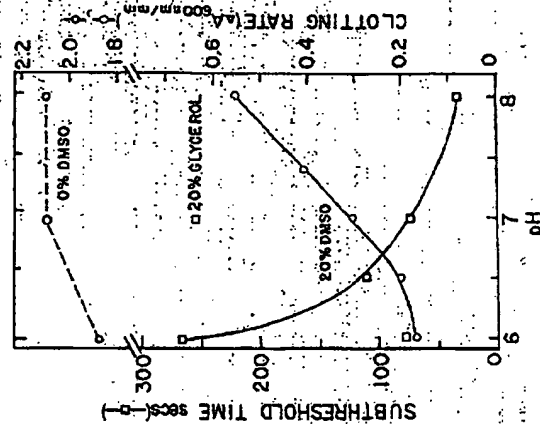


FIGURE 9. Effects of pH and DMSO on fibrinogen clotting. Experimental conditions were as described in the legend for FIGURE 8. The subthreshold time was the time until the first increase in opacity.



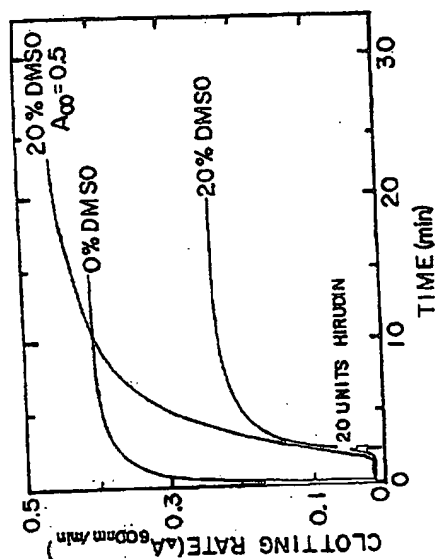


FIGURE 10. The time course of fibrinogen clotting in the presence of DMSO and hirudin. Experimental conditions were as described in the legend for FIGURE 8, except that the pH was 7.0 and the temperature was 39°C.

(FIGURE 10). At the time hirudin was added, the system that contained no DMSO was completely clotted. These results clearly indicate that DMSO inhibits the generation of fibrin monomers by thrombin.

To determine whether DMSO was inhibiting thrombin as a classical competitive or noncompetitive inhibitor, plots of  $1/v$  ( $v$  = clotting rate) against DMSO concentration were made. Atypical curves, resulting as straight lines, could be obtained only if  $1/v$  was plotted versus  $[DMSO]^2$ , which indicated that this was a second order-type inhibition. DMSO had no appreciable effect on the thrombin-catalyzed hydrolysis of tosyl-arginine methyl ester. It thus appeared that the inhibition of clotting by DMSO was not related to a direct inhibition of thrombin.

FIGURE 11A shows a plot of DMSO concentration versus  $1/1-i$ , where  $i = 1 - v_1/v_0$  and  $v_1$  is the velocity, or rate of formation, in the presence of DMSO, of the critical fibrin monomer concentration. The curve is similar to those that have been ascribed to the binding of inhibitor to substrate,<sup>17</sup> which results in a reduced concentration of effective substrate. The data from clotting-rate measurements also followed this relationship.

To determine whether there was an appreciable effect of DMSO on the polymerization of fibrin monomers, a solution of fibrin monomers was prepared at pH 5.3; and it was allowed to polymerize in the presence and absence of DMSO at pH 6.6. The rate of aggregation was measured by the rate of increase in opacity at 350 nm. In the presence of DMSO, the time course—versus—absorbance curve was sigmoidal. The sigmoidicity increased as the DMSO concentration was raised. In this case, the initial lag phase appeared to represent an effect of DMSO on the aggregation of monomers to small linear or intermediate-size polymers. After the initial slow increase in absorbance, a rapid first-order clotting occurred. The initial rates of fibrin aggregation were found to be ca. half as sensitive to DMSO as those of the thrombin-catalyzed clotting of fibrinogen.

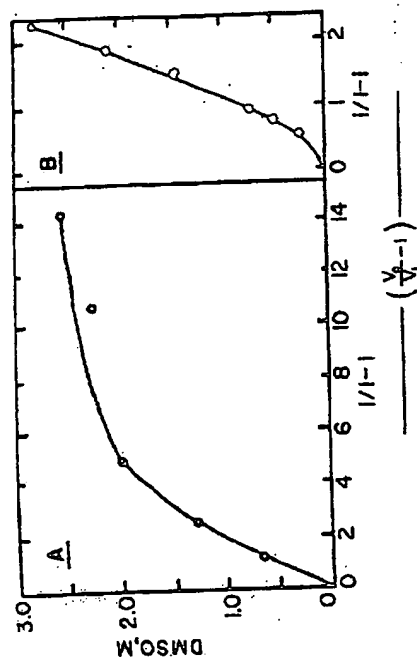


FIGURE 11. Studies of the kinetics of DMSO inhibition of (A) formation of the critical fibrin monomer concentration and (B) fibrin monomer aggregation. The temperature was 25°C. The pH was 7.0 for study of the rate of formation of the critical concentration of fibrin monomers from fibrinogen ( $\circ$ — $\circ$ ) and 6.6 for the rate of fibrin monomer aggregation ( $\circ$ — $\circ$ ).  $i = 1 - v_1/v_0$  where  $v_1$  is the velocity of the inhibited reaction.

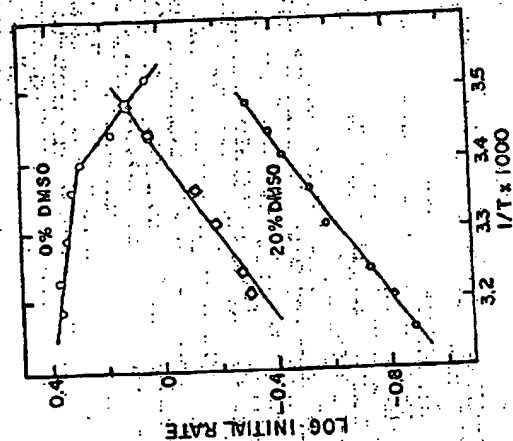


FIGURE 12. Effects of temperature and DMSO on fibrinogen clotting. Conditions were as described in the legend to FIGURE 8, except that the assays were performed over a temperature range of 13–40°C. ( $\circ$ — $\circ$ ) = clotting rates with no DMSO; ( $\circ$ — $\circ$ ) = clotting rates at 20% DMSO. ( $\circ$ — $\circ$ ) = rate of formation of the critical fibrin monomer concentration in the presence of 20% DMSO.

When the DMSO concentration was plotted against the  $i/1-i$  for fibrin monomer polymerization, a curve was obtained similar to those reported to be caused by partial inhibition due to substrate displacement (Figure 11B).<sup>37</sup> It thus appears that DMSO binds not only with fibrinogen, but also with fibrin monomer at certain of the sites of polymerization. The nature of the DMSO effect in this case appears to be due to binding of ionic or hydrophilic groups, because the temperature dependence of the polymerization rate in the presence of DMSO was positive (the greatest inhibition occurred at low temperatures).

We next investigated the temperature dependence of the DMSO effects on the rate of clotting and the rate of development of a critical fibrin monomer concentration. As can be seen in Figure 12, both parameters show a negative energy of activation and  $\Delta H^\circ$  (change in the rate of enthalpy). This finding is consistent with the idea that hydrophobic interactions between DMSO and fibrinogen are a significant mechanism. The temperature dependence of the clotting rate of fibrinogen in the absence of DMSO showed a positive energy of activation and was biphasic, which suggests that at least two of the rate constants in the overall clotting process have different temperature coefficients. This effect was not seen in the presence of DMSO, possibly because the combination of thrombin with fibrinogen became rate-limiting.

Studies of the uv absorption spectra of DMSO and fibrinogen were performed because DMSO has been used extensively in solvent perturbation studies,<sup>38</sup> as in contrast to previous work, it was found that the greatest spectral change occurred in the region of 190-200 nm; at this level, DMSO exhibited a strong absorption maximum when present in 0.01-0.001% water solutions and a hypochromicity of 30-40% when mixed with fibrinogen. When mixed with 10<sup>-3</sup> M amino acid solutions, DMSO exhibited a hypochromicity only with tyrosine.

#### DISCUSSION

There are two properties of DMSO that appear to explain many of its effects on subunit proteins: its affinity for proton-donor groups, and the presence of hydrophobic as well as hydrophilic groups on the DMSO molecule. Thus the information that is available on the effects of low levels of DMSO on subunit proteins such as GDH is consistent with the interpretation that the primary effect of DMSO is the formation of hydrogen bonds with proton-donor groups on the surface of the molecule, which may differentially stabilize a particular conformation such as the inactive monomer. The strong stabilizing effects of DMSO on GDH at low temperatures suggest that DMSO may be useful for stabilizing labile protein or enzyme preparations, and possibly also for the storage of tissues and organs. Although DMSO is widely used for the preservation of cells and tissues in the frozen state, little work has been done on the possible use of DMSO in preserving tissues or cells in the cold but unfrozen state.

The reversal of the inhibitory effects of DMSO on GDH by ADP, an allosteric activator, and the synergistic effect of DMSO with D<sub>2</sub>O both suggest that it has effects on hydrophilic bonding and water bridges. Effects of this type appear to be generally reversible, so long as the DMSO concentration is less than 20% and/or the temperature is less than 25°C. These are probably also the optimal conditions for the use of DMSO as a solvent to carry drugs through the skin into localized areas, where it would be desirable to use the lowest possible concentrations of DMSO and low temperatures, in order to minimize the irreversible effects on structural and functional proteins.

At higher concentrations or at temperatures approaching 37°C, in addition to its effects on hydrophilic bonding, DMSO may rupture hydrophobic bonds. In the case of either GDH or  $\beta$ -glucuronidase, higher DMSO levels or higher temperatures were correlated with an irreversible loss of enzyme activity; hence this can be considered as protein "denaturation." In view of the lack of appreciable effects of the deuterium isotope on the denaturation of  $\beta$ -glucuronidase, it would appear that hydrophobic bonding may be of particular importance in the maintenance of the structure of this enzyme.

The inhibitory effects of DMSO on fibrinogen clotting were maximal at high temperatures and high DMSO concentrations, which suggests that a significant mechanism of DMSO action in this case may also be interference with hydrophobic interactions. While the effects of DMSO on clotting appear to be related to its effects on hydrophobic bonding, the dependence of the degree of inhibition on the pH of the medium, and the inhibition of fibrin monomer aggregation by DMSO at low temperatures, suggest that the effects of hydrophilic bonding are also important. The effects of hirudin show that the initial rate of fibrin monomer formation by thrombin is inhibited, which suggests that DMSO is inhibiting the initiation of clotting by thrombin. This appears to be due to a competition between DMSO and thrombin for binding sites on fibrinogen, rather than to inhibition of thrombin action.

Denaturation of proteins in localized areas by topical applications of 50-100% DMSO may be useful in the treatment of some types of traumatic injuries, because denaturation of many proteins appears to be a necessary prerequisite for enzymatic digestion by lysosomal proteases.<sup>39</sup> After DMSO treatment, the subsequent turnover of necrotic tissue due to the migration of macrophages or by other phagocytic cells into the area might be appreciably facilitated. This may explain why topical application of DMSO at 6-hour intervals has been found useful in veterinary practice for the treatment of open, infected wounds of long duration.<sup>40</sup>

The inactivation of  $\beta$ -glucuronidase by DMSO may also be a useful indicator of the DMSO concentrations that have been reached in dermal regions *in vivo* following topical applications of DMSO. Since this enzyme activity is readily detected by means of fluorescent or cytochemical stains,<sup>41</sup> the depth of tissue exposed to critical DMSO levels could be investigated.

#### SUMMARY

The effects of DMSO are thought to result from the formation of hydrogen bonds with proton-donor groups on biopolymers, which are stronger than those formed with water. Since DMSO contains methyl groups, however, effects on hydrophobic bonding in proteins could be expected at higher DMSO levels. Our studies of the effects of DMSO on model subunit proteins can be interpreted in the above terms. At a concentration of 20% or less, DMSO changed glutamate dehydrogenase into the inactive monomer, and the effects were fully reversible with the activator (ADP). Higher DMSO levels resulted in irreversible inactivation. The predominant effect noted on  $\beta$ -glucuronidase was irreversible inactivation by 20% or more DMSO at 37°C. Purified  $\beta$ -glucuronidase exhibited an activation in 20% DMSO at high substrate levels; this resulted from an apparent substrate inhibition in the absence of DMSO. DMSO inhibited the clotting of fibrinogen by purified thrombin, but the major effect appeared to be due to competition between thrombin and DMSO for binding sites on fibrinogen. These effects appear to be largely due to interactions between DMSO and hydrophobic bonding in fibrinogen, although

DMSO also appears to interfere with the aggregation of fibrin monomers through its effects on hydrophilic groups. These results suggest that reversible alterations in protein structure are the major effect of exposure of subunit proteins to low DMSO levels at low temperatures, while irreversible denaturation of subunit proteins may be an appreciable effect at higher temperatures and higher DMSO concentrations.

#### ACKNOWLEDGMENTS

The authors gratefully acknowledge the assistance of Mr. Gregory E. Johnson in carrying out many of the experiments reported here. Also, we are indebted to Mr. Takeshi Minagawa, Mr. Emerson Golf, Mr. Fred Rupprecht, and Mrs. Elsie Spencer for aiding in the preparation of this manuscript, and to Drs. Robert K. Jones and Raymond E. Pfeiffer of Lovelace Foundation for critically reviewing the manuscript.

#### REFERENCES

1. LEWIN, S. 1967. The conformation stabilizing potential of water in biopolymers and its stabilization by deuteration. *Studia Biophys.* 4: 29.
2. LEWIN, S. 1967. Some aspects of hydration and stability of the native state of DNA. *J. Theoret. Biol.* 17: 182.
3. HENDERSON, R. F., T. R. HENDERSON & B. M. WOODEN. 1970. Effects of D<sub>2</sub>O on the association-dissociation equilibrium in subunit proteins. *J. Biol. Chem.* 245: 3733.
4. NEMETHY, G. & H. A. SCHERAGA. 1964. Structure of water and hydrophobic bonding in proteins. IV. The thermodynamic properties of liquid deuterium oxide. *J. Chem. Phys.* 41: 68.
5. HENDERSON, R. F. & T. R. HENDERSON. 1969. Effects of D<sub>2</sub>O on the allosteric properties of glutamic dehydrogenase. *Arch. Biochem. Biophys.* 129: 86.
6. RAMMLER, D. H. & A. ZAFFARONI. 1967. Biological implications of DMSO based on a review of its chemical properties. *Ann. N.Y. Acad. Sci.* 141: 13.
7. HERSKOVITS, T. T. 1962. Nonaqueous solutions of DNA: Factors favoring the stability of the helical configuration in solution. *Arch. Biochem. Biophys.* 97: 474.
8. SCHERAGA, H. A., G. NEMETHY & T. Z. STENBERG. 1962. The contribution of hydrophobic bonds to the thermal stability of proteins. *J. Biol. Chem.* 237: 2506.
9. HENDERSON, T. R., R. F. HENDERSON & G. E. JOHNSON. 1969. The effect of dimethyl sulfoxide on the allosteric transitions of glutamic dehydrogenase. *Arch. Biochem. Biophys.* 132: 242.
10. FISHMAN, W. H. 1965.  $\beta$ -Glucuronidase. In *Methods of Enzymatic Analysis*. H. U. Bergmeyer, Ed.: 869. Academic Press Inc., New York, N.Y.
11. FISHMAN, W. H. & P. BRANFELD. 1955. Glucuronidases. *Methods Enzymol.* 1: 262.
12. RAMMLER, D. H. 1967. The effect of DMSO on several enzyme systems. *Ann. N.Y. Acad. Sci.* 141: 291.
13. MARLER, E. & C. TANFORD. 1964. The molecular weight of the peptide chains of L-glutamate dehydrogenase. *J. Biol. Chem.* 239: 4217.
14. PAGE, E. & C. GODIN. 1969. On the determination of the molecular weight of protein subunits on Sephadex G-200 in the presence of detergent. *Glutamate dehydrogenase*. *Can. J. Biochem.* 47: 401.
15. EISENBERG, H. & O. M. TOWNS. 1968. Molecular weight of the subunits of oligomeric and associated forms of bovine liver glutamate dehydrogenase. *J. Mol. Biol.* 31: 37.
16. DESSEN, P. & D. PANTALONI. 1969. Glutamate dehydrogenase. Structure quaternaire et propriétés rotatoires. *European J. Biochem.* 8: 292.
17. SUNO, H. & W. BURCHARD. 1968. Sedimentation coefficient and molecular weight of beef liver glutamate dehydrogenase at the microgram and the milligram level. *European J. Biochem.* 6: 202.

18. SUNO, H., I. PILZ & M. HERBST. 1969. Studies of glutamate dehydrogenase. 5. The x-ray small-angle investigation of beef liver glutamate dehydrogenase. *European J. Biochem.* 7: 517.
19. BRANFELD, P., H. C. BRANFELD, J. S. NISSELBAUM & W. H. FISHMAN. 1954. Dissociation and activation of  $\beta$ -glucuronidase. *J. Amer. Chem. Soc.* 76: 4872.
20. BRANFELD, P., S. JACOBSON & H. C. BRANFELD. 1957. "Activator-competitive" enzyme inhibition. Interrelation of dissociation, activation, inhibition and surface inactivation of  $\beta$ -glucuronidase. *Arch. Biochem. Biophys.* 69: 198.
21. DAVIS, H. L., N. DAVIS & A. L. CLAMONS. 1967. Procoagulant and nerve-blocking effects of DMSO. *Ann. N.Y. Acad. Sci.* 141: 310.
22. HERSKOVITS, T. T. 1967. Difference spectroscopy. *Methods Enzymol.* 11: 748.
23. COFFEY, J. W. & C. DEDUYA. 1968. Digestive activity of lysosomes. I. The digestion of proteins by extracts of rat liver lysosomes. *J. Biol. Chem.* 243: 3255.
24. LEVSESQUE, F. 1967. Effects of DMSO on open wounds in horses. *Ann. N.Y. Acad. Sci.* 141: 490.
25. PHILLIPS, H. M. & J. L. YORK. 1973. Bovine fibrinogen. I. Effects of amidation on fibrin monomer aggregation. *Biochemistry* 12: 3637.
26. PHILLIPS, H. M. & J. L. YORK. 1973. Bovine fibrinogen. 2. Effects of tyrosine modification on fibrin monomer aggregation. *Biochemistry* 12: 3642.
27. REINER, J. M. 1966. Behavior of Enzyme Systems, p. 192. Van Nostrand-Reinhold Co., New York, N.Y.



PubMed

National  
Library  
of MedicineMy NCBI  
[Sign In] [Register]

PubMed

Nucleotide

Protein

Genome

Structure

OMIM

PMC

Journals

Books

for   

Limits

Preview/Index

History

Clipboard

Details

Display

Abstract

Show

20

Sort by

Send to

All: 1

Review: 0

☐ 1: Ann N Y Acad Sci. 1975 Jan 27;243:38-53.[Related Articles, Links](#)**Effects of dimethyl sulfoxide on subunit proteins.****Henderson TR, Henderson RF, York JL.**

The effects of DMSO are thought to result from the formation of hydrogen bonds with proton-donor groups on biopolymers, which are stronger than those formed with water. Since DMSO contains methyl groups, however, effects on hydrophobic bonding in proteins could be expected at higher DMSO levels. Our studies of the effects of DMSO on model subunit proteins can be interpreted in the above terms. At a concentration of 20% or less, DMSO changed glutamate dehydrogenase into the inactive monomer and the effects were fully reversible with the activator (ADP). Higher DMSO levels resulted in irreversible inactivation. The predominant effect noted on beta-glucuronidase was irreversible inactivation by 20% or more DMSO at 37 degrees C. Purified beta-glucuronidase exhibited an activation in 20% DMSO at high substrate levels; this resulted from an apparent substrate inhibition in the absence of DMSO. DMSO inhibited the clotting of fibrinogen by purified thrombin, but the major effect appeared to be due to competition between thrombin and DMSO for binding sites on fibrinogen. These effects appear to be largely due to interactions between DMSO and hydrophobic bonding in fibrinogen, although DMSO also appears to interfere with the aggregation of fibrin monomers through its effects on hydrophilic groups. These results suggest that reversible alterations in protein structure are the major effect of exposure of subunit proteins to low DMSO levels at low temperatures, while irreversible denaturation of subunit proteins may be an appreciable effect at higher temperatures and higher DMSO concentrations.

PMID: 236713 [PubMed - indexed for MEDLINE]

Display  Show  Sort by  Send to [Write to the Help Desk](#)[NCBI](#) | [NLM](#) | [NIH](#)[Department of Health & Human Services](#)[Privacy Statement](#) | [Freedom of Information Act](#) | [Disclaimer](#)

## Fourier transform Raman spectroscopy of interactions between the penetration enhancer dimethyl sulfoxide and human stratum corneum<sup>a</sup>

Angela N.C. Anigbogu<sup>a</sup>, Adrian C. Williams<sup>a</sup>, Brian W. Barry<sup>a,\*</sup>,  
Howell G.M. Edwards<sup>b</sup>

<sup>a</sup> Postgraduate Studies in Pharmaceutical Technology, The School of Pharmacy, University of Bradford, Bradford BD7 1DP, UK

<sup>b</sup> Chemistry and Chemical Technology, University of Bradford, Bradford BD7 1DP, UK

Received 17 February 1995; accepted 20 April 1995

### Abstract

The stratum corneum, the outermost layer of human skin, is the major barrier to transdermal delivery of most drugs. Dimethyl sulfoxide (DMSO) is an established penetration enhancer. To assess its mechanism of flux enhancement, Fourier transform (FT) Raman spectroscopy was used to study the effects of a series of aqueous solutions of DMSO on hydrated human stratum corneum following treatment for 1 h. The results showed changes in the stratum corneum keratin from an  $\alpha$ -helical to a  $\beta$ -sheet conformation. In addition, at concentrations  $\geq 60\%$  v/v, at which DMSO enhances drug flux, there was evidence of interactions with stratum corneum lipids. These observations suggest that the skin penetration enhancement produced by DMSO not only involves changes in protein structure but may also be related to alterations in stratum corneum lipid organization, besides any increased drug partitioning effects.

**Keywords:** Penetration enhancer; Human stratum corneum; Dimethyl sulfoxide; Water; Fourier transform Raman spectroscopy

### 1. Introduction

Human skin functions as an excellent barrier in two directions, controlling the loss of water and other body constituents while preventing the

entry of noxious substances from the external environment. The percutaneous route for drug administration holds several advantages over the oral or systemic routes such as the avoidance of first pass gut and hepatic metabolism, the ability to deliver drugs continuously, potentially fewer side effects, better patient compliance and ease of rapid cessation of therapy (Barry, 1983; Weissinger, 1993). Widespread use of the skin for drug delivery is, however, limited because of the aforementioned barrier properties.

<sup>a</sup> Preliminary data were presented at the British Pharmaceutical Conference, Reading, UK, September, 1993.

\* Corresponding author.

Human skin consists essentially of three tissue layers, the multi-layered epidermis, the underlying dermis containing a matrix of connective tissue woven from fibrous protein and the deep subcutaneous fatty layer. The outermost stratum of the epidermis, the stratum corneum or horny layer, is recognized as contributing the rate-limiting step in the barrier function of human skin to most drugs (Blank, 1953; Barry, 1983). This tissue typically consists of 10-15 layers of flattened, keratinized dead cells embedded in a lipid-rich matrix and may be about 10  $\mu\text{m}$  when dry but usually swells to several times this thickness when hydrated. The barrier properties of the stratum corneum are controlled by its composition: 75-80% proteins, 5-15% lipids and 5-10% unidentified material on a dry weight basis (Wilkes et al., 1973).

There has been considerable research effort devoted to improving the percutaneous penetration of drugs either for local therapeutic effect or for systemic therapy. One approach has been the use of penetration enhancers which are chemicals that can decrease reversibly the barrier properties of the stratum corneum. Dimethyl sulfoxide (DMSO) is a dipolar aprotic solvent with a wide range of physical and chemical properties to which its diverse physiological and pharmacological activities are attributable. It is the earliest and the most widely studied skin penetration enhancer. It has been found to improve the permeation of a wide range of ionic and non-ionic compounds of molecular weight below 3000 at concentrations exceeding 60% (Ritschel, 1969) and a product containing a 5% solution of the anti-viral agent idoxuridine in DMSO is available for clinical use. Tetracycline hydrochloride in DMSO is also commercially available for the treatment of *Acne vulgaris* and various other patents for dermatological formulations containing DMSO have been filed.

Several theories have been advanced to explain the mechanisms of action of DMSO enhancement of skin permeability including: extraction of skin lipids (Allenby et al., 1969; Embury and Dugard, 1971); denaturation of stratum corneum proteins (Elfbaum and Laden, 1968); formation of hydrogen-bonded complexes with

stratum corneum lipids (Al-Saidan et al., 1987); and the distortion and intercellular delamination of stratum corneum as a result of high osmotic stresses caused by transportation of both DMSO and water into the tissue from admixtures containing both solvents (Chandrasekaran et al., 1977). More recent studies suggest that DMSO exerts its rôle in enhancement of drug permeation by not only extracting soluble components of the horny structure but also by delaminating the horny layer and denaturing the proteins (Kurihara-Bergstrom et al., 1986, 1987). It has been proposed that part of the effects of DMSO arises from its solvent properties and thus, at high concentrations, it may promote partitioning of lipophilic drugs into the stratum corneum (Barry, 1987). Results of Fourier transform infrared (FTIR) spectroscopic investigations suggest that DMSO changes stratum corneum protein conformations (Oertel, 1977). Based on results of recent differential scanning calorimetric studies, it has been suggested that DMSO acts by displacing bound protein water, leaving a looser structure (Barry, 1987). Despite the wide ranging studies that have been performed with DMSO, its mechanisms of action as a penetration enhancer still remain unclear.

Fourier transform (FT) Raman spectroscopy has recently been used to characterize human skin (Williams et al., 1992). Wavenumber positions ( $\nu$ ,  $\text{cm}^{-1}$ ) of bands in a Raman spectrum depend on both the atomic masses and the force constant. Vibrations involving light atoms occur at higher frequency positions than those of heavy atoms; for example, the stretching vibration of  $\text{H}_2\text{O}$  is seen at approx.  $3400 \text{ cm}^{-1}$  while that of  $\text{D}_2\text{O}$  occurs at approx.  $2400 \text{ cm}^{-1}$ . The force constant is a measure of molecular bond stiffness. Tightly bound groups have stronger force constants and vibrations involving them appear at higher frequencies than those involving looser bound groups, so that, for example,  $\text{C}=\text{C}$  stretching modes occur at around  $1500 \text{ cm}^{-1}$  whereas  $\text{C}-\text{C}$  modes are seen at around  $1000 \text{ cm}^{-1}$ .

A comparison of several Raman spectroscopic techniques demonstrated minimal inter- and intra-cadaver variations in molecular vibrations

arising from human stratum corneum constituents (Williams et al., 1993). Recently, we have shown the versatility of the technique in studies of terpene penetration enhancer action on human skin (Anigbogu et al., 1993). Since Raman scattering by water is weak, the interference from water seen in infrared studies of hydrated human stratum corneum is minimized. In the study presented here, FT Raman spectroscopy was used to probe molecular interactions between aqueous solutions of DMSO and human stratum corneum constituents. The technique was also applied to studies of interactions between DMSO and water.

## 2. Materials and methods

### 2.1. Chemicals

Spectroscopic grade dimethyl sulfoxide (DMSO) was obtained from Sigma Chemical Co., Poole, UK with a stated purity of 99 + %. Deuterium-exchanged dimethyl sulfoxide ( $\text{DMSO-}d_6$ ) and deuterium oxide ( $\text{D}_2\text{O}$ ) were supplied by Aldrich Chemical Company, Gillingham, UK, both with stated purities of 99.9%. Bovine keratin powder was purchased from ICN Biomedicals, Inc., Ohio, U.S.A. The chemicals were used without further purification. Mixtures of DMSO or  $\text{DMSO-}d_6$  with deuterium oxide or distilled water were made ranging from 10 to 90% v/v in increments of 10% v/v.

### 2.2. Preparation of stratum corneum

Caucasian abdominal skin was obtained post mortem and stored in double-sealed evacuated polyethylene bags at  $-20^\circ\text{C}$  prior to use (Harrison et al., 1984). The samples used in this study were from eight donors, 54% female, and had a mean age of  $79 \pm 9$  (S.D.) years. Epidermal membranes were prepared by heat separation (Kligman and Christophers, 1963); excess subcutaneous fat and connective tissue were removed from the skin which was then immersed in water at  $60^\circ\text{C}$  for 45 s. The epidermal membrane was gently teased off and floated stratum corneum

side up overnight at  $22 \pm 1^\circ\text{C}$  on an aqueous solution of trypsin (0.0001% w/v) and sodium hydrogen carbonate (0.5% w/v). The digested epidermal remnants were removed by swabbing. The stratum corneum membranes were washed with distilled water, rinsed in cold acetone for 10 s to remove surface contaminants and then stored over silica gel in an evacuated desiccator until required.

The stratum corneum samples were hydrated to a water content of  $\geq 60\%$  w/dry weight over a saturated aqueous solution of sodium sulfate which provides a relative humidity of 97% at  $25^\circ\text{C}$ . The hydrated samples of whole stratum corneum were treated by complete immersion in the desired concentration of aqueous DMSO or  $\text{DMSO-}d_6$  for 1 h after which any excess enhancer was removed by blotting. All treatments were performed in triplicate.

### 2.3. Lipid extraction of stratum corneum and keratin powder

Sheets of human stratum corneum membranes prepared as described above were exhaustively delipidized by a modification of the protocol detailed by Roberts and Lillywhite (1983). The stratum corneum membranes were soaked at  $32^\circ\text{C}$  in (i) chloroform/methanol (2:1) for 24 h followed by (ii) soaking in acetone for 4 h and then (iii) hexane for 24 h followed by (iv) ethanol/diethyl ether (8:92) for 24 h. At all stages during the lipid extraction, the flasks containing the samples and the solvents were gently shaken to aid the extraction. The samples were evacuated to remove excess solvent. Lipid-extracted stratum corneum did not take up appreciable water by the method used in hydrating whole stratum corneum. Samples were therefore floated in water to hydrate before analysis. Bovine keratin powder was subjected to the same rigorous extraction process to ensure the removal of any lipid contaminants.

### 2.4. Fourier transform Raman spectroscopy

FT Raman spectra of aqueous solutions of DMSO,  $\text{DMSO-}d_6$ , untreated whole human stratum corneum, lipid-extracted stratum corneum

and DMSO- $d_6$ -treated whole stratum corneum were obtained using a Bruker FRA 106 FT Raman accessory mounted on an IFS 66-FTIR optical bench. Several Raman bands are common to molecules containing the same functional groups, termed 'characteristic frequencies', such as the C-H bands common to organic species. Therefore, to examine the C-H vibrational frequencies of stratum corneum constituents without interference from those of DMSO, fully deuterated DMSO was used. The atomic masses of the deuterated form are higher and thus the C-D bonds vibrate at lower frequencies than the C-H bonds and in a region where the skin is devoid of

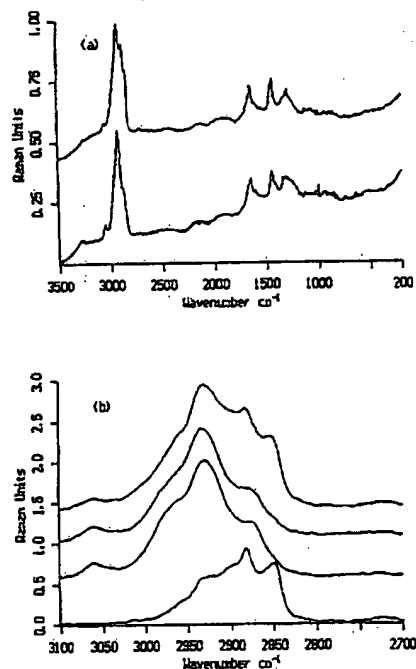


Fig. 1. FT Raman spectra of (a) hydrated whole stratum corneum (upper trace) and lipid-extracted human stratum corneum (bottom trace) over the wavenumber range 3500-200  $\text{cm}^{-1}$  and (b) whole stratum corneum (top trace), lipid-extracted stratum corneum, lipid-extracted keratin powder and lipid fraction of stratum corneum (bottom trace) over the 3500-2700  $\text{cm}^{-1}$  range.

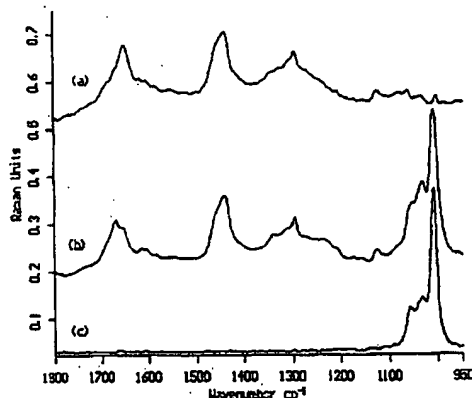


Fig. 2. FT Raman spectra of (a) untreated stratum corneum, (b) stratum corneum treated with DMSO- $d_6$  for 1 h and (c) pure DMSO- $d_6$ . The spectra clearly show the presence of dimethyl sulfoxide in the skin.

any vibrations, so allowing interference-free assessments of vibrational modes.

The liquid samples were presented in a 2  $\text{cm}^3$  quartz cuvette with a mirrored rear surface while the stratum corneum samples were presented in a stainless-steel cup of diameter approx. 2 mm to a near-infrared Nd:YAG laser operating at a wavelength of 1.064  $\mu\text{m}$  with an output power of 750 mW. The liquid samples were subjected to full laser power and typically 200 scans were collected at a resolution of 4  $\text{cm}^{-1}$ . The stratum corneum samples were, however, exposed to a laser power of approx. 450 mW to avoid fluorescence and sample degradation and the spectra represent an average of 4000 scans at a resolution of 4  $\text{cm}^{-1}$ . The FT Raman accessory is equipped with a liquid-nitrogen cooled germanium diode detector with an extended spectral bandwidth which covered the wavenumber range 3500-50  $\text{cm}^{-1}$ . Spectral response was corrected for white light and the observed band wavenumbers, calibrated against the internal laser frequency, were correct to better than  $\pm 1 \text{ cm}^{-1}$ .

## 2.5. Curve fitting

Opus data files generated on the Bruker FRA 106 FT Raman accessory were translated into



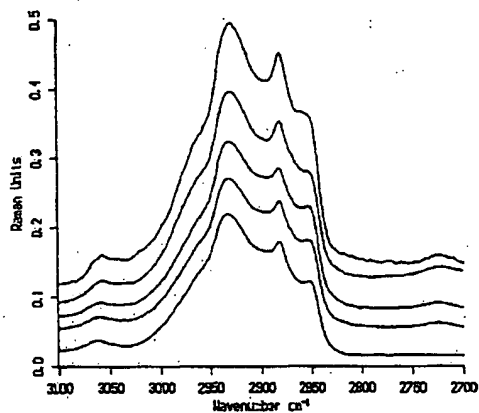


Fig. 3. FT Raman spectra of the CH stretching modes in untreated stratum corneum (bottom trace) and stratum corneum treated with 20, 40, 60% and pure DMSO- $d_6$  (top trace).

JCAMP files and curves were fitted using Lab Calc software (Galactic Industries Corp.). The program is flexible and allows the user a choice of parameters to input for the curve fitting. At the start, initial approximations were made about the number of bands present, their positions, widths and types (i.e., Gaussian, Lorentzian, log-normal or mixture). For the present study, the band type specification was a Gaussian/Lorentzian mixture. The program fitted a linear baseline to each spectrum and used the initial approximations and iteration to find a combination of the heights, positions, widths and areas that best fitted the data.

### 3. Results

All samples of stratum corneum used in this study were prepared by trypsin digestion of heat-separated epidermal membranes and all spectra were corrected for instrument response. Because of the natural variability that occurs in human skin, there were some minor differences in the wavenumber positions of some bands from sample to sample but the trends observed for each treatment were the same. The results presented

here are therefore representative and not the mean values from all replicates.

Fig. 1a shows typical FT Raman spectra of hydrated whole (untreated) and lipid-extracted human stratum corneum respectively over the wavenumber range 3500–200  $\text{cm}^{-1}$  and Fig. 1b illustrates spectra over the range 3500–2700  $\text{cm}^{-1}$  for whole (untreated), lipid extracted stratum corneum, lipid-extracted bovine keratin powder and the lipid fraction of stratum corneum obtained by subtracting the spectrum of the lipid extracted stratum corneum from that of whole (untreated) stratum corneum. There is a marked similarity between the spectrum of lipid-extracted stratum corneum and lipid-extracted bovine keratin powder.

Fig. 2 illustrates FT Raman spectra over the 1800–950  $\text{cm}^{-1}$  range of untreated stratum corneum, stratum corneum treated with pure deuterated DMSO, and pure deuterated DMSO. This figure shows that the DMSO is devoid of vibrational modes which would interfere with the amide I band ( $\text{C}=\text{O}$  stretching around 1650  $\text{cm}^{-1}$ ) in the stratum corneum. Fig. 3 details the C-H stretching region (3100–2700  $\text{cm}^{-1}$ ) of untreated stratum corneum and stratum corneum treated with different aqueous concentrations of

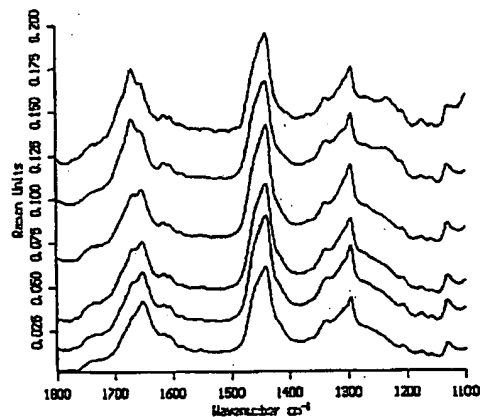


Fig. 4. FT Raman spectra over the wavenumber range 1800–1100  $\text{cm}^{-1}$  of untreated stratum corneum (bottom trace), and stratum corneum treated with 20, 40, 60, 80% and pure DMSO- $d_6$  (top trace).

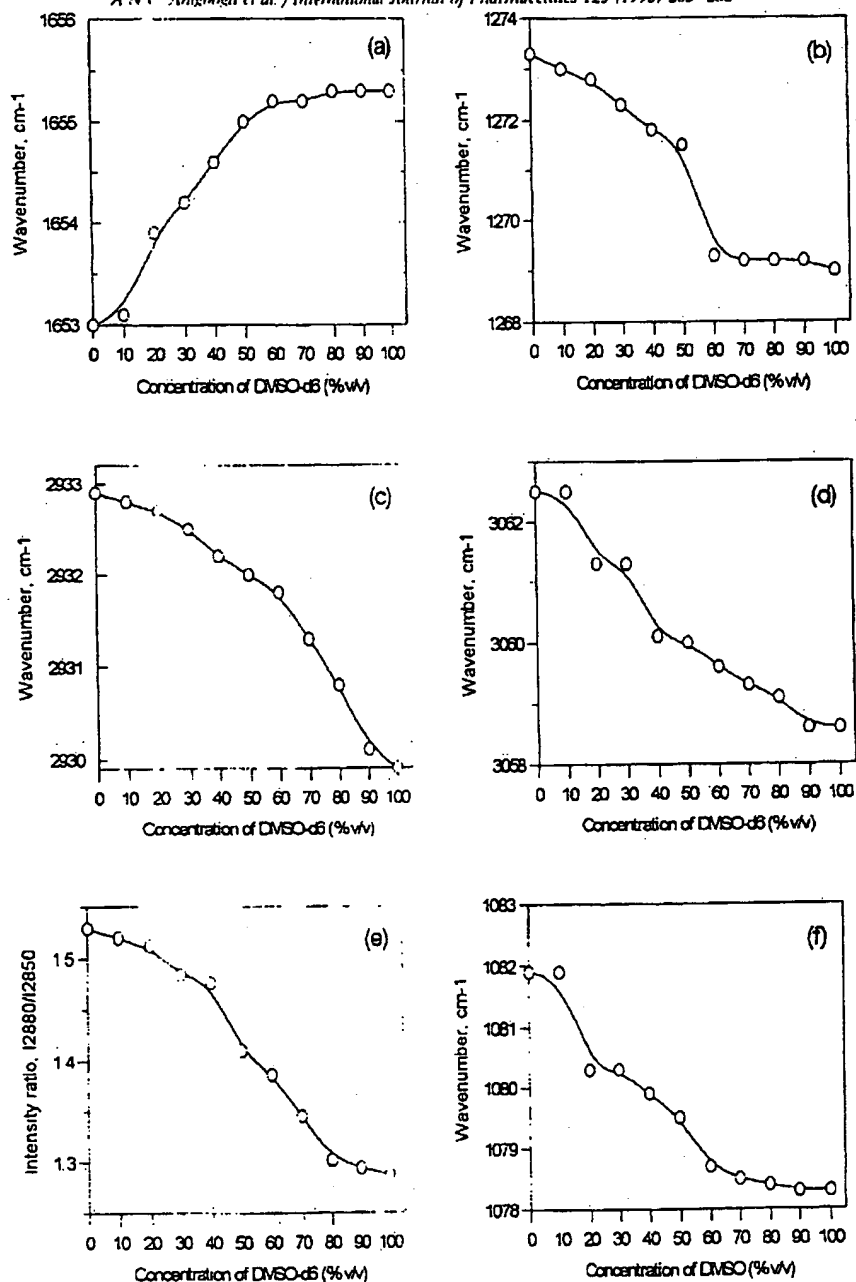


Fig. 5. Frequency and intensity ratio changes in stratum corneum as a function of aqueous DMSO- $d_6$  (a-e) and DMSO concentration (f): (a) amide I band of protein, (b) amide III band of protein, (c)  $\text{CH}_2$  symmetric stretching vibration of stratum corneum, (d) C-H (olefinic) stretching mode of stratum corneum, (e)  $I_{1280}/I_{1285}$  ratio of stratum corneum lipids, and (f) C-C skeletal stretch (random conformation) of stratum corneum lipids.

deuterium-exchanged DMSO ( $\text{DMSO-}d_6$ ). Fig. 4 provides FT Raman spectra in the 1800–1100  $\text{cm}^{-1}$  range of untreated stratum corneum and stratum corneum treated with various concentrations of aqueous deuterium-exchanged DMSO ranging from 20% v/v to pure. Fig. 5 shows graphs derived from Fig. 1–4.

Fig. 6 represents profiles obtained from curve fitting of the amide I band in whole and lipid-extracted human stratum corneum. Fig. 7a is a graph showing the proportions of Raman signal arising from the various vibrational modes of

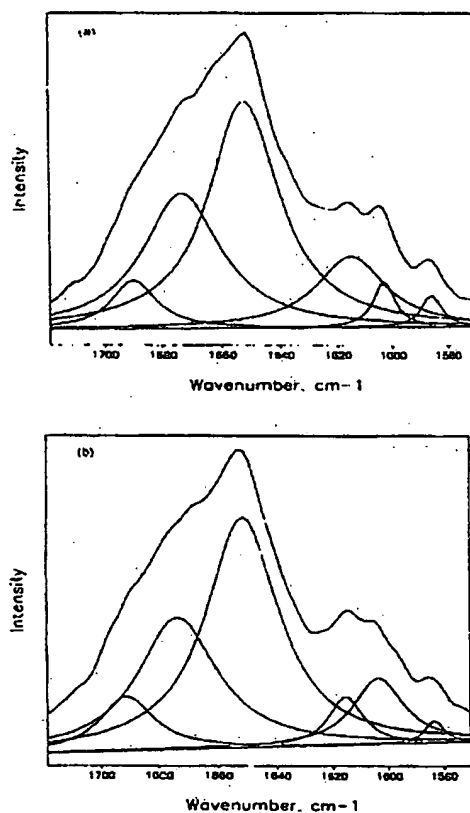


Fig. 6. Profiles obtained from curve-fitting the amide I band in (a) whole stratum corneum and (b) lipid-extracted stratum corneum.

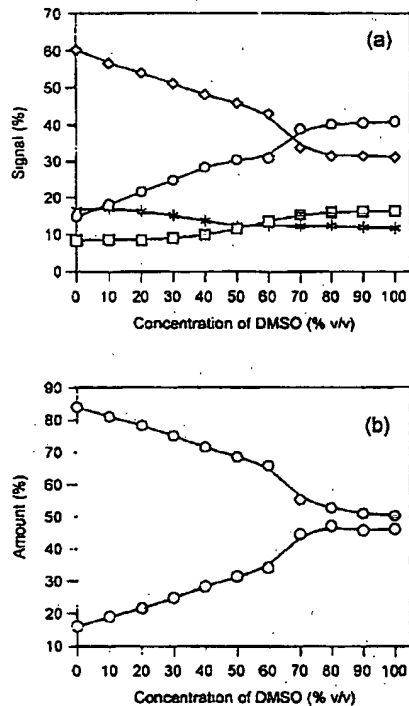


Fig. 7. (a) Changes in the Raman signal arising from the amide I mode of  $\alpha$ -helical keratin ( $\diamond$ ), the symmetrical parallel mode of anti-parallel  $\beta$ -pleated sheets ( $\circ$ ), the asymmetrical parallel mode of anti-parallel  $\beta$ -pleated sheets ( $\square$ ) and unidentified protein residues ( $*$ ), in human stratum corneum with different concentrations of aqueous DMSO. (b) Profile showing amount of  $\alpha$ -helical keratin ( $\diamond$ ) and  $\beta$ -pleated sheets ( $\circ$ ) in human stratum corneum at different concentrations of DMSO, expressed as the percentage of total amount,  $\alpha$ -helical +  $\beta$ -pleated keratin.

keratin at different DMSO concentrations. The graph shows an initial steady increase in the signal due to the symmetrical parallel amide I mode of the anti-parallel  $\beta$ -pleated sheets being formed up to 60% v/v DMSO with a sudden increase to 70% v/v DMSO. The signal from the asymmetrical parallel amide I mode of anti-parallel  $\beta$ -sheets was fairly constant between 0 and 40% v/v DMSO with a slight increase thereafter up to 70% v/v DMSO. In stratum corneum

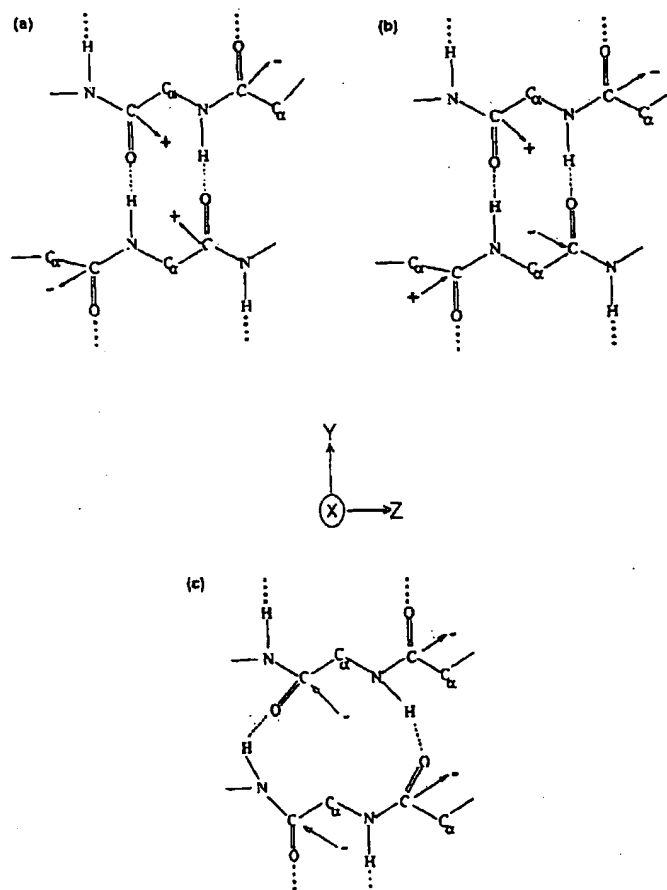


Fig. 8. A schematic illustration of the vibrational modes for (a) symmetrical parallel amide I mode of anti-parallel  $\beta$ -pleated sheets, (b) asymmetrical parallel amide I mode of anti-parallel  $\beta$ -pleated sheets and (c) perpendicular amide I mode of parallel  $\beta$ -pleated sheets observed in human stratum corneum (redrawn from Miyazawa, 1960).

treated with 80% v/v to pure DMSO, the signal was again fairly uniform. There was a slight but steady decrease in the signal arising from the unidentified protein residues between 0 and 60% v/v DMSO beyond which there was no appreciable further decrease in the signal. The amount (%) of  $\alpha$ -helical keratin and  $\beta$ -pleated sheets relative to one another with different concentra-

tions of aqueous DMSO are shown in Fig. 7b. With increasing concentrations of DMSO, the amount of  $\alpha$ -helix in the stratum corneum decreased while the amount of  $\beta$ -sheet structures increased.

Fig. 8 shows the actual vibrational modes of parallel and anti-parallel  $\beta$ -sheets redrawn from Miyazawa (1960).

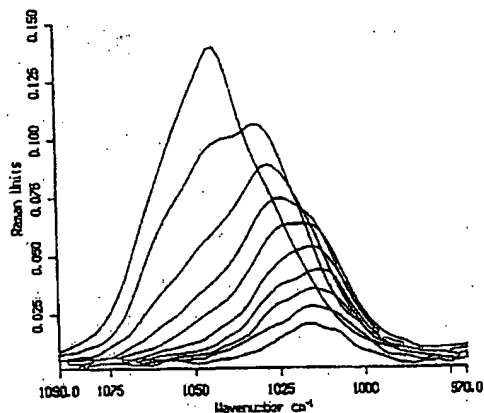


Fig. 9. FT Raman spectra of DMSO-water mixtures in the S=O stretching region of dimethyl sulfoxide in concentrations ranging from 10% v/v (bottom trace) to pure (top trace) in 10% v/v intervals.

Fig. 9 and 10 show spectra of DMSO-deuterium oxide mixtures in the S=O stretching and O-D stretching regions respectively.

#### 4. Discussion

Assignments of the bands in the spectra for human stratum corneum (Fig. 1a) consistent with the observed Raman active vibrational modes have been made (Barry et al., 1992), and the main features are summarized in Table 1.

Of particular importance to this study are the CH stretching modes in the 3100–2700  $\text{cm}^{-1}$  region; the C=O stretching mode at about 1650  $\text{cm}^{-1}$  (amide I band) arising predominantly from the  $\alpha$ -keratin in the stratum corneum corneocytes; the band at about 1274  $\text{cm}^{-1}$  assigned as the CN stretching and NH deformation of protein (amide III band) and weaker bands at about 1030, 1062, 1082 and 1126  $\text{cm}^{-1}$  assigned as C-C stretching modes which yield information about skeletal structures in a molecule. These bands (1030–1126  $\text{cm}^{-1}$ ) have been used to assess lipid bilayer packing in model membrane systems (Carey, 1982). The amide I and III bands have been shown to arise from 'in-plane' vibrations of

the peptide bond -CONH- [24] and differences in position, dichroism and intensity of these bands have been used extensively in conformational analysis of proteins (Carey, 1982; Hudson and Mayne, 1987).

The bands in the C-H stretching region, 3100–2700  $\text{cm}^{-1}$ , are clearly complex and contain overlapping vibrational modes. In previous literature reports detailing infrared spectroscopic investigations of human stratum corneum (Golden et al., 1986; Knutson et al., 1986; Krill et al., 1992), it had been assumed that the intercellular lipids were the major contributors to all the bands arising from the C-H groups. To investigate this assumption, we extensively extracted the lipids, adopting a protocol that would ensure the removal of most of the different classes of lipids found in the stratum corneum, rather than just applying chloroform-methanol (2:1) as usually used for lipid extraction. Even though some covalently bound lipids in the stratum corneum may not be removed, our method of extraction ensured that most of the lipids were removed and this process was usually complete within 72 h. Extension of the time period for lipid extraction to 168 h did not remove further lipids as shown by Raman spectroscopy.

Our results show that following extensive lipid extraction, the C-H olefinic stretching mode for stratum corneum at about 3060  $\text{cm}^{-1}$  remained invariant suggesting that it mostly derives from the keratin, while the C-H aliphatic stretching mode at about 2725  $\text{cm}^{-1}$  was entirely removed, indicating it arises essentially from the intercellular lipids. The band at about 2852  $\text{cm}^{-1}$  assigned as a  $\text{CH}_2$  symmetric stretching mode, is not present in the spectrum of the extracted stratum corneum, suggesting that this band arises mostly from intercellular lipids. The band at about 2883  $\text{cm}^{-1}$ , assigned as a  $\text{CH}_2$  asymmetric stretching mode is markedly reduced in intensity but a fraction of this band remains, indicating that it is mainly due to the intercellular lipids but may have a contribution from the keratin. The band at about 2931  $\text{cm}^{-1}$  which has been assigned as a  $\text{CH}_3$  symmetric stretching mode is however only slightly reduced in intensity suggesting that most of the vibrations responsible for this band arise

Table 1  
FT Raman spectral assignments of the main vibrational modes for human stratum corneum

Wavenumber (cm <sup>-1</sup> ) <sup>a</sup>	Assignments and approximate description of vibrational modes <sup>b</sup>
3060w	$\nu(\text{CH})$ olefinic
2958m, sh	$\nu(\text{CH}_2)$ Asym
2931s	$\nu(\text{CH}_2)$ Sym
2883m	$\nu(\text{CH}_2)$ Asym
2852m	$\nu(\text{CH}_2)$ Sym
1652s	$\nu(\text{C}=\text{O})$ amide I ( $\alpha$ -helix)
1585w	$\nu(\text{C}=\text{C})$ olefinic
1552w	$\delta(\text{NH})$ and $\nu(\text{CN})$ amide II
1438s	$\delta(\text{CH}_2)$ scissoring
1296m	$\delta(\text{CH}_2)$
1274m	$\nu(\text{CN})$ and $\delta(\text{NH})$ amide III ( $\alpha$ -helix)
1244w, sh	$\delta(\text{CH}_2)$ wagging; $\delta(\text{CN})$ amide III, disorder
1172w	$\nu(\text{CC})$
1126mw	$\nu(\text{CC})$ skeletal, <i>trans</i> conformation
1082mw	$\nu(\text{CC})$ skeletal, random conformation
1062mw	$\nu(\text{CC})$ skeletal, <i>trans</i> conformation
1031mw	$\nu(\text{CC})$ skeletal, <i>cis</i> conformation
1002m	$\nu(\text{CC})$ aromatic ring
644w	$\nu(\text{CS})$
623w	$\nu(\text{CS})$

Data are wavenumber positions of bands in a representative spectrum resulting from 4000 scans at a resolution of 4 cm<sup>-1</sup>. Asym, asymmetric; Sym, symmetric. Abstracted from Barry et al. (1992).

<sup>a</sup> s, strong; m, medium; w, weak; sh, shoulder.

<sup>b</sup>  $\nu$ , stretch;  $\delta$ , deformation.

from the keratin component of the stratum corneum with a minor contribution from the lipids.

Similarly, of the four C-C skeletal stretching modes in the spectrum of stratum corneum, the one found at about 1031 cm<sup>-1</sup> remained prominent after lipid extraction, suggesting it is derived from keratin, while the other three at about 1062, 1082 and 1126, cm<sup>-1</sup> were markedly reduced, indicating they arise mainly from the intercellular lipid alkyl chains.

All the changes discussed above are summarized in Table 2. The spectrum of the resultant extracted stratum corneum we obtained is in fact markedly similar to the spectrum of commercially available keratin powder (Fig. 1b) which we also subjected to extensive solvent extraction to remove lipid contaminants.

Even though stratum corneum lipids contain very long chain (C<sub>24</sub>-C<sub>35</sub>) saturated ceramides as well as long chain acids, cholesterol esters, triglycerides and hydrocarbons, an examination of the amino acid composition of the stratum corneum keratin shows that at least between 65 and 75% of the amino acid residues found in the stratum corneum have aliphatic side chains (Crounse, 1963; Baden and Bonar, 1968; Wood and Blandon, 1985; Krill et al., 1992). If we consider that the stratum corneum, in addition to

Table 2  
FT Raman spectral assignments for some vibrational modes in human stratum corneum deduced following extensive lipid-extraction

Wavenumber (cm <sup>-1</sup> ) <sup>a</sup>	Assignments and approximate description of vibrational modes <sup>b</sup>	Origin of vibration
3060w	$\nu(\text{CH})$ olefinic	predominantly protein
2931s	$\nu(\text{CH}_2)$ Sym	mostly protein but with significant lipid contribution
2883m	$\nu(\text{CH}_2)$ Asym	mostly lipids with minor protein contribution
2852m	$\nu(\text{CH}_2)$ Sym	essentially lipids
2725w	$\nu(\text{CH})$ aliphatic	essentially lipids
1126mw	$\nu(\text{CC})$ skeletal, <i>trans</i> conformation	mainly lipid with minor protein contribution
1082mw	$\nu(\text{CC})$ skeletal, random conformation	mainly lipid with minor protein contribution
1062mw	$\nu(\text{CC})$ skeletal, <i>trans</i> conformation	mainly lipid with minor protein contribution
1031mw	$\nu(\text{CC})$ skeletal, <i>cis</i> conformation	mostly protein with small lipid contribution

Samples were exhaustively delipidized as described in section 2. Data are wavenumber positions of C-H and C-C vibrational modes from representative spectra of 4000 scans obtained at resolution of 4 cm<sup>-1</sup>.

<sup>a</sup> s, strong; m, medium; w, weak; sh, shoulder.

<sup>b</sup>  $\nu$ , stretch; Asym, asymmetric; Sym, symmetric.

Table 3  
FT Raman spectral assignments of the main vibrational modes for dimethyl sulfoxide (DMSO) and deuterium exchanged dimethyl sulfoxide (DMSO- $d_6$ )

Wavenumber (cm <sup>-1</sup> ) <sup>a</sup>	DMSO- $d_6$	Assignments and approximate description of vibrational modes <sup>b</sup>
2997s		$\nu(\text{CH}_3)$ Asym.
2914vs		$\nu(\text{CH})$ Sym.
2891w sh		$\nu(\text{CH}_3)$ Sym.
	2249s	$\nu(\text{CD}_3)$ Asym.
	2125vs	$\nu(\text{CD})$ Sym.
	1996w	$\nu(\text{CD}_2)$ Sym.
1420m		$\delta(\text{CH})$
1310w		$\delta(\text{CH}_2\text{-S})$ Sym.
	1057m sh	$\delta(\text{CH})$ degenerate
	1032m sh	
1044m		$\nu(\text{S}=\text{O})$
	1008s	$\nu(\text{S}=\text{O})$
955w		$\delta(\text{CH}_3)$ rock
	821vw	$\delta(\text{CH}_2)$ rock
	761m	$\delta(\text{CH}_2)$ rock
6700s		$\nu(\text{C-S-C})$ Asym.
670s		$\nu(\text{C-S-C})$ Sym.
	614vs	$\nu(\text{CS})$ Asym.
384m		$\delta(\text{C-S}=\text{O})$
335s	341m	$\delta(\text{C-S}=\text{O})$
308m	308s	$\delta(\text{C-S-C})$
	264ms	$\delta(\text{C-S-C})$

Asym., asymmetric; Sym., symmetric. Samples of DMSO and DMSO- $d_6$  were presented in a 2 cm<sup>3</sup> quartz cuvette to a near-infrared Nd:YAG laser. Data represent wavenumber positions of bands in spectra generated from 200 scans at a resolution of 4 cm<sup>-1</sup>.

<sup>a</sup> v, very; s, strong; m, medium; w, weak; sh, shoulder.

<sup>b</sup>  $\nu$ , stretch;  $\delta$ , deformation.

some unidentified material, consists mainly of proteins (75–80%) and lipids (5–15%), a large contribution from the proteins to the vibrations in the C-H regions is to be expected.

DMSO possesses several distinctive and characteristic bands and assignments for the observed Raman active vibrational modes of non-deuterated and deuterium-exchanged DMSO are in Table 3. Of particular interest are the bands in the 1050–1000 cm<sup>-1</sup> region assigned as S=O stretching modes. The appearance of these bands in the spectrum of stratum corneum following a 1 h treatment indicates the presence of DMSO in

the tissue. In the 1700–1250 cm<sup>-1</sup> region where the amide I and III bands occur in the stratum corneum, DMSO is devoid of any vibrations and hence changes observed in the stratum corneum spectra after treatment with DMSO must arise from changes in the molecular environment of the amide bonds and are not due to interference from DMSO bands.

Contrary to the conclusions of a recent X-ray diffraction study by Garson et al. (1991) which indicated that human stratum corneum keratin was mainly in the  $\beta$  form, FT Raman vibrations recorded for human stratum corneum show that the proteins exist predominantly in the  $\alpha$ -helix conformation as indicated by the positions of the amide I and III bands at about 1650 and 1274 cm<sup>-1</sup>, respectively (Barry et al., 1992). The solvents used in our study for lipid extraction did not change protein conformation as the amide I band in the extracted stratum corneum was also at about 1650 cm<sup>-1</sup>.

At low applied concentrations of DMSO (around 20% v/v), there were minor yet real changes in spectral features arising from C-H stretching modes of stratum corneum (Fig. 3). Deuterated DMSO was used for this investigation and the CD modes were clearly separated from the CH vibrational modes of stratum corneum. The bands at about 2881 and 2850 cm<sup>-1</sup> in untreated stratum corneum are asymmetric and become more asymmetrical in stratum corneum treated with various concentrations of DMSO. Generally, all the bands in the 3100–2700 cm<sup>-1</sup> region broaden in stratum corneum treated with DMSO.

Fig. 4 is a comparison of the FT Raman spectra over the 1800–1100 cm<sup>-1</sup> wavenumber range of untreated stratum corneum and stratum corneum treated with various concentrations of DMSO. Compared with an untreated sample, following application of increasing concentrations of DMSO, the amide I band shifts significantly and reproducibly by about 2 cm<sup>-1</sup> to higher wavenumbers (Fig. 5a). There was a small but steady shift in the position of the amide I band to higher wavenumbers from 10 to 60% v/v DMSO. From 70% v/v to pure DMSO there was no appreciable shift in the position of this band as

shown by the plateau in the graph. The intensity of the amide I band relative to the neighbouring  $\text{CH}_2$  scissoring mode decreases markedly with the appearance of a new band at about  $1673\text{ cm}^{-1}$ . The amide III band shifts to a lower wavenumber by about  $4\text{ cm}^{-1}$  from approx.  $1273\text{ cm}^{-1}$  to approx.  $1269\text{ cm}^{-1}$  (Fig. 5b). This shift was gradual from 10 to 50% v/v DMSO with a sudden increase in the magnitude of shift at 60% v/v DMSO as seen from the change in the slope of the graph. Thereafter, there was no further appreciable shift in the position of the amide III band. These changes are consistent with conversion of the protein from an  $\alpha$ -helical conformation to  $\beta$ -pleated sheets that has been observed in other natural proteins and synthetic polypeptides (Tu, 1982). These changes were observed with concentrations of DMSO as low as 20% v/v. Treatment with increasing concentrations of DMSO produced increasing amounts of  $\beta$ -pleated sheet form relative to  $\alpha$ -helix, and with pure DMSO, the intensity of the  $\beta$ -pleated sheet form predominated.

In the absence of calibration data for proteins with known  $\alpha$ -helical and  $\beta$ -sheet composition, we employed curve-fitting for the first time, to separate the bands in the amide I region of untreated stratum corneum and stratum corneum treated with various concentrations of aqueous DMSO in order to determine semi-quantitatively the proportions of  $\alpha$ -helical and  $\beta$ -sheet proteins present in stratum corneum before and after treatment. Although curve fitting has limitations, with careful choice and use of parameters, overlapping bands found in heterogeneous systems such as human skin can be effectively and correctly separated (Maddams, 1980). In the work reported here, for all the bands curve-fitted, the statistical goodness of fit was better than 99.9% but visual inspection was still employed as suggested by Maddams (1980).

Using X-ray diffractometry to study changes in palmar cuttings caused by heat, Baden et al. (1973) reported that in addition to a predominantly  $\alpha$ -helical content, epidermis and stratum corneum contains 5-10% anti-parallel  $\beta$ -sheet and that parallel  $\beta$ -sheets (initial concentration not stated), formed as a result of heat-induced

conformational changes in the  $\alpha$ -helices. The profiles in Fig. 6a and b show the experimentally generated Raman spectra from human stratum corneum (top traces) with the derived composites from curve fitting underlying each. These profiles resulting from curve fitting of our spectra show that the observed amide I band in human stratum corneum following mild heat separation is a composite of three bands at about  $1650$ ,  $1670$  and  $1695\text{ cm}^{-1}$  attributed to  $\alpha$ -helices, the symmetrical parallel Amide I mode of anti-parallel  $\beta$ -pleated sheets and the asymmetrical parallel amide I mode of anti-parallel  $\beta$ -pleated sheets respectively (Walton and Blackwell, 1973; Tu, 1986). Anti-parallel  $\beta$ -pleated sheets actually have four Raman-active vibrational modes of which the symmetrical parallel amide I mode of anti-parallel  $\beta$ -pleated sheets, at about  $1670\text{ cm}^{-1}$ , is the strongest and most easily observable. The other three modes are usually much weaker and may in fact not be detectable. From the profiles in Fig. 6a we were also able to detect the asymmetrical parallel amide I mode of anti-parallel  $\beta$ -pleated sheets at about  $1695\text{ cm}^{-1}$ . The remaining two, symmetrical and asymmetrical perpendicular amide I vibrational modes of the anti-parallel  $\beta$ -pleated sheets, were not detectable in the spectra of human stratum corneum before and after treatment with DMSO. The bands at about  $1585$ ,  $1606$  and  $1618\text{ cm}^{-1}$  are presumed to arise from unidentified protein residues.

From the areas under the bands, we calculated the proportion of the Raman signal in untreated stratum corneum arising from  $\alpha$ -helical keratin to be approx.  $60 \pm 9\%$ , from the symmetrical parallel amide I mode of anti-parallel  $\beta$ -pleated sheets to be approx.  $15 \pm 3\%$ , and from the asymmetrical parallel amide I mode of anti-parallel  $\beta$ -pleated sheets to be approx.  $8 \pm 2\%$ ; approx.  $17 \pm 4\%$  was from unidentified protein residues [(S.E.),  $n = 4$ ]. These results are presented graphically in Fig. 7a. Anti-parallel  $\beta$ -pleated sheet in human stratum corneum gives rise to two vibrational amide I modes at approx.  $1670$  and  $1695\text{ cm}^{-1}$  whereas there is a single amide I mode at about  $1652\text{ cm}^{-1}$  arising from the  $\alpha$ -helical keratin. To confirm that the two observed modes of



anti-parallel  $\beta$ -pleated sheets are indeed due to the same species, we calculated the ratio of the areas of symmetrical/asymmetrical parallel amide I modes of anti-parallel  $\beta$ -sheets in stratum corneum treated with different concentrations of DMSO. If the two modes arise from different molecular species, we would expect a trend in the ratios, either increasing or decreasing with increasing concentrations of DMSO. Regression analysis, however, showed no correlation between DMSO concentration and symmetrical/asymmetrical  $\beta$ -keratin ratio ( $r = 0.065$ ); the mean ratio was  $2.53 \pm 0.21$ . This is strong evidence that the two modes (symmetrical and asymmetrical) arise from a single  $\beta$ -keratin molecule.

In order to estimate the relative proportion of  $\beta$ -keratin to  $\alpha$ -helical keratin in the stratum corneum, we averaged the areas under the two modes arising from anti-parallel  $\beta$ -keratin. This average value was then added to the area of the  $\alpha$ -helical band to obtain the total area of  $\alpha$ -helical and anti-parallel  $\beta$ -sheet keratin produced following treatment with different concentrations of DMSO. To calculate the amounts of  $\alpha$ -helical keratin and  $\beta$ -pleated sheets present in stratum corneum from the areas under the bands, we assumed a linear relationship between amount and the signal arising from various modes of the two conformations following treatment with DMSO. The amount of each type of conformation was then obtained as percent fraction of the total.

The amounts of  $\alpha$ -helical and anti-parallel  $\beta$ -pleated sheet keratin relative to one another in the stratum corneum at different DMSO concentrations are shown in Fig. 7b, expressed as a percentage of  $\alpha$ -helical plus  $\beta$ -pleated keratin. On first observation, the amount of  $\beta$ -pleated sheets so calculated in untreated stratum corneum (approx. 16%) as detected by Raman spectroscopy coupled with curve fitting appeared somewhat higher than the previously reported amounts of 5-10% (Baden et al., 1973). To assess if this high proportion arises as an artefact from our method of preparation of stratum corneum (trypsinizing epidermal membranes previously heat-separated at 60°C), we also collected Raman spectra from samples of stratum corneum pre-

pared by scraping abdominal skin thus avoiding such treatment. Following curve fitting and calculation of the areas under the bands, similar levels of symmetrical parallel amide I mode of anti-parallel  $\beta$ -pleated sheets and asymmetrical parallel amide I mode of anti-parallel  $\beta$ -pleated sheets and  $\alpha$ -helical keratin were found in stratum corneum scrapings as in heat-separated stratum corneum. This suggests that the temperature we used for our sample preparation together with the extremely mild trypsinization procedure did not change stratum corneum proteins from  $\alpha$ -helices to  $\beta$ -sheets.

The amide I band arises predominantly (about 80%) from C=O stretching vibrations of the CONH group and to determine if C=O vibrations from the fatty acids were contributing significantly to this band we also curve-fitted the amide I band in lipid-extracted stratum corneum. Similar profiles (Fig. 6b) and values were obtained as for whole stratum corneum suggesting that indeed there are more  $\beta$ -pleated sheets in stratum corneum than have previously been reported (Baden et al., 1973).

Following treatment with increasing concentrations of DMSO solutions, the signals arising from symmetrical parallel amide I mode of anti-parallel  $\beta$ -pleated sheets and asymmetrical parallel amide I mode of anti-parallel  $\beta$ -pleated sheets increased while the signal from the  $\alpha$ -helical keratin decreased (Fig. 7a). There was initially a small but steady increase in the amounts of anti-parallel  $\beta$ -pleated sheets formed up to 60% v/v DMSO. Then there was an abrupt increase in the amount of anti-parallel  $\beta$ -pleated sheets as shown by the change in the slope of the graph in Fig. 7b; beyond 70% v/v the amount formed was essentially constant. With pure DMSO, the amount of anti-parallel  $\beta$ -pleated sheets structures in the stratum corneum was approx. 46% (Fig. 7b).

The band attributed to the perpendicular amide I mode of the parallel  $\beta$ -pleated sheets at about  $1632 \text{ cm}^{-1}$  appeared for the first time in the Raman spectrum of stratum corneum treated with 90% v/v aqueous DMSO. The area of the parallel  $\beta$ -pleated sheets formed, was added to that of  $\alpha$ -helical keratin and anti-parallel  $\beta$ -pleated sheets and the amount calculated as per-

cent fraction of the total. The amount of parallel  $\beta$ -pleated sheets represents about 3% of the total  $\alpha$ -helical and  $\beta$ -sheet structures in human stratum corneum. Similar amounts were produced by pure DMSO. The parallel amide I mode of the parallel  $\beta$ -pleated sheets at about  $1645\text{ cm}^{-1}$  was not observed. The band at about  $1652\text{ cm}^{-1}$  arising from the  $\alpha$ -helical keratin was however, still present at approx. 51% showing that the conversion to  $\beta$ -sheets was not complete even with pure DMSO.

The vibrational modes of the parallel and anti-parallel  $\beta$ -sheets discussed above are shown in Fig. 8. In anti-parallel  $\beta$ -sheets, each unit cell contains four peptide groups arising from two adjacent chains. Adjacent chains can move in phase or out of phase. Specifically, in the symmetrical parallel amide I mode of anti-parallel  $\beta$ -sheets at approx.  $1670\text{ cm}^{-1}$ , adjacent peptide groups move in phase. Similarly, adjacent groups in the asymmetrical parallel amide I mode of anti-parallel  $\beta$ -sheets at approx.  $1695\text{ cm}^{-1}$  also move in phase. Adjacent groups across interchain hydrogen bonds in the perpendicular amide I mode of parallel  $\beta$ -pleated sheets move out of phase. The plus and minus signs represent the  $x$  components of the transition moments of the peptide groups pointing upward and downward, respectively, in the plane of the paper.

The changes outlined above suggest that DMSO, in addition to altering the protein conformation, also affects the intercellular lipids in stratum corneum. The lipids in the stratum corneum are arranged in a multiply bilayered structure. At physiological temperatures and in their unperturbed state, stratum corneum lipids exist in various phases; crystalline, gel and liquid crystalline forms with the gel phase predominating (White et al., 1988). In the gel phase, lipid backbone C-C bonds are arranged in a zig-zag manner such that the alkyl chains are maximally extended, affording close packing. This is the all-*trans* structure which has the lowest energy and lateral motion is highly restricted (Lee, 1975). With thermal or chemical perturbation, *trans* conformers convert to *gauche* conformers along the alkyl chains. The energy associated with the structure is higher and the carbon atoms are less

rigidly held together and thus C-C single bonds along the alkyl chains vibrate with a greater degree of motional freedom. This increasing mobility along the alkyl chain is associated with a decrease in the microviscosity of the hydrocarbon region of the lipid bilayer. The lipids are thus thought to exist in a more fluid-like state and this is termed the liquid crystalline phase.

The force constants of the C-C bonds in *trans* and *gauche* conformations are different and as such the stretching vibrations occur at different frequencies. It has been shown that C-H stretching vibrations are sensitive to changes in their environment and are thus significantly affected by changes in the conformation of the adjoining C-C bonds (Snyder et al., 1982; Casal and Mantsch, 1984). Changes observed in the frequencies of the C-H vibrations are therefore an indirect measure of structural changes in the lipids. Shifts to lower wavenumbers of up to  $3\text{ cm}^{-1}$  in the frequency of the  $\text{CH}_3$  symmetric stretching vibration of stratum corneum (from approx.  $2933\text{ cm}^{-1}$  to approx.  $2930\text{ cm}^{-1}$ ) were observed after treatment with different concentrations of DMSO (Fig. 3). As mentioned earlier, there are contributions from both the lipids and proteins to this vibrational mode and these changes observed following treatment with DMSO may be indicative of interactions between DMSO and stratum corneum lipids and proteins (Fig. 5c shows a graphical representation of these shifts). The C-H olefinic stretching mode, mainly due to stratum corneum keratin, also shifted by  $4\text{ cm}^{-1}$  to lower frequencies from approx.  $3062\text{ cm}^{-1}$  to approx.  $3058\text{ cm}^{-1}$  over the range 0-100% DMSO (Fig. 5d).

The intensity ratio ( $I_{2880}/I_{2850}$ ) of the peak heights of the bands at about  $2880$  and  $2850\text{ cm}^{-1}$ , corresponding to the C-H asymmetric and symmetric stretching frequencies of the methylene groups arising mainly from the lipids, has been used to study the structure and phase transitions of the hydrocarbons in model phospholipid membranes such as dipalmitoyl phosphatidylcholine (DPPC) and polymethylene chains (Gaber and Peticolas, 1977; Snyder et al., 1978). The  $I_{2880}/I_{2850}$  ratio measures both lateral packing in the extended chains of the lipid bilayer and conformational order/disorder seen in gel and

liquid crystalline phases. A broad asymmetric band underlies the  $\text{CH}_2$  asymmetric stretching mode at approx.  $2880\text{ cm}^{-1}$  (Snyder et al., 1978). This broad band is involved in Fermi resonance interaction with the first overtone of a methylene bending mode at approx.  $1440\text{ cm}^{-1}$  and contributes to the intensity of the  $2880\text{ cm}^{-1}$  band. When the population of *gauche* conformers in the lipid bilayers of the stratum corneum increases following treatment with  $\text{DMSO-d}_6$ , the chain symmetry disappears and with it the resonance condition ceases. The contribution from the first overtone of the  $1440\text{ cm}^{-1}$  band disappears and therefore, the relative intensity of the  $2880\text{ cm}^{-1}$  band decreases, whereas the  $2850\text{ cm}^{-1}$  is not affected with its intensity remaining essentially constant. Consequently, the intensity ratio ( $I_{2880}/I_{2850}$ ) decreases with an increase in the number of *gauche* conformers in the system. Fig. 5e shows a plot of the  $I_{2880}/I_{2850}$  ratio of stratum corneum as a function of DMSO concentration. Although the magnitude of this change is less than that obtained for thermally induced conformational changes in DPPC (Brown et al., 1973; Litman et al., 1991), it is reproducible and does suggest the production of intramolecular chain disorder arising from *trans-gauche* isomerization of the lipid alkyl chains within the bilayer. There was initially a small decrease in the intensity ratio from the untreated control to stratum corneum treated with 40% v/v DMSO. This was followed by a more rapid decrease between 40 and 80% v/v DMSO after which the rate of change fell.

Further evidence for this disorder is seen in the changes in the C-C skeletal stretching region, whereby the alkyl C-C backbone yields information about membrane structure and fluidity. The  $1062$  and  $1126\text{ cm}^{-1}$  bands arise from the *trans* conformation of the C-C stretch while the  $1082\text{ cm}^{-1}$  band is thought to be mainly due to the *gauche* conformation of the C-C stretch. Deuterated DMSO, however, also has bands in the  $1000\text{--}1050\text{ cm}^{-1}$  region and to study changes in the C-C modes of the skin, aqueous solutions of non-deuterated DMSO were therefore used. With increasing concentrations of DMSO, the intensi-

ties of the  $1126$  and  $1062\text{ cm}^{-1}$  bands greatly diminish, consistent with fewer *trans* conformers, whereas the  $1082\text{ cm}^{-1}$  band broadens, increases in intensity and shifts to lower frequencies by up to  $7\text{ cm}^{-1}$  (Fig. 5f) consistent with a greater number of *gauche* conformers. These results are in good agreement with those obtained for chloroform-induced disordering of DPPC chains (Gaber and Peticolas, 1977). It is observed, however, that the changes in the C-C skeletal band at  $1082\text{ cm}^{-1}$  occurred between 0 and 60% v/v DMSO after which there was no further appreciable change. It may well be that since this band arises mainly from *gauche* conformers of the lipids, the maximum fluidity attained by stratum corneum lipids denoted by changes in this band were achieved at 60% v/v DMSO and hence no further shift in the frequency of this band at higher DMSO concentrations. In a previous FTIR study of the effect of DMSO on stratum corneum constituents, Oertel (1977) was unable to show these changes in the alkyl backbone region of the lipids because vibrational features below  $1300\text{ cm}^{-1}$  in the infrared spectrum of stratum corneum are usually very weak and poorly resolved.

Overall, the results from this study show a concentration-dependence in the action of DMSO on stratum corneum lipids and proteins and correlates with data from earlier DSC studies (Barry, 1987).

DMSO is a powerful dipolar aprotic solvent which forms an association complex with water at a concentration of about 67% v/v DMSO through dipole-dipole interactions and through hydrogen bonding interactions which are stronger than those formed between water molecules (Cowie and Toporowski, 1961). Figs. 9 and 10 illustrate changes in the S=O stretching mode of DMSO and the O-D bands of  $\text{D}_2\text{O}$ , respectively. The S=O stretching Raman band in pure DMSO occurs at about  $1045\text{ cm}^{-1}$ . With increasing amounts of water, the position of this band gradually shifts to lower frequencies until, in the 10% v/v aqueous solution, it occurs at approx.  $1014\text{ cm}^{-1}$ . There were also changes in the O-D bands of water when present with different proportions

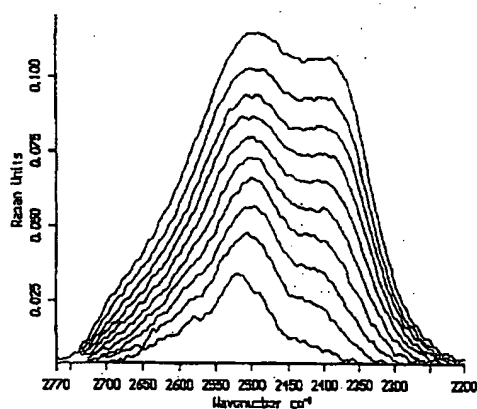


Fig. 10. FT Raman spectra of DMSO-water mixtures in the O-D stretching region of deuterium oxide in concentrations ranging from 10% v/v (bottom trace) to pure (top trace) at intervals of 10% v/v.

of DMSO. Both of these phenomena correlate with results from other studies (Scherer et al., 1973; Bertoluzza et al., 1979).

The nature of DMSO-water binary mixtures has been the subject of many investigations and it is generally agreed that at high concentrations, DMSO breaks up the structure of water. It is likely that the structural effects of DMSO on water present in biological systems can help explain its various biological properties. The obvious site for such interactions in the skin is at the polar head group regions of the lipids, and with keratin where water is present. It is worth noting that in the skin, similar shifts were observed in the S=O stretching mode of DMSO as those observed when it was mixed with water. Results from small angle X-ray scattering (SAXS) studies have shown that the repeat distance between lipid lamellae found in untreated human stratum corneum remained unchanged upon treatment with water, indicating that no swelling between the lipid bilayers occurred and therefore water did not intercalate between the bilayers (Bouwstra et al., 1991). This implies that water in extensively hydrated skin is mainly associated with the keratin component of the corneocytes. In the native

form, the conformational integrity of a protein is dependent upon bound water which forms a hydration sheath. DMSO may substitute or displace this bound water and in so doing alter the protein conformation as observed in the present study.

However, these protein structural changes cannot fully explain the actions of DMSO as at concentrations similar to those at which it is known to enhance drug flux, DMSO was shown to affect stratum corneum lipids and the intercellular domain is presumed to be the main site of the resistance to solute transport for most drugs. In addition, DMSO may promote the partitioning of lipophilic drugs into the stratum corneum.

In conclusion, therefore, DMSO appears to absorb into the corneocytes whose keratin conformation tends to alter from an  $\alpha$ -helix to  $\beta$ -sheets. In the lipid domains, DMSO appears to disturb the multilamellar lipid bilayers by causing conformational changes from an all *trans* gel phase to a *trans-gauche* liquid crystalline phase. Overall, the action of DMSO on the keratin and lipids thus results in looser or more permeable structures which are presumably responsible at least in part for the observed increases in the flux of very many drugs following DMSO treatment.

#### Acknowledgements

A.N.C.A. thanks the Commonwealth Scholarship Commission for a studentship.

#### References

- Allenby, A.C., Fletcher, J., Schock, C. and Tees, T.E.S., The effect of heat, pH and organic solvents on the electrical impedance and permeability of excised human skin. *Br. J. Dermatol.*, 81 (Suppl. 4) (1969) 31-39.
- Al-Saidan, S.M.H., Selkirk, A.B. and Winfield, A.J., Effect of dimethylsulphoxide concentration on the permeability of neonatal rat stratum corneum to alkanols. *J. Invest. Dermatol.*, 89 (1987) 426-429.
- Anigbogu, A.N.C., Williams, A.C., Barry, B.W. and Edwards, H.G.M., Fourier transform Raman spectroscopy in the study of interactions between terpene penetration enhancers and human stratum corneum. In Brain, K.R., James, V.J. and Walters, K.A. (Eds), *Prediction of Percutaneous Penetration*, STS, Cardiff, 1993, pp. 27-36.

- Baden, H.P. and Bonar, L., The  $\alpha$ -fibrous proteins of the epidermis. *J. Invest. Dermatol.*, 51 (1968) 478-483.
- Baden, H.P., Goldsmith, L.A. and Bonar, L., Conformational changes in the  $\alpha$ -fibrous protein of epidermis. *J. Invest. Dermatol.*, 60 (1973) 215-218.
- Barry, B.W., *Dermatological Formulations: Percutaneous Absorption*, Dekker, New York, 1983.
- Barry, B.W., Mode of action of penetration enhancers in human skin. *J. Controlled Release*, 6 (1987) 85-97.
- Barry, B.W., Edwards, H.G.M. and Williams, A.C., Fourier transform Raman and infrared vibrational study of human skin: assignment of spectral bands. *J. Raman Spectrosc.*, 23 (1992) 641-645.
- Bertoluzza, A., Bonora, S., Battaglia, M.A. and Monti, P., Raman and infrared study on the effects of dimethyl sulphoxide (DMSO) on water structure. *J. Raman Spectrosc.*, 8 (1979) 231-235.
- Blank, I.H., Further observations on factors which influence the water content of the stratum corneum. *J. Invest. Dermatol.*, 21 (1953) 259-271.
- Bouwstra, J.A., De Vries, M.A., Gooris, G.S., Bras, W., Brussee, J. and Ponc, M., Thermodynamic and structural aspects of the skin barrier. *J. Controlled Release*, 15 (1991) 209-220.
- Brown, K.G., Petricolas, W.L. and Brown, E., Raman studies of conformational changes in model membrane systems. *Biochim. Biophys. Res. Commun.*, 54 (1973) 358-364.
- Carey, P.R., *Biochemical Applications of Raman and Resonance Raman Spectroscopies*, Academic Press, New York, 1982.
- Casal, H.L. and Mantsch, H.H., Polymorphic phase behaviour of phospholipid membranes studied by infrared spectroscopy. *Biochim. Biophys. Acta*, 779 (1984) 381-401.
- Chandrasekaran, S.K., Campbell, P.S. and Michael, A.S., The effect of dimethyl sulphoxide on drug permeation through human skin. *AIChE J.*, 23 (1977) 810-815.
- Cowie, J.M.G. and Toporowski, P.M., Association in the binary liquid system, dimethyl sulphoxide-water. *Can. J. Chem.*, 39 (1961) 2240.
- Crounse, R.G., Epidermal keratin: a re-evaluation. *Nature*, 200 (1963) 539-542.
- Elftbaum, S.G. and Laden, K., The effect of dimethyl sulphoxide on percutaneous absorption: a mechanistic study. III. *J. Soc. Cosmet. Chem.*, 19 (1968) 841-847.
- Embery, G. and Dugard, P.H., The isolation of dimethyl sulphoxide soluble components from human epidermal preparations: a possible mechanism of action of dimethyl sulphoxide in effecting percutaneous migration phenomena. *J. Invest. Dermatol.*, 57 (1971) 308-311.
- Gaber, B.P. and Petricolas, W.L., On the quantitative interpretation of biomembrane structure by Raman spectroscopy. *Biochim. Biophys. Acta*, 465 (1977) 260-274.
- Garson, J., Doucet, J., Leveque, J. and Tsoucaris, G., Oriented structure of stratum corneum revealed by X-ray diffraction. *J. Invest. Dermatol.*, 96 (1991) 43-49.
- Golden, G.M., Guzek, D.B., Harris, R.R., McKie, J.E. and Potts, R.O., Lipid thermotropic transitions in human stratum corneum. *J. Invest. Dermatol.*, 86 (1986) 255-259.
- Harrison, S.M., Barry, B.W. and Dugard, P.H., Effects of freezing on human stratum skin permeability. *J. Pharm. Pharmacol.*, 36 (1984) 261-262.
- Hudson, B.S. and Mayne, L.E., Peptides and protein side chains. In Spiro, T.G. (Ed.), *Biological Applications of Raman Spectroscopy*, Wiley, New York, 1987, pp. 181-209.
- Kligman, A.M. and Christophers, E., Preparation of isolated sheets of human stratum corneum. *Arch. Dermatol.*, 88 (1963) 70-73.
- Knutson, K., Potts, R.O., Guzek, D.B., Golden, G.M., McKie, J.E., Lambert, W.J. and Higuchi, W.I., Macro and molecular physical-chemical considerations in understanding drug transport in the stratum corneum. *J. Controlled Release*, 2 (1986) 67-87.
- Krill, S.L., Knutson, K. and Higuchi, W.I., The stratum corneum lipid thermotropic phase behaviour. *Biochim. Biophys. Acta*, 1112 (1992) 281-286.
- Kurihara-Bergstrom, T., Flynn, G.L. and Higuchi, W.I., Physical study of percutaneous absorption enhancement by dimethyl sulfoxide: dimethyl sulfoxide mediation of vidarabine (ara-A) permeation of hairless mouse skin. *J. Invest. Dermatol.*, 89 (1987) 274-280.
- Kurihara-Bergstrom, T., Flynn, G.L. and Higuchi, W.I., Physicochemical study of percutaneous absorption enhancement by dimethyl sulfoxide: kinetic and thermodynamic determinants of dimethyl sulfoxide mediated mass transfer of alkanols. *J. Pharm. Sci.*, 75 (1986) 479-486.
- Lee, A.G., Functional properties of biological membranes: a physical chemical approach. *Prog. Biophys. Mol. Biol.*, 29 (1975) 3-56.
- Litman, B.J., Lewis, N.E. and Levin, I.W., Packaging characteristics of highly unsaturated bilayer lipids: Raman spectroscopic studies of multilamellar phosphatidylcholine dispersions. *Biochemistry*, 30 (1991) 313-319.
- Maddams, W.F., The scope and limitations of curve-fitting. *Appl. Spectrosc.*, 34 (1980) 245-267.
- Miyazawa, T., Perturbation treatment of the characteristic vibrations of polypeptide chains in various configurations. *J. Chem. Phys.*, 32 (1960) 1647-1652.
- Oertel, R.P., Protein conformational changes induced in human stratum corneum by organic sulphoxides: an infrared spectroscopic investigation. *Biopolymer*, 16 (1977) 2329-2345.
- Ritschel, W.A., Sorption promoters in biopharmaceutics. *Angew. Chem. Int. Ed.*, 8 (1969) 699-710.
- Roberts, J.B. and Lillywhite, H.B., Lipids and the permeability of epidermis from snake skin. *J. Exp. Zool.*, 228 (1983) 1-9.
- Scherer, R.G., Go, M.K. and Kint, S., Raman spectra and structure of water in dimethyl sulphoxide. *J. Phys. Chem.*, 77 (1973) 2108-2117.

- Snyder, R.G., Hsu, S.L. and Krimm, S., Vibrational spectra in the C-H stretching region and the structure of the polymethylene chain. *Biochim. Biophys. Acta*, 34A (1978) 395-406.
- Snyder, R.G., Strauss, H.L. and Elliger, C.A., C-H stretching modes and the structure of n-alkyl chains. 1. Long, disordered chains. *J. Phys. Chem.*, 86 (1982) 5145-5150.
- Tu, A.T., Peptide backbone conformation and microenvironment of protein side chains. In Clark, R.J.H. and Hester, R.E. (Eds), *Spectroscopy of Biological Systems*, Wiley, New York, 1986, pp. 47-112.
- Tu, A.T., *Raman Spectroscopy in Biology: Principles and Applications*, Wiley, New York, 1982, pp. 187-233.
- Walton, A.G. and Blackwell, J., Infrared and Raman spectroscopy. *Biopolymers*, Academic Press, New York, 1973, pp. 168-228.
- Weissinger, J., Transdermal delivery of drugs and topical applications: non-clinical regulatory considerations. In Gurny, R. and Teubner, A., (Eds), *Dermal and Transdermal Drug Delivery: New Insights and Perspectives*, Wissenschaftliche Verlagsgesellschaft, Stuttgart, 1993, pp. 187-193.
- White, S.H., Mirejovsky, D. and King, G.I., Structure of the lamellar lipid domains and corneocyte envelopes of murine stratum corneum: an X-ray diffraction study. *Biochemistry*, 27 (1988) 3725-3732.
- Wilkes, G.L., Brown, J.A. and Wildnauer, R.H., The biochemical properties of skin. *CRC Crit. Rev. Bioeng.*, (1973) 453-495.
- Williams, A.C., Barry, B.W., Edwards, H.G.M. and Farwell, D.W., A critical comparison of some Raman spectroscopic techniques for studies of human stratum corneum. *Pharm. Res.*, 10 (1993) 1642-1647.
- Williams, A.C., Edwards, H.G.M. and Barry, B.W., Fourier transform Raman spectroscopy: a novel application for examining human stratum corneum. *Int. J. Pharm.*, 81 (1992) R11-R14.
- Wood, E.J. and Blandon, P.T., *The Human Skin*, Edward Arnold, London, 1985.

# Medicated Topicals

**Lawrence H Block, PhD**

Professor of Pharmaceutics

Duquesne University School of Pharmacy

Pittsburgh, PA 15282

The application of medicinal substances to the skin or various body orifices is a concept doubtless as old as humanity. The papyrus records of ancient Egypt describe a variety of such medications for external use. Galen described the use in Roman times of a forerunner to today's vanishing creams.

Medications are applied in a variety of forms reflecting the ingenuity and scientific imagination of pharmacists through the centuries. New modes of drug delivery have been developed to remedy the shortcomings of earlier vehicles or, more recently, to optimize drug delivery. Conversely, some external

medications have fallen into disuse because of changes in the practice of medicine.

Medications are applied to the skin or inserted into body orifices in liquid, semisolid or solid form. Ophthalmics and topical aerosol products will not be discussed in this chapter. Ophthalmic use imposes particle size, viscosity and sterility specifications that require separate, detailed discussion (see Chapter 43). The complexity of pharmaceutical aerosol systems necessitates their inclusion elsewhere (see Chapter 50).

## BIOPHARMACEUTICAL ASPECTS OF THE ROUTES OF ADMINISTRATION

### EPIDERMAL AND TRANSDERMAL DRUG DELIVERY

#### The Skin

The skin often has been referred to as the largest of the body organs: an average adult's skin has a surface area of about 2 m<sup>2</sup>. It is probably the heaviest organ of the body. Its accessibility and the opportunity it affords to maintain applied preparations intact for a prolonged time have resulted in its increasing use as a route of drug administration, whether for local, regional, or systemic effects.

Anatomically, human skin may be described as a stratified organ with three distinct tissue layers: the epidermis, the dermis and the subcutaneous fat layer (Fig 44-1).

Epidermis, the outermost skin layer, comprises stratified squamous epithelial cells. Keratinized, flattened remnants of these actively dividing epidermal cells accumulate at the skin surface as a relatively thin region (about 10  $\mu$ m thick) termed the stratum corneum, or horny layer. The horny layer is itself lamellar with the keratinized cells overlapping one another, linked by intercellular bridges and compressed into about 15 layers. The lipid-rich intercellular space in the stratum corneum comprises lamellar matrices with alternating hydrophilic layers and lipophilic bilayers formed during the process of keratinization. The region behaves as a tough but flexible coherent membrane.

The stratum corneum also is markedly hygroscopic—far more so than other keratinous materials such as hair or nails. Immersed in water the isolated stratum corneum swells to about three times its original thickness, absorbing about four to five times its weight in water in the process. The stratum corneum functions as a protective physical and chemical barrier and is only slightly permeable to water. It retards water loss from underlying tissues, minimizes ultraviolet light pene-

tration, and limits the entrance of microorganisms, medications, and toxic substances from without. The stratum corneum is abraded continuously. Thus, it tends to be thicker in regions more subject to abrasion or the bearing of weight. Its regeneration is provided by rapid cell division in the basal cell layer of the epidermis. Migration or displacement of dividing cells toward the skin surface is accompanied by differentiation of the epidermal cells into layers of flat, laminated plates, as noted above. An acidic film (pH ranging between 4 and 6.5, depending on the area tested) made up of emulsified lipids covers the surface of the stratum corneum.

The dermis apparently is a gel structure-involving a fibrous protein matrix embedded in an amorphous, colloidal, ground substance. Protein, including collagen and elastin fibers, is oriented approximately parallel to the epidermis. The dermis supports and interacts with the epidermis, facilitating its conformation to underlying muscles and bones. Blood vessels, lymphatics, and nerves are found within the dermis, though only nerve fibers reach beyond the dermal ridges or papillae into the germinative region of the epidermis. Sweat glands and hair follicles extending from the dermis through the epidermis provide discontinuities in an otherwise uniform integument.

The subcutaneous fat layer serves as a cushion for the dermis and epidermis. Collagenous fibers from the dermis thread between the accumulations of fat cells, providing a connection between the superficial skin layers and the subcutaneous layer.

**HAIR FOLLICLES AND SWEAT GLANDS**—Human skin is sprinkled liberally with surface openings extending well into the dermis. Hair follicles, together with the sebaceous glands that empty into the follicles, make up the pilosebaceous unit. Apocrine and eccrine sweat glands add to the total.

**PILOSEBACEOUS UNITS**—Human hair consists of compacted keratinized cells formed by follicles. Sebaceous glands empty into the follicle sites to form the pilosebaceous unit. The hair follicles are surrounded by sensory nerves; thus, an important function of human hair is sensory. Human hair varies enormously within the same individual, even within the same

could enhance vehicle-skin partitioning efficiency and drug permeation.

**PENETRATION ENHANCERS**—This term has been used to describe substances that facilitate absorption through the skin. While most materials have a direct effect on the permeability of the skin, other so-called enhancers (eg, polyols, such as glycerin and propylene glycol) appear to augment percutaneous absorption by increasing the thermodynamic activity of the penetrant, thereby increasing the effective escaping tendency and concentration gradient of the diffusing species. Penetration enhancers with a direct effect on skin permeability include solvents, surfactants, and miscellaneous chemicals such as urea and *N,N*-diethyl-*m*-toluamide (Table 44-3).<sup>16,17</sup> The mechanism of action of these enhancers is complex since these substances also may increase penetrant solubility. Nonetheless, the predominant effect of these enhancers on the stratum corneum is either to increase its degree of hydration or disrupt its lipoprotein matrix. In either case, the net result is a decrease in resistance to penetrant diffusion. (The formulator should note that the inclusion of a penetration enhancer in a topical formulation mandates additional testing and evaluation to ensure the absence of enhancer-related adverse effects.)

Foremost among the solvents that affect skin permeability is water. As noted above, water is a factor even for *anhydrous* transdermal delivery systems due to their occlusive nature. Due to its safety and efficacy, water has been described as the ultimate penetration enhancer. Other solvents include the classic enhancer, dimethyl sulfoxide (DMSO), which is of limited utility because of its potential ocular and dermal toxicity, its objectionable taste and odor (a consequence of its absorption and subsequent biotransformation), and the need for concentrations in excess of 70% to promote absorption. Analogs of

**Table 44-3. Penetration Enhancers<sup>a</sup>**

<b>Solvents</b>	Water
	Alcohols
	Methanol
	Ethanol
	2-Propanol
	Alkyl methyl sulfoxides
	Dimethyl sulfoxide
	Decylmethyl sulfoxide
	Tetradecylmethyl sulfoxide
	Pyrrolidones
	2-Pyrrolidone
	<i>N</i> -Methyl-2-pyrrolidone
	<i>N</i> -(2-Hydroxyethyl)pyrrolidone
	Laurocapram
	Miscellaneous solvents
	Acetone
	Dimethyl acetamide
	Dimethyl formamide
	Tetrahydrofurfuryl alcohol
<b>Amphiphiles</b>	
	<i>L</i> - $\alpha$ -Amino acids
	Anionic surfactants
	Cationic surfactants
	Amphoteric surfactants
	Nonionic surfactants
	Fatty acids and alcohols
<b>Miscellaneous</b>	
	Clofibric acid amides
	Hexamethylene lauramide
	Proteolytic enzymes
	Terpenes and sesquiterpenes
	$\alpha$ -Bisabolol
	<i>d</i> -Limonene
	Urea
	<i>N,N</i> -Diethyl- <i>m</i> -toluamide

<sup>a</sup> Adapted from References 16 and 17.

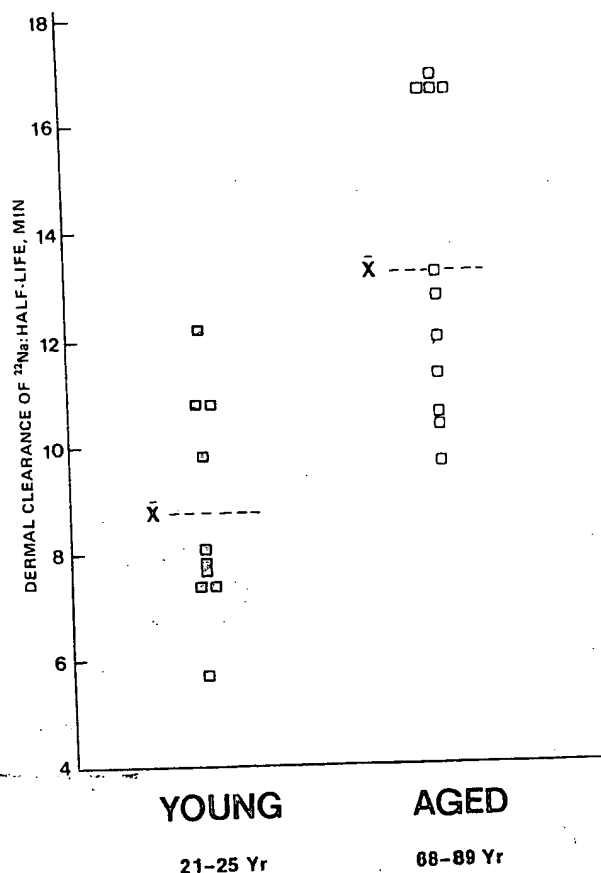


**Figure 44-7.** Dermal clearance of <sup>22</sup>Na in young and aged subjects after intradermal injection (data from Reference 19).

DMSO such as decylmethyl sulfoxide are used currently in some topical formulations. In contrast with other solvents, laurocapram (1-dodecylazacycloheptan-2-one; Azone) has been shown to function effectively at low concentrations ( $\leq 5\%$ ). Furthermore, Azone's effect on skin permeability persists long after a single application, due apparently to its prolonged retention within the stratum corneum.

Surfactants, long recognized for their ability to alter membrane structure and function, can have a substantial effect on skin permeability.<sup>18</sup> However, given the irritation potential of surfactants applied chronically, their utility as penetration enhancers is limited. Their effect on permeability may be complicated further by surfactant-monomer aggregation to form micelles and the concomitant solubilization of the permeant. As the impact of surfactants on skin permeability of a penetrant is problematic, the effect of their inclusion in a formulation should be evaluated using appropriate *in vitro* and *in vivo* studies.

**STRATUM CORNEUM BARRIER EFFICACY AND DERMAL CLEARANCE**—Even though *in vitro* studies of percutaneous transport may reflect the resistance of the skin to drug diffusion, there is no way such studies can characterize adequately the transfer of diffusing drug into the microvasculature of the dermis and its subsequent transfer into general circulation.

Christophers and Kligman<sup>19</sup> evaluated the dermal clearance of <sup>22</sup>Na from the midback skin of volunteers following the intradermal injection of <sup>22</sup>Na as normal saline solution. The dermal clearances, expressed in terms of the half-life for disappearance of radioactivity, are plotted in Figure 44-7.<sup>19</sup> Similar results were obtained with disappearance of skin fluorescence after intradermal injection of sodium fluorescein. The



## OINTMENTS

Ointments are semisolid preparations intended for external application to the skin or mucous membranes; usually, but not always, they contain medicinal substances. The types of ointment bases used as vehicles for drugs are selected or designed for optimum delivery of the drugs and also to contribute emolliency or other quasi-medicinal qualities. Ointment properties vary, since they are designed for specific uses, ease of application, or extent of application.

The official definition of ointment in its present form was introduced in the USP XV in 1955. The definition is broad and encompasses petrolatum, ie, oleaginous bases, emulsion bases—either water-in-oil (W/O) or oil-in-water (O/W)—and the so-called water-soluble bases.

In unofficial terms, oleaginous bases are described as ointments, but emulsion bases may be termed creams or lotions. Either of these containing large amounts of solids is termed a paste. All of these subclasses are defined officially as ointments.

Pharmaceutical authors have a penchant for defining *ideal* preparations, eg, the ideal base, the ideal vehicle, and so on. In practice, of course, there is no such thing. An individual cannot be all things to all people; neither can an ointment base be ideal for all drugs, all situations, or all skins, for that matter. An ointment base functioning as a drug vehicle should be optimized for a specific drug and, insofar as possible, for specific disease states or skin conditions.

It is, of course, possible to define certain specific requirements for an ointment base to be used for extemporaneous compounding. Such a base should be nonirritating, easily removable, nonstaining, stable, non-pH-dependent, and widely compatible with a variety of medicaments. When one adds the stipulation that the base must release the same variety of medicaments, the implausibility of such definitions becomes evident.

### Classification and Properties of Ointment Bases

The USP recognizes four general classes of ointment bases, hereunder categorized into five classes for the purpose of indicating more definitively some differences in the principal properties of the bases.

#### HYDROCARBON BASES (OLEAGINOUS)

Example: White Petrolatum, White Ointment

1. Emollient
2. Occlusive
3. Non-water-washable
4. Hydrophobic
5. Greasy

#### ABSORPTION BASES (ANHYDROUS)

Examples: Hydrophilic Petrolatum; Anhydrous Lanolin

1. Emollient
2. Occlusive
3. Absorb water
4. Anhydrous
5. Greasy

#### ABSORPTION BASES (W/O TYPE)

Examples: Lanolin, Cold Cream

1. Emollient
2. Occlusive
3. Contain water
4. Some absorb additional water
5. Greasy

#### WATER-REMOVABLE BASES (O/W TYPE)

Example: Hydrophilic Ointment

1. Water-washable
2. Nongreasy
3. Can be diluted with water
4. Nonocclusive

#### WATER-SOLUBLE BASES

Example: Polyethylene Glycol Ointment

1. Usually anhydrous
2. Water-soluble and washable
3. Nongreasy
4. Nonocclusive
5. Lipid-free

The selection of the optimum vehicle from the classification above may require compromises so often encountered in drug formulation. For example, stability or drug activity might be superior in a hydrocarbon base; however, acceptability is diminished because of the greasy nature of the base. The water solubility of the polyethylene glycol bases may be attractive, but the glycol(s) may be irritating to traumatized tissue. Drug activity and percutaneous absorption may be superior when using a hydrocarbon base; however, it may be prudent to minimize percutaneous absorption by the use of a less occlusive base.

## OINTMENT BASES

### Hydrocarbon Bases

Hydrocarbon bases are usually petrolatum *per se* or petrolatum modified by waxes or liquid petrolatum to change viscosity characteristics. Liquid petrolatum gelled by the addition of a polyethylene resin also is considered a hydrocarbon ointment base, albeit one with unusual viscosity characteristics.

Hydrocarbon ointment bases are classified as oleaginous bases along with bases prepared from vegetable fixed oils or animal fats. Bases of this type include lard, benzoinated lard, olive oil, cottonseed oil, and other oils. Such bases are emollient but generally require addition of antioxidants and other preservatives. They are now largely of historic interest.

Petrolatum USP is a tasteless, odorless, unctuous material with a melting range of 38 to 60°; its color ranges from amber to white (when decolorized). Petrolatum often is used externally, without modification or added medication, for its emollient qualities.

Petrolatum used as an ointment base has a high degree of compatibility with a variety of medicaments. Bases of this type are occlusive and nearly anhydrous and thus provide optimum stability for medicaments such as antibiotics. The wide melting range permits some latitude in vehicle selection, and the USP permits addition of waxy materials as an aid in minimizing temperature effects.

Hydrocarbon bases, being occlusive, increase skin hydration by reducing the rate of loss of surface water. Bases of this kind may be used solely for such a skin-moisturizing effect, eg, white petroleum jelly as noted above. Skin hydration on the other hand may increase drug activity. Studies have indicated that steroids have increased activity, as measured by vasoconstrictor effects, when applied to the skin in a hydrocarbon vehicle. Stoughton consistently found the same steroid more active when applied in a petrolatum vehicle than when applied in a cream (ie, O/W emulsion) vehicle.

A gelled mineral oil vehicle represents a unique addition to this class of bases that comprises refined natural products. Liquid petrolatum may be gelled by addition of a polyethylene. When approximately 5% of low-density polyethylene is added, the mixture heated and then shock-cooled, a soft, unctuous, colorless material resembling white petrolatum is produced. The mass maintains unchanged consistency over a wide temperature range. It neither hardens at low temperatures nor melts at reasonably high temperatures. Its useful working range is between  $-15^{\circ}$  and  $60^{\circ}$ . Excessive heat, ie, above  $90^{\circ}$ , will destroy the gel structure.

On the basis of *in vitro* studies, drugs may be released faster from the gelled mineral oil vehicle than from conventional petrolatum. This quicker release has been attributed to easier migration of drug particulates through a vehicle that is essentially a liquid than through petrolatum.

Despite the advantages hydrocarbon or oleaginous vehicles provide in terms of stability and emolliency, such bases have the considerable disadvantage of greasiness. The greasy or oily material may stain clothing and is difficult to remove. In terms of patient acceptance, hydrocarbon bases, ie, ointments, rank well below emulsion bases such as creams and lotions.

## Absorption Bases

Absorption bases are hydrophilic, anhydrous materials or hydrous bases that have the ability to absorb additional water. The former are anhydrous bases, which absorb water to become W/O emulsions; the latter are W/O emulsions, which have the ability to absorb additional water. The word absorption in this connotation refers only to the ability of the base to absorb water. Both types of base are exemplified by Anhydrous Lanolin and Lanolin. The former is converted to the latter by the addition of 30% water. The latter in turn will absorb additional amounts of water.

Hydrophilic Petrolatum USP is an anhydrous absorption base. The W/O emulsifying property is conferred by the inclusion of cholesterol. This composition is a modification of the original formulation, which contained anhydrous lanolin. The lanolin was deleted because of reports of allergy; cholesterol was added. Inclusion of stearyl alcohol and wax adds to the physical characteristics, particularly firmness and heat stability.

### HYDROPHILIC PETROLATUM USP

Cholesterol	30 g
Stearyl Alcohol	30 g
White Wax	80 g
White Petrolatum	860 g
To make	1000 g

Melt the stearyl alcohol and white wax together on a steam bath, then add the cholesterol and stir until it completely dissolves. Add the white petrolatum and mix. Remove from the bath, and stir until the mixture congeals.

Lanolin is a complex mixture of substances. Its ability to absorb water is probably a characteristic of the material rather than a single component. The chemistry of lanolin has been studied in detail. Such studies have resulted in the introduction of a large variety of lanolin derivatives and separated fractions. Available now are lanolin alcohols, dewaxed lanolins, acetylated lanolins, ethoxylated lanolins, hydrogenated lanolins, lanolin esters, and other products. Most of these derivatives have been produced for specific purposes, such as improved emulsification characteristics or to reduce allergic reactivity.

The specific compounds responsible for lanolin allergy remain unknown; however, the greater portion of lanolin allergens resides in the wool wax alcohols fraction. Thus, fractional separation to obtain, for example, the so-called liquid lanolins substantially reduces the incidence of allergic reactions. Given

the plethora of lanolin fractions, derivatives, modifications, and levels of purity, it is quite possible, even likely, that lanolin-sensitive individuals can tolerate specific lanolin products.

Absorption bases, particularly the emulsion bases, impart excellent emolliency and a degree of occlusiveness on application. The anhydrous types can be used when the presence of water would cause stability problems with specific drug substances, eg, antibiotics. Absorption bases also are greasy when applied and are difficult to remove. Both of these properties are, however, less obvious than with hydrocarbon bases.

Commercially available absorption bases include Aquaphor (Beiersdorf) and Polysorb (Fougera). Nivea Cream (Beiersdorf) is a hydrated emollient base. Absorption bases, either hydrous or anhydrous, are seldom used as vehicles for commercial drug products. The W/O emulsion system is more difficult to deal with than the more conventional O/W systems, and there is, of course, reduced patient acceptance because of greasiness.

## Water-Removable Bases

Water-washable bases or emulsion bases, commonly referred to as creams, represent the most commonly used type of ointment base. By far the majority of commercial dermatologic drug products are formulated in an emulsion or cream base. Emulsion bases are washable and removed easily from skin or clothing. Emulsion bases can be diluted with water, although such additions are uncommon.

As a result of advances in synthetic cosmetic chemistry the formulator of an emulsion base can be faced with a bewildering variety of selections. Fortunately, the emulsion base can be subdivided into three component parts, designated as the oil phase, the emulsifier, and the aqueous phase. The medicinal agent may be included in one of these phases or added to the formed emulsion.

The oil phase, sometimes called the internal phase, is typically made up of petrolatum and/or liquid petrolatum together with one or more of the higher-molecular-weight alcohols, such as cetyl or stearyl alcohol. Stearic acid may be included if the emulsion is to be based on a soap formed *in situ*, eg, triethanolamine stearate. A calculated excess of stearic acid in such a formulation will produce a pearlescent appearance in the finished product.

For drug-delivery vehicles, simplified systems are in order to minimize component interactions, either physical or chemical, and, of course, to minimize cost. Hydrophilic Ointment USP is a typical emulsion base. The composition is as follows:

### HYDROPHILIC OINTMENT USP

Methylparaben	0.25 g
Propylparaben	0.15 g
Sodium Lauryl Sulfate	10 g
Propylene Glycol	120 g
Stearyl Alcohol	250 g
White Petrolatum	250 g
Purified Water	370 g
To make about	1000 g

Melt the stearyl alcohol and the white petrolatum on a steam bath, and warm to about  $75^{\circ}$ . Add the other ingredients, previously dissolved in the water and warmed to  $75^{\circ}$ , and stir the mixture until it congeals.

Stearyl alcohol and petrolatum constitute an oil phase with the proper smoothness and comfort for the skin. Stearyl alcohol also serves as an adjuvant emulsifier. Petrolatum in the oil phase also contributes to the water-holding ability of the overall formulation.

A glance at the cosmetic literature and such volumes as the Cosmetic, Toiletry and Fragrance Association's *International Cosmetic Ingredient Dictionary* impresses one with the enormous number and variety of emulsion-base components, particularly oil-phase components. Many of these substances im-

**2 0** T H E D I T I O N

---

# Remington: The Science and Practice of Pharmacy

**ALFONSO R GENNARO**

Chairman of the Editorial Board  
and Editor

QV  
704  
P388p  
2000  
ref

**Remington: The Science and Practice of Pharmacy . . .** A treatise on the theory and practice of the pharmaceutical sciences, with essential information about pharmaceutical and medicinal agents; also, a guide to the professional responsibilities of the pharmacist as the drug information specialist of the health team . . . A textbook and reference work for pharmacists, physicians, and other practitioners of the pharmaceutical and medical sciences.

**EDITORS**

Alfonso R Gennaro, *Chair*

Nicholas G Popovich

Ara H Der Marderosian

Roger L Schnaare

Glen R Hanson

Joseph B Schwartz

Thomas Medwick

H Steve White

**AUTHORS**

The 119 chapters of this edition of *Remington* were written by the editors, by members of the Editorial Board, and by the authors listed on pages viii to x.

**Managing Editor**

John E Hoover, BSc (Pharm)

**Editorial Assistant**

Bonnie Brigham Packer, RNC, BA

**Director**

Philip P Gerbino 1995–2000

Twentieth Edition—2000

Published in the 180th year of the  
**PHILADELPHIA COLLEGE OF PHARMACY AND SCIENCE**

10-5-01

Editor: Daniel Limmer  
Managing Editor: Matthew J. Hauber  
Marketing Manager: Anne Smith

Lippincott Williams & Wilkins

351 West Camden Street  
Baltimore, Maryland 21201-2436 USA

227 East Washington Square  
Philadelphia, PA 19106

All rights reserved. This book is protected by copyright. No part of this book may be reproduced in any form or by any means, including photocopying, or utilized by any information storage and retrieval system without written permission from the copyright owner.

The publisher is not responsible (as a matter of product liability, negligence or otherwise) for any injury resulting from any material contained herein. This publication contains information relating to general principles of medical care which should not be construed as specific instructions for individual patients. Manufacturers' product information and package inserts should be reviewed for current information, including contraindications, dosages and precautions.

*Printed in the United States of America*

Entered according to Act of Congress, in the year 1885 by Joseph P Remington, in the Office of the Librarian of Congress, at Washington DC

Copyright 1889, 1894, 1905, 1907, 1917, by Joseph P Remington

Copyright 1926, 1936, by the Joseph P Remington Estate

Copyright 1948, 1951, by the Philadelphia College of Pharmacy and Science

Copyright 1956, 1960, 1965, 1970, 1975, 1980, 1985, 1990, 1995, by the Philadelphia College of Pharmacy and Science

Copyright 2000, by the University of the Sciences in Philadelphia

*All Rights Reserved*  
Library of Congress Catalog Card Information is available  
ISBN 0-683-306472

*The publishers have made every effort to trace the copyright holders for borrowed material. If they have inadvertently overlooked any, they will be pleased to make the necessary arrangements at the first opportunity.*

*The use of structural formulas from USAN and the USP Dictionary of Drug Names is by permission of The USP Convention. The Convention is not responsible for any inaccuracy contained herein.*

*Notice—This text is not intended to represent, nor shall it be interpreted to be, the equivalent of or a substitute for the official United States Pharmacopeia (USP) and/or the National Formulary (NF). In the event of any difference or discrepancy between the current official USP or NF standards of strength, quality, purity, packaging and labeling for drugs and representations of them herein, the context and effect of the official compendia shall prevail.*

HEALTH SCIENCES LIBRARY  
UNIVERSITY OF CINCINNATI

To purchase additional copies of this book call our customer service department at (800) 638-3030 or fax orders to (301) 824-7390. International customers should call (301) 714-2324.

00 01 02 03 04  
1 2 3 4 5 6 7 8 9 10

## Penetration Enhancement of Transdermal Delivery—Current Permutations and Limitations

*Carryn H. Purdon,<sup>1</sup> Chad G. Azzi,<sup>1</sup> Jin Zhang,<sup>1</sup> Eric W. Smith,<sup>1</sup>  
& Howard I. Maibach<sup>2</sup>*

<sup>1</sup>College of Pharmacy, University of South Carolina, Columbia, South Carolina, USA; <sup>2</sup>Department of Dermatology, University of California, San Francisco, California, USA

Address all correspondence to Eric W. Smith, College of Pharmacy, University of South Carolina, Columbia, South Carolina, 29208; esmith@cop.sc.edu

**Referees:** Dr. Bozena B. Michniak, Department of Pharmacology and Physiology, University of Medicine and Dentistry of New Jersey, Newark NJ 07103; Dr. Kenneth B. Sloan, Department of Medicinal Chemistry, College of Pharmacy, University of Florida, Gainesville FL 32610

**ABSTRACT:** In order to achieve enhanced topical drug delivery, it is necessary to make physical or biomolecular structural alterations to the stratum corneum by suitable techniques or by the use of specific chemical agents or drug carriers. The role of the chemical penetration enhancer is to reversibly alter the barrier properties of the stratum corneum by disruption of the membrane structures or by maximizing drug solubility within the skin. Alternatively, permeant delivery to the dermal vasculature using one of several physical methods to reduce diffusional resistance within the skin may be used to promote drug penetration. In the present article, we summarize the major facets of the diverse spectrum of penetration enhancement techniques that include modification of the stratum corneum, lipid-based delivery systems, drug/vehicle interactions, bypassing the stratum corneum, and electrical techniques of enhancement.

**KEY WORDS:** penetration enhancer, barrier, skin, stratum corneum, delivery systems, vehicles, electrical techniques

### I. INTRODUCTION

Optimized drug delivery systems common today achieve a balance between the physicochemical requisites for stability of active and inactive constituents, preserva-

tion against microbial spoilage, and, most importantly, presentation of the drug to the skin in a system that will allow appropriate release of the active.<sup>1</sup>

The transdermal permeation of drugs occurs via diffusion through the intact epidermis and through the skin appendages—i.e., hair follicles and sweat glands—that form shunt pathways through the stratum corneum (SC). However, these skin appendages occupy only 0.1% of the total human skin surface, and the contribution of this pathway is usually considered to be small. The barrier function of mammalian skin is principally attributed to the intercellular lipid bilayers of the outer 10–20  $\mu\text{m}$  of the epidermis, the SC.<sup>2</sup> The barrier properties of this layer are based on the specific composition of the SC lipids<sup>3</sup> and, in particular, the exceptional structural arrangement of the intercellular lipid matrix and the lipid envelope surrounding the cells.<sup>4</sup> The SC organization has often been described by the “brick and mortar” model,<sup>5</sup> in which extracellular lipid accounts for approximately 10% of the dry weight of this layer, and 90% is intracellular protein (mainly keratin).<sup>6,7</sup> The SC lacks phospholipids but is enriched in ceramides and neutral lipids (cholesterol, fatty acids, cholesteryl esters) that are arranged in a bilayer format and form so-called “lipid channels.”<sup>8</sup>

Two penetration pathways may be identified through the intact SC: the *intercellular lipid* route and the *transcellular* route through the corneocytes. In both cases the permeant must diffuse through the intercellular lipid bilayer matrix.<sup>9</sup> The ability of topically applied agents to interact with the intercellular lipids therefore dictates the degree to which percutaneous absorption may be enhanced. Several pathways could be involved in this process. Penetration is enhanced via the transcellular route by swelling of the intracellular protein matrix, which necessitates alteration of protein structure within the corneocytes. The passage of drug molecules by the intercellular route could occur via the lipoidal pathway or the aqueous pathway. In the lipoidal pathway, penetration could be enhanced by altering the crystallinity of the intercellular lipid bilayer through an increase in hydration of the lipid polar head groups. Alternatively, the lipid hydrophobic tails could be disordered to achieve the same effect. Increased drug partitioning could also be facilitated in the aqueous spaces between the lipid bilayers.<sup>10</sup> Regardless of the mechanism of action, in order to achieve enhanced drug delivery, biomolecular structural alterations must be made within the skin by suitable agents or drug carriers.<sup>11</sup>

Numerous articles in this field have been published in recent years. Moser et al.<sup>12</sup> and Hadgraft<sup>13</sup> reviewed passive enhancement strategies in topical and transdermal drug delivery. Foldvari<sup>14</sup> discussed several chemical penetration enhancers, lipid-based delivery systems, the relationship between liposome composition and drug permeation, and the possible mechanism of action of lipid vesicle-mediated drug delivery. Asbill and Michniak<sup>15</sup> discussed transdermal activity of percutaneous penetration enhancers and retarders. Suhonen et al.<sup>16</sup> reviewed the skin barrier structure and function and the mechanisms of action of some well established permeation promoters, with a focus on their impact on SC structural alterations. Junginger and

Verhoef<sup>17</sup> reviewed novel types of macromolecular penetration enhancers, such as anionic polyacrylates and cationic chitosan derivatives. Bach and Lippold<sup>18</sup> reviewed the quantification of penetration enhancement. Chung<sup>19</sup> presented the feasibility of proliposomes as a sustained transdermal dosage form and the role of the SC in the enhanced delivery of drugs from liposomes. Barry<sup>20</sup> reviewed novel mechanisms and devices to enable successful transdermal drug delivery focusing on drug/vehicle interactions, the role of vesicles and particles, modification of the SC by hydration, and chemical enhancers. In addition, enhancement methods are described that bypass or remove the SC tissue via microneedles, ablation of the barrier layer, follicular delivery, electrically assisted methods, or the use of synergistic interactions between chemical enhancers, ultrasound, iontophoresis, and electroporation. These methods are outlined in Table 1.

The present article attempts to summarize the major facets of the diverse spectrum of penetration enhancement techniques that have recently been reported. We have broadly classified the modes of penetration enhancement in terms of a chemical, vehicle, physical, or electrical basis; realizing that *any* disruption of the SC usually affects several of the defined transdermal absorption parameters. Attempting to assign a single, specific mechanism of enhancement action is, therefore, difficult in many cases.

## II. MODIFICATION OF THE SC

### II.A. Sulfoxides

Dimethylsulfoxide (DMSO) is an effective penetration enhancer that promotes permeation by reducing skin resistance to drug molecules or by augmenting drug partitioning from the dosage form.<sup>21</sup> Several theories have been advanced to explain the mechanisms of action of DMSO enhancement of skin permeability, including: extraction of skin lipids,<sup>22</sup> denaturation of SC proteins,<sup>23</sup> formation of hydrogen-bonded complexes with SC lipids,<sup>24</sup> and the distortion and intercellular delamination of the SC as a result of high osmotic stresses caused by transportation of both DMSO and water into the tissue from admixtures containing both solvents.<sup>25</sup> More recent studies suggest that DMSO exerts its role in enhancement of drug permeation by not only extracting soluble components of the SC, but also by delaminating the horny layer and denaturing the proteins.<sup>26,27</sup> Results of Fourier transform infrared (FTIR) spectroscopic investigations suggest that DMSO changes SC protein conformations.<sup>28</sup> Despite the wide-ranging studies that have been performed with DMSO, its specific mechanisms of action as a penetration enhancer still remain unclear.

DMSO is a dipolar, aprotic solvent that is miscible in both aqueous and polar



TABLE 1. Chemical and Physical Means of Penetration Enhancement

Class		Examples	Mechanisms
<b>Chemical Enhancement</b>			
Sulfoxides		Dimethylsulfoxide	Extracting soluble components of the SC, delaminating the horny layer, denaturing the proteins
Alcohols		Ethanol, octanol	Enhancing the solubility of drugs, disruption of the SC integrity through extraction of biochemicals,
Polyols		Propylene glycol	Solubility modification
Fatty Alcohols		Lauryl alcohol, oleyl alcohol	Increasing drug solubility and partitioning, disruption of the barrier function of the skin, ion-pair formation
Fatty Acids		Oleic acid, lauric acid, linoleic acid, capric acid	Increasing drug solubility and partitioning, disruption of the barrier function of the skin, ion-pair formation
Esters		Ethyl acetate, octyl acetate	Disruption of lipid packing, influence partitioning between vehicle and skin
Amines and amides	Urea	Dimethylacetamide, 1-alkyl-4-imidazolin-2-one	Facilitating hydration of the SC, disruption of lipid
	Pyrrolidones	1-dodecyl-azacycloheptan-2-one, 2-pyrrolidinone-1-acetic acid dodecyl ester	Fluidizing the lipids along the intercellular lipid domains in the SC, changing the SC lipid arrangement
Terpenes		D-limonene, menthol	Disruption of lipid packing within the bilayers, disturbance in the stacking of the bilayers
Surfactants	Anionic	Sodium laurate, sodium cholate	Altering the barrier function of the SC, removal of water-soluble agents, emulsifying sebum
	Cationic	Cetyltrimethyl ammonium bromide	
	Nonionics	Poloxamer, lecithin	
Cyclodextrins		$\alpha$ -, $\beta$ - and $\gamma$ -cyclodextrin	Inclusion of drugs into molecular cavity
Oxazolidinones		4-decyloxazolidin-2-one	Localizing drugs in the skin layers

Oxazolidinones	4-decyloxazolidin-2-one	Localizing drugs in the skin layers
----------------	-------------------------	-------------------------------------

# TRANSDERMAL PENETRATION ENHANCEMENT

Chitosan	Poly [b-(1-4)-2-amino-2-deoxy-D-glucopyranose]	Ionic interactions with negatively charged sites on the cell surface and tight junctions
Lipid Based Delivery System	Liposomes	Interacting with skin lipids
	Transfersomes	Squeezing through polar channels under a hydration gradient
	Ethosomes	Ethanol fluidizes both ethosomal lipids and bilayers of the SC intercellular lipid
Drug-vehicle Interactions	Supersaturated Solution	Elevating thermodynamic activity of drug
	Microemulsions	Disruption of the SC lipids, increasing the partitioning of the drug into the skin
<b>Physical Enhancement</b>		
Circumventing The SC	Microneedle Array	Penetrates to epidermal layer
	Stratum corneum ablation	Ablating the stratum corneum, eg. Skin stripping
Electrical Techniques of Enhancement	Iontophoresis	Driving charged species by electrical repulsion, increasing the permeability of skin by the flow of electric current, affecting the flux of uncharged molecules and large polar peptides by electroosmosis
	Ultrasound	Disturbing the lipid packing in SC by cavitation
	Electroporation	Creating transient pores through the SC by electrical pulse
Radio-wave Energy	Radiofrequency thermal ablation	Creating an array of small microchannels across the SC by microablating skin cells using radiofrequency energy

organic solvents; therefore, it may be easily incorporated into pharmaceutical formulations. High concentrations, usually greater than 60%, are required to produce a penetration enhancement effect. Unfortunately, at this high concentration, DMSO has been shown to produce adverse skin reactions. Kim et al.<sup>29</sup> synthesized novel transdermal penetration enhancers by replacing the oxygen atom of the DMSO with a nitrogen atom, an arylsulfonyl, aroyl, or aryl group. Like DMSO, these iminosulfuranes are polar, aprotic compounds; however, the polarity of iminosulfuranes can also be modulated by placing diverse substituents at the aromatic core of the molecule. The lipophilicity of iminosulfuranes is greater than that of DMSO, suggesting that an increased partitioning of these agents into the SC produces the enhanced penetration effect. These compounds were designed to be used at lower concentrations (below 10%) and were predicted to result in less skin irritation than DMSO and thereby be more acceptable for use in commercial products.

Anigbogu et al.<sup>30</sup> used Fourier transform Raman spectroscopy to study the effects of a series of aqueous solutions of DMSO on hydrated human SC, following treatment for 1 hour, to assess its mechanism of flux enhancement. The results showed changes in the SC keratin from an  $\alpha$ -helical to  $\beta$ -sheet conformation. In addition, at concentrations greater than 60% v/v, at which DMSO enhances drug flux, there was evidence of interactions with SC lipids. These observations suggest that the skin penetration enhancement produced by DMSO not only involves changes in protein structure but may also be related to alterations in SC lipid organization, in addition to any increased drug partitioning effects.

## II.B. Alcohols

Alcohols may influence transdermal penetration by several mechanisms. The alkyl chain length of the alkanols is an important parameter in the promotion of permeation enhancement. Augmentation appears to increase as the number of carbon units increases, up to a limiting value of 6–8 methylene groups.<sup>31</sup> In addition, lower molecular weight alkanols are thought to act as solvents, enhancing the solubility of drugs in the matrix of the SC.<sup>31</sup> Disruption of the SC integrity through extraction of biochemicals by the more hydrophobic alcohols may also contribute to enhanced mass transfer through this tissue.<sup>32</sup>

The skin penetration enhancement effect of saturated fatty alcohols has been demonstrated in many in vitro studies.<sup>33,34</sup> However, the skin irritation of saturated fatty alcohols has not been studied systematically. Kanikkannan and Singh<sup>35</sup> investigated the skin permeation enhancement effect and skin irritation of a series of saturated fatty alcohols in hairless rats using melatonin as a model compound. Octanol and nonanol were found to be the most useful enhancers for the transfer-

mal deliv  
and a reas  
volunteers  
informatio

Ande  
decanol, u  
rated fatty  
concentra  
parabolic  
and perme  
melatonin  
as the lev  
increase i

## II.C Poly

The molec  
their effi  
markedly  
molecule;  
dependin  
glycol is t  
proteinac  
permeatio  
penetrati

Benzene, acetone, and methanol were used as artificial feed mixtures. Propylene was used as a solubility test gas. The feed compositions, vapor pressures, and vapor-liquid equilibrium data were taken from the literature.<sup>1</sup> In each case, propylene was present with high concentration in the medium-boiling components of the feed. The feed was cooled and introduced into the column at the top. The hydrocarbon vapor was condensed in the condenser and the propylene was removed from the liquid by passing it through a propylene-selective membrane.

# *Critical Reviews™ in Therapeutic Drug Carrier Systems*

**Ajay K. Banga, PhD, Editor-in-Chief**

*Professor, Pharmaceutical Sciences*  
Mercer University  
3001 Mercer University Drive  
Atlanta GA 30341-4155  
banga\_ak@mercer.edu

**Srini Tenjarla, PhD, Associate Editor**

*Associate Director*  
Shire Pharmaceutical Development  
1901 Research Boulevard, Suite 500  
Rockville MD 20850 --  
stenjarla@us.shire.com



begell house, inc.  
Publishers

# Physicochemical Study of Percutaneous Absorption Enhancement by Dimethyl Sulfoxide: Dimethyl Sulfoxide Mediation of Vidarabine (ara-A) Permeation of Hairless Mouse Skin

Tamie Kurihara-Bergstrom, Ph.D.,\* Gordon L. Flynn, Ph.D., and William I. Higuchi, Ph.D.†  
College of Pharmacy, The University of Michigan, Ann Arbor, Michigan, U.S.A.

Dimethyl sulfoxide's (DMSO) concentration-dependent influences on its own permeation rate through hairless mouse skin and on the concurrent permeation rates of water and the antiviral drug vidarabine (ara-A) have been studied at 37°C using in vitro diffusion cells. Solubilities of ara-A in DMSO-water mixtures were also determined in order to assess ara-A's relative thermodynamic activity in the binary solvent media used in the mass transfer studies. Solubilities increased exponentially with increasing percentages of DMSO. Activity coefficients decreased accordingly. When the same DMSO medium was placed in each side of diffusion cell (balanced solvent configuration) permeability coefficients for ara-A decreased exactly as ara-A's solubility increased up to a 50% DMSO concentration, indicating the observed decreases in the mass transfer coefficients have thermodynamic origins. When DMSO media were placed in either the donor or receiver side of the cell up to the

same 50% concentration point and opposed by a normal saline medium on the other side (asymmetric solvent configurations), the permeability of ara-A did not decrease and at some DMSO levels was substantially increased, behavior in marked departure from thermodynamic control. The behavior disparity between the 2 configurations of the cell suggests that cross-currents of solvents play a role in permeability enhancement. Regardless of solvent configuration, permeability coefficients for ara-A at 90 and 100% DMSO strengths were exaggeratedly large, consistent with severe impairment of the stratum corneum. Similar overall permeability behavior was observed for the 2 solvents, water and DMSO. Possible underlying mechanisms for these effects and the relative importance of the various mechanisms of DMSO enhancement as a function of DMSO's concentration and configuration are discussed. *J Invest Dermatol* 89:274-280, 1987

Despite the fact that vidarabine (ara-A) has been used successfully by injection in the treatment of herpes infections [1,2], the local application of ara-A to control herpes simplex manifestations of the skin has not been altogether successful. Ando and colleagues [3,4] suggested that the low efficacy of topical ara-A is due to an extremely low permeability of ara-A through skin. In this regard ara-A and its antiviral analogs have several suboptimal properties for local administration that cannot be overlooked. Vidarabine for instance, is an extremely polar, relatively large molecule, suggesting it should be very difficult to deliver through a membrane structure as compact and functionally nonpolar as

the stratum corneum. Because of this difficulty, skin permeation-enhancing solvents have been tried clinically in hopes of improving the clinical effectiveness of such agents [5,6]. Since dimethyl sulfoxide (DMSO) has been the principal solvent chosen for this purpose, and since it has been shown to alter and enhance the skin permeability of other compounds [7-10], DMSO has been evaluated as a promoting agent of ara-A's permeation. Specific objectives were to determine the effect of DMSO on the permeation rate of ara-A in vitro (hairless mouse skin) and, generally, to explore the thermodynamic and kinetic limits of action of DMSO in enhancing transport of this prototypical antiviral nucleoside.

The permeability coefficient,  $P_{sc}$ , of ara-A through the skin's principal barrier layer, the stratum corneum, can be explicitly defined in terms of the effective thickness ( $h_{sc}$ ), the effective diffusivity ( $D_{sc}$ ), and the effective partition coefficient ( $K_{sc}$ ) between the operative diffusional domain of the stratum corneum and DMSO-water solutions:

$$P_{sc} = \frac{D_{sc} \cdot K_{sc}}{h_{sc}} \quad (\text{Eq 1})$$

The terms  $h_{sc}$ ,  $D_{sc}$ , and  $K_{sc}$  are indicated as effective because it is not possible to separate these parameters experimentally and assign them exact values. As long as the external solvent contacting the skin does not concentrate in and alter the horny layer or does not occlude the skin and hydrate the horny layer, the thickness

Manuscript received May 12, 1986; accepted for publication February 23, 1987.

This work supported through National Institutes of Health grant NIDR DE-02731.

\*Present address: Basic Pharmaceuticals Research, CIBA-GEIGY Corporation, 444 Saw Mill Road, Ardsley, New York 10502.

†Present address: Department of Pharmaceutics, College of Pharmacy, The University of Utah, Salt Lake City, Utah 84112.

Reprint requests to: Gordon L. Flynn, Ph.D., College of Pharmacy, The University of Michigan, Ann Arbor, Michigan 48109-1065.

Abbreviations:

ara-A: vidarabine

DMSO: dimethyl sulfoxide

of the stratum corneum and the permeant's diffusivity,  $D_{sc}$ , will remain unchanged, and equation 1 can be written as:

$$P_{sc} = (\text{constant}) K_{sc} \quad (\text{Eq. 2})$$

The partition coefficient,  $K_{sc}$ , represents the equilibrium distribution coefficient of the permeant (ara-A in the present studies) between the phase of stratum corneum acting as the mass conducting medium (conduit phase) and the external solvent, which in these studies, is water, DMSO, or DMSO-water mixtures. Providing that the solvency of the conduit phase within the horny layer for ara-A is also unaffected by the external presence of DMSO solvent, then the partition coefficient of ara-A should strictly reflect the changing affinity of the applied phase for ara-A as the strength of DMSO is increased. Behavior regimes in which all these critical assumptions apply are evident upon comparing solubility and permeability trends. This was done previously for alkanols [11] and it was observed that the skin was unaffected by DMSO to a 50% concentration as long as the organic solvent was placed on both sides of the skin membrane.

The mole fraction solubility,  $X_2$ , of a permeant as ara-A in the applied phase is related to its activity in solution,  $a_2$ , by:

$$a_2 = \gamma_2 X_2 \quad (\text{Eq. 3})$$

where  $\gamma_2$  is the activity coefficient. The activity,  $a_2$ , will be constant in saturated solutions, barring a change in the crystal structure, as the percentage concentrations of the solvents in a binary mixture are changed. Thus, at saturation,  $\gamma_2$ , the solute activity coefficient, must change oppositely and in proportion to changes in  $X_2$  in order to maintain the product of  $\gamma_2$  and  $X_2$  constant. Since  $K_{sc} = \gamma_2/\gamma_{skin}$  and providing  $\gamma_{skin}$  is constant, the permeability coefficient should decrease in exact proportion to the solubility increase unless diffusivity in the barrier tissues is altered. Conformity to this expectation indicates simple thermodynamic control of the permeation process. Lack of conformity indicates in a very general way that there has been structural alteration within the membrane. This critical test was applied to the data for ara-A's permeation of hairless mouse skin under various circumstances of operation of the diffusion cell.

## MATERIALS AND METHODS

**Materials** The key materials used in these studies were  $^3\text{H}$ -vidarabine (10.1 Ci/mmol) and vidarabine, gifts from Warner Lambert/Parke-Davis, Ann Arbor, Michigan; and  $^3\text{H}$ -water (0.6 Ci/ml),  $^{14}\text{C}$ -dimethyl sulfoxide (10 mCi/mmol), and a commercial liquid scintillation cocktail (Aqualos) from New England Nuclear, Boston, Massachusetts. Normal saline (Abbot Laboratories, North Chicago, Illinois) was used to make the permeation solutions and as a receiver solution component. Reagent grade dimethyl sulfoxide (Fisher Scientific Co., Fairlawn, New Jersey) was the other solvent used for preparing the donor and receiver media. It was also used to prepare the media for the solubility studies along with double-distilled water.

**Diffusion Gels** Small glass diffusion cells, each consisting of 2 half-cells, were used. These had half-cell compartment volumes of 1.5 ml and individually measured effective diffusional areas ranging from 0.542–0.675 cm<sup>2</sup>. Each half-cell had a sampling port of 1 cm length and a stirring port of 3 cm length. Motors (Hurst Mfg. Co., Princeton, New Jersey) mounted above the cell and attached to stirring shafts passing through the stirring port were used to stir the media in the half-cells at 150 rpm. The stirring shafts had small teflon propellers threaded onto their ends. Skin membranes were placed between the half-cells and the unit was clamped together by a spring clamp. The cells were then immersed in a 37°C bath so that only the sampling and stirring ports broke through the liquid surface.

**Membrane Preparation** Male hairless mice 35–40 days of age (Skin Cancer Research Institute, Temple University Medical Center, Philadelphia, Pennsylvania) were sacrificed by spinal cord dislocation and square sections of abdominal skin, approximately

3 cm in each dimension, were immediately excised. Adhering fat and other visceral debris were removed from the skin undersurface before the skin was completely cut from the animal. After placing the skin sections between the half-cells, protruding, excess skin was trimmed off. The elapsed time from sacrifice of an animal to the beginning of a diffusion run was a few minutes.

**Permeation Procedure** After assembly of a cell, the donor and receiver sides were partially filled (1 ml) with the media for a given experiment. The media were either normal saline, DMSO-water mixtures (30%, 50%, 75%, or 90% DMSO) or neat DMSO. Some experiments were run with the same medium in both compartments of the cell (balanced configuration), whereas in others DMSO medium was placed in either the donor or receiver half-cell and saline was placed in the other side (asymmetric configurations). Balancing the medium eliminates net diffusive flows of the solvents. By varying the placement of the DMSO media in the asymmetric configurations, DMSO was caused to diffuse both with and against the diffusive direction of ara-A with net water diffusion opposing DMSO's in each case. The 2 asymmetric configurations allowed examination of the influence of concurrent diffusion of the solvents with or against ara-A.

The contents of a freshly filled cell were mixed for 5 min to temperature equilibration. Then 200  $\mu\text{l}$  samples from each cell side were counted to make certain there was no residual radioactivity remaining from previous runs. This was strictly precautionary, because between runs, the cells were washed, rinsed liberally, soaked in permanganate cleaning solution overnight, and then cleaned again. The radioisotope free donor compartment was charged with 200  $\mu\text{l}$  containing from 1–5  $\mu\text{Ci}$  of radiolabeled permeant(s) and 200  $\mu\text{l}$  of appropriate solvent were added to the receiver. In studies in which solvent flows themselves were measured, the radiolabeled charge was sometimes placed in the half-cell contacting the dermis and diffusion was followed from receiver to donor.

Initial concentrations of the radiolabeled material were based on samples withdrawn from the half-cells 2 min after adding the radiochemical charge. At every 1000 s thereafter for a total of 7000 s (usual case) or longer, 100  $\mu\text{l}$  samples were drawn from the half-cell opposing that containing the radioactive permeant. Fresh solvent of the appropriate composition was added to replace the solvent removed in sampling and corrections in sample concentrations were made to account for the attending dilution involved.

Samples were directly transferred to vials containing 10 ml of scintillation cocktail. These were assayed on a liquid scintillation counter (Beckman LS 9000 Scintillation Counter, Beckman Instruments, Fullerton, California). Each sample was counted for 10 min.

**Data Analysis** The concentration of radiolabel in the receiver half-cell was plotted as a function of time after correction was made for the dilution of sampling. The steady state region was identified graphically and the slope through the data in this region was estimated using least squares analysis. The permeability coefficient for a run was then calculated from:

$$P = \frac{V_r \cdot \frac{dc}{dt}}{A \cdot \Delta C} \quad (\text{Eq. 4})$$

where:

$P$  = permeability coefficient (cm/h),

$V_r$  = receiver volume (1.4 cm<sup>3</sup>),

$\frac{dc}{dt}$  = rate of change of concentration (flux rate) in the receiver compartment in the steady state (counts/100  $\mu\text{l}$  sample/10 min counting time),

$\Delta C$  = initial radiochemical concentration in the donor chamber (counts/100  $\mu$ l sample/10 min counting time), and

A = diffusional area ( $\text{cm}^2$ ).

**Solubility Determinations** Large excesses of crystalline ara-A were equilibrated with the pure solvents and binary solvent mixtures in well stirred jacketed flasks set up on a magnetic stirrer. Samples from the ara-A slurries were withdrawn periodically by syringe and, after coupling on a filter holder, were filtered through fluoropore filters (Millipore Corp., Bedford, Massachusetts) having a 0.5  $\mu$ m pore size. This effectively removed all particulate matter. The samples were appropriately diluted with water and assayed. Sampling was continued until a solubility plateau was obtained (Fig 1).

High-performance liquid chromatography (Waters Chromatography Division, Millipore Corp., Milford, Massachusetts) was used to assay for solubility. The mobile phase was methanol: water, 20:80, and the column was a  $\mu$ -Bondapak C-18 reverse-phase type. Solvent was passed through the system at 2.0 ml/min and at this flow rate the retention time was 4 min. Standard solutions of ara-A were prepared in 10% DMSO for calibration of the integrated area at 254 nm. The injection volume for stan-

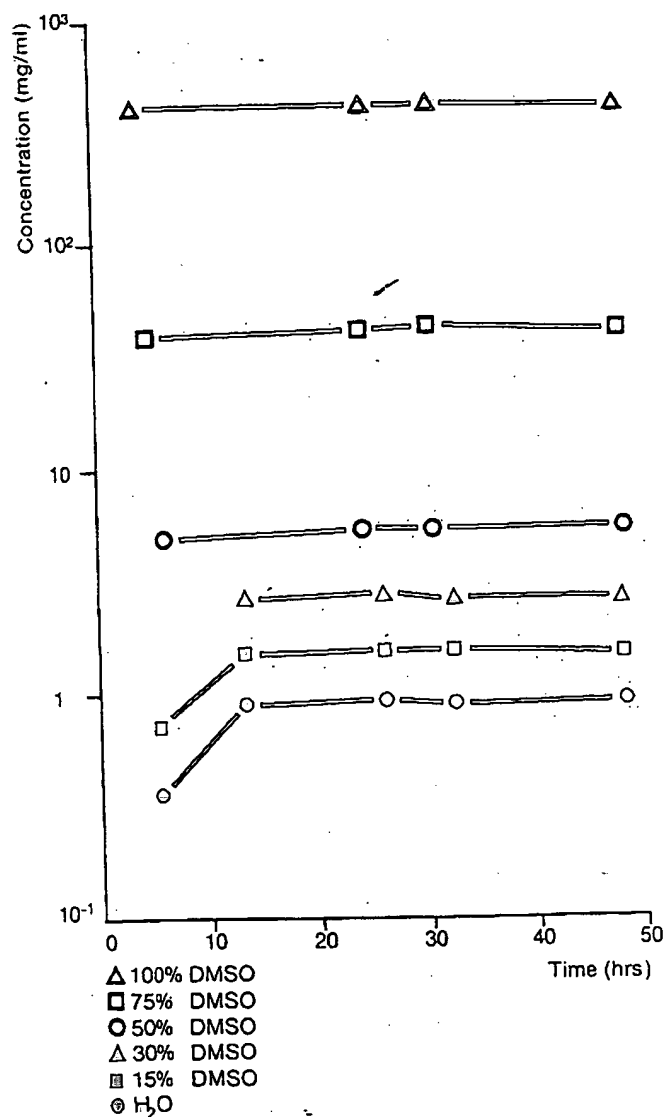


Figure 1. Solution profiles for ara-A in varying DMSO concentrations at 37°C as a function of time.

Table I. Comparison of Permeability Coefficients of Vidarabine Administered to Hairless Mouse Skin in Dimethyl Sulfoxide-Water Media

System (donor-receiver)	$P \times 10^9$ (cm/h)	Ratio (A)/(B)
(A) Saline-saline	$(3.16 \pm 0.34) \times 10^{-2}$	1.1
(B) Saline-saline	$(3.10 \pm 0.58) \times 10^{-2}$	
(A) 30% $(\text{CH}_3)_2\text{SO}_4$ -saline	$(1.33 \pm 0.56) \times 10^{-2}$	1.8
(B) 30% $(\text{CH}_3)_2\text{SO}_4$ -30% $(\text{CH}_3)_2\text{SO}_4$	$(7.96 \pm 3.80) \times 10^{-3}$	
(A) 50% $(\text{CH}_3)_2\text{SO}_4$ -saline	$(8.81 \pm 1.80) \times 10^{-2}$	14.4
(B) 50% $(\text{CH}_3)_2\text{SO}_4$ -50% $(\text{CH}_3)_2\text{SO}_4$	$(6.19 \pm 1.64) \times 10^{-3}$	
(A) 75% $(\text{CH}_3)_2\text{SO}_4$ -saline	$(5.15 \pm 1.95) \times 10^{-1}$	59.8
(B) 75% $(\text{CH}_3)_2\text{SO}_4$ -75% $(\text{CH}_3)_2\text{SO}_4$	$(1.09 \pm 0.81) \times 10^{-2}$	
(A) 90% $(\text{CH}_3)_2\text{SO}_4$ -saline	$(5.19 \pm 2.46) \times 10^{-1}$	0.94
(B) 90% $(\text{CH}_3)_2\text{SO}_4$ -90% $(\text{CH}_3)_2\text{SO}_4$	$(5.57 \pm 1.17) \times 10^{-1}$	
(A) 100% $(\text{CH}_3)_2\text{SO}_4$ -saline	$1.29 \pm 0.23$	0.07
(B) 100% $(\text{CH}_3)_2\text{SO}_4$ -100% $(\text{CH}_3)_2\text{SO}_4$	$18.9 \pm 1.64$	

In set A the dimethyl sulfoxide was placed in the donor compartment only (one of the two possible asymmetric cell configurations). In set B identical dimethyl sulfoxide solutions were placed on both sides of the skin (balanced configuration).

\*Average of three results and standard deviation.

dard and unknown solutions was 20  $\mu$ l. The sensitivity range of the chromatographic system was determined to be 0.1  $\mu$ g/ml and excellent linearity was observed over the range of concentrations used for assay. Areas from standard solutions were routinely determined prior to quantification of unknown samples.

## RESULTS

Permeability coefficients obtained for ara-A in both the balanced and the asymmetric solvent configurations of the cells are given in Table I. The DMSO media were placed in contact with the external (stratum corneum) surface of the skin in the asymmetric mode in these experiments. The ratios of the permeability coefficients in the 2 modes of operation are given in the *right-hand column*. Data for the 2 different asymmetric configurations of the cell are given in Table II. Ratios of the data for the 2 configurations are provided in the *right-hand column*. With the exception of the saline-to-saline control experiment, data for the asymmetric configuration with the organic solvent phase in contact with the stratum corneum represent separate experiments. This was because matched samples of skin were taken from the animals and compared as sets. The agreement in the results of common experiments in the first and second data sets is reasonable.

Data for the concurrent permeation of DMSO, water, and ara-A are given in Table III. These experiments also involved the gathering of totally independent ara-A data. It can be seen that

Table II. Comparison of Permeability Coefficients of Vidarabine Administered to Hairless Mouse Skin in Dimethyl Sulfoxide-Water Media

System (donor-receiver)	$P \times 10^9$ (cm/h)	Ratio (A)/(C)
(A) Saline-saline	$(3.16 \pm 0.34) \times 10^{-2}$	1.1
(C) Saline-saline	$(3.10 \pm 0.58) \times 10^{-2}$	
(A) 30% $(\text{CH}_3)_2\text{SO}_4$ -saline	$(2.11 \pm 1.17) \times 10^{-2}$	0.5
(C) Saline-30% $(\text{CH}_3)_2\text{SO}_4$	$(4.89 \pm 3.11) \times 10^{-2}$	
(A) 50% $(\text{CH}_3)_2\text{SO}_4$ -saline	$(4.91 \pm 2.44) \times 10^{-2}$	0.4
(C) Saline-50% $(\text{CH}_3)_2\text{SO}_4$	$(1.32 \pm 0.60) \times 10^{-1}$	
(A) 75% $(\text{CH}_3)_2\text{SO}_4$ -saline	$(4.68 \pm 1.48) \times 10^{-1}$	4.06
(C) Saline-75% $(\text{CH}_3)_2\text{SO}_4$	$(1.53 \pm 1.20) \times 10^{-1}$	
(A) 100% $(\text{CH}_3)_2\text{SO}_4$ -saline	$(8.12 \pm 1.91) \times 10^{-1}$	0.9
(B) Saline-100% $(\text{CH}_3)_2\text{SO}_4$	$(9.27 \pm 1.78) \times 10^{-1}$	

In these cases the solvents are configured in the asymmetric modalities. In set A the dimethyl sulfoxide media were in contact with the stratum corneum, whereas in set B the dimethyl sulfoxide media were placed against the dermal side of the skin membranes.

\*Average of three results and standard deviation.

Table III. Concurrent Permeation Rate of Vidarabine, Dimethyl Sulfoxide, and Water Through Hairless Mouse Skin

% Dimethyl Sulfoxide	Permeability Coefficient $\times 10^3$ (cm/h) <sup>a</sup>			
	P vidarabine <sup>b</sup>	P dimethyl sulfoxide <sup>b</sup>	P H <sub>2</sub> O <sup>b,d</sup>	P H <sub>2</sub> O <sup>c</sup>
0	$(3.37 \pm 1.19) \times 10^{-2}$		$1.30 \pm 0.18$	$1.90 \pm 0.22$
15	$(2.45 \pm 0.20) \times 10^{-2}$	$(6.02 \pm 0.72) \times 10^{-2}$		
30	$(3.90 \pm 1.52) \times 10^{-2}$	$(6.93 \pm 3.00) \times 10^{-2}$	$1.82 \pm 0.32$	$1.77 \pm 0.42$
50	$(4.69 \pm 1.70) \times 10^{-1}$	$(9.98 \pm 3.52) \times 10^{-1}$	$1.48 \pm 0.58$	$2.72 \pm 0.55$
75	$(7.74 \pm 1.22) \times 10^{-1}$	$4.16 \pm 1.11$	$21.4 \pm 10.3$	$65.5 \pm 16.1$
100	$1.09 \pm 0.10$	$4.13 \pm 0.05$		$150 \pm 20.0$

<sup>a</sup>Average of four results and standard deviation.<sup>b</sup>Donor  $\rightarrow$  receiver.Receiver  $\rightarrow$  donor.<sup>c</sup>Permeability coefficients of individual species identified by subscripts.

these asymmetric data agree well with like data from the first 2 sets.

Solubility data are shown in Fig 1. It is notable that the solubility equilibrium was achieved in a day's time in all instances. The plateaus (and plateau standard deviations) were  $0.972 \pm 0.016$ ,  $1.72 \pm 0.02$ ,  $2.71 \pm 0.07$ ,  $5.72 \pm 0.08$ ,  $44.5 \pm 0.87$ , and  $433 \pm 21$  mg/ml for water, 15%, 30%, 50%, 75%, and neat DMSO respectively.

### DISCUSSION

Kligman [12] may have been the first to document the marked concentration dependency of DMSO's ability to enhance skin permeation when he noted that fluorescein's permeation of ex-

cised human skin membranes was nil until the concentration of DMSO in the medium used to apply fluorescein exceeded 50%. From there fluorescein's permeability increased systematically and dramatically to a DMSO strength of 90%. Substantial back diffusion of water was also noted by Kligman [12] and was given as the reason the penetration rate dropped back between 90 and 100% DMSO. Subsequently, Sweeney and colleagues [13] showed it took DMSO concentrations above 60% to accelerate tritiated water's permeation of skin. Elfbaum and Laden demonstrated much the same to be true for DMSO mediation of picric acid permeation of skin [14] and, in related experiments, saw the same kind of concentration dependency for the swelling of hair fibers [15]. Whealing reactions of intact skin share this general concentration dependency [16]. More recently, work by Kurihara-Bergstrom and associates [11] has shown that the permeation behaviors of simple alkanols as methanol, butanol, and octanol through hairless mouse skin are similarly dependent on DMSO's solution strength. The present experiments performed on hairless mouse skin further support the idea that it takes a highly enriched DMSO media to produce pronounced enhancements of permeability. Being more detailed and systematic than most past works, subtleties of behavior not previously apparent are also revealed. For example; although the data for the balanced and asymmetric configurations, plotted in Fig 2, follow patterns that fit expectations drawn from the literature, these data also show that the manner of configuration of the solvent phases external to the mouse skin has a remarkable effect on permeation.

In the balanced configuration, the permeability coefficient of ara-A systematically declines to 50% DMSO and remains smaller than the permeability coefficient from saline even to a 75% DMSO concentration. Extraordinarily large increases in permeability are noted, however, when DMSO's strength is increased first to 90% and then to 100%. In the normal asymmetric configuration with DMSO in contact with the stratum corneum, the permeability coefficient drops slightly from the value found in saline to that in 30% DMSO (not significant) and then increases sharply at the 50% DMSO strength. In 50% DMSO it is over twice the magnitude of the reference saline value ( $p < 0.01$ ) and over 14 times the value found for balanced configuration at 50% DMSO ( $p < 0.05$ ). An eight-fold further increase is seen at 75% DMSO where the asymmetric value is now about 60 times higher than the value in the comparable balanced configuration, a highly statistically significant difference ( $p < 0.01$ ). No further increase is noted in permeability when the DMSO strength is raised to 90%, a concentration at which the curves for the asymmetric and balanced configurations intersect. In neat DMSO the permeability coefficient in the asymmetric configuration is at its highest at  $1.3 \times 10^{-3}$  cm/h. This is now a highly significant ( $p < 0.001$ ) 14.6 times smaller than found in the balanced mode, however.

The decline in permeability in the balanced configuration to the 50% DMSO concentration is due to an increasing ability of the increasingly concentrated DMSO media to solvate ara-A. This ability is directly and relatively reflected accurately in solubility patterns. At any predetermined concentration of ara-A, the in-

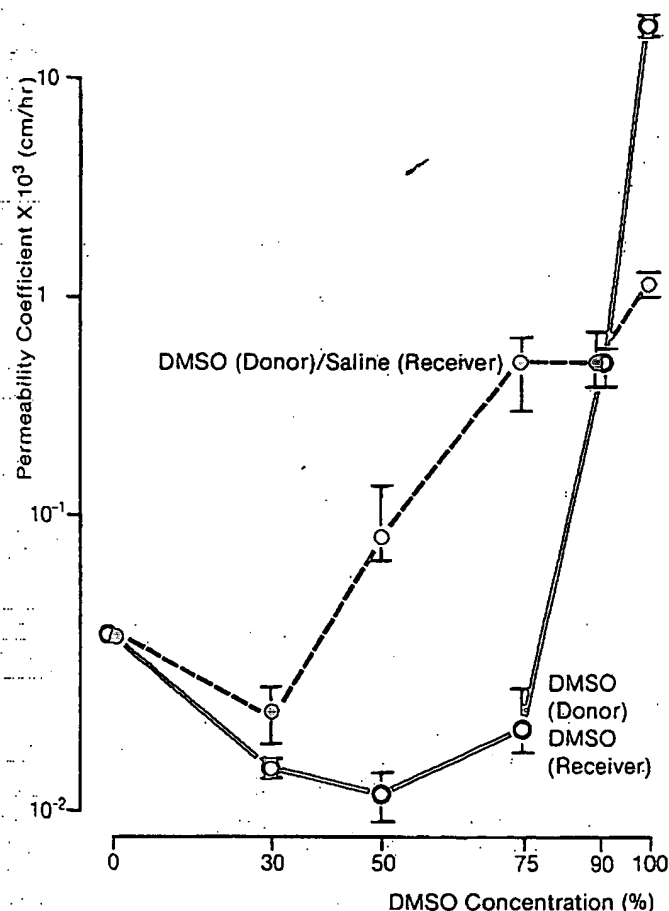


Figure 2. Comparison of permeability coefficients of ara-A through hairless mouse skin in DMSO-water media (DMSO-saline). Closed circles, DMSO media were in contact with the stratum corneum only; open circles, DMSO media were placed on both sides of the skin.



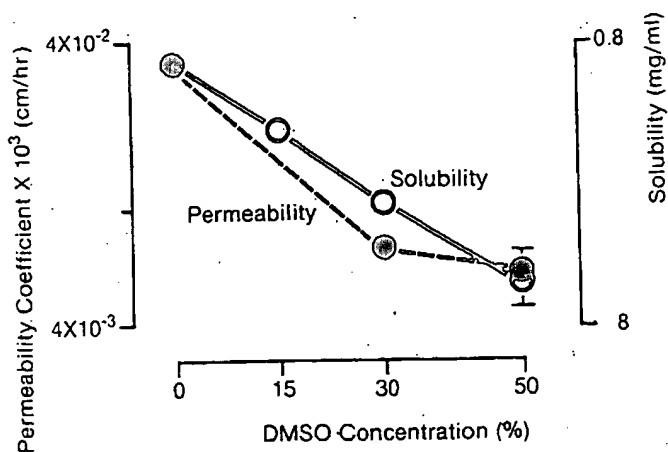


Figure 3. Comparison of permeability coefficient and solubility of ara-A between water and 50% DMSO-water media. Closed circles, permeability coefficients; open circles, solubility.

creasing ability of DMSO enriched media to solvate the compound directly translates to decreased stratum corneum-water partitioning, and everything else equal, proportionally decreased flux. This is reflected directly in the permeability coefficient, which is a concentration normalized parameter. Since the six-fold decrease in permeability from saline to 50% DMSO is matched by a six-fold increase in solubility over the same range of DMSO concentration (Fig 3), it appears that to the 50% DMSO strength in the balanced configuration DMSO's influence is strictly thermodynamic, a conclusion in keeping with results of experiments with select alkanols [11]. The permeability coefficients of ara-A applied in 75, 90, and 100% DMSO in the balanced configuration take a dramatic upwards turn, a marked qualitative departure from the thermodynamic (partitioning) trend. This unequivocally indicates DMSO has in some way altered the properties of the stratum corneum at these higher levels.

In contrast, unmistakable stratum corneum impairment by DMSO is seen at the 50% strength when this solvent medium is placed in only the donor compartment. This appears to be somewhat true for the 30% medium as well. Thus, the way the solvents are configured around the skin membrane itself has a marked influence on permeability. The data compiled in Table III indicate there are large net cross-currents of water and DMSO in the asymmetric circumstances, the major difference between the balanced and asymmetric modes. The inference is strong that the diffusive exchange of solvents causes disruption of the horny layer's structure. This idea is in keeping with the proposed enhancement mechanism of Chandrasekaran and coworkers [10], who were the first to note that, when configured asymmetrically, DMSO and water produce a separation of stratum corneum cell layers, presumably through osmotically derived stresses. Given the behaviors seen in the balanced configuration, it would appear the solvent cross-flows are of singular importance to DMSO permeability enhancement in the asymmetric modality at the intermediate DMSO concentrations. At concentrations above 50% other factors of enhancement must necessarily come into play given that marked enhancement of permeability is seen in the balanced configuration. It was previously demonstrated [11] that under the conditions of these experiments, substantial amounts of soluble organic substances are eluted from the skin, presumably mostly lipids, above the 50% DMSO strength, with the amounts extracted increasing sharply as DMSO is further enriched. By eluting soluble substances, the solvent induces a porosity on the skin and diffusion can proceed through solvent-filled channels in the stratum corneum matrix.

Concentrated DMSO is also capable of directly denaturing the keratin protein of the horny layer and disrupting ordered lipid structures, additional factors that may be involved when DMSO

is applied in essentially an undiluted state. It is notable that there is crossover of the 2 profiles at the 90% DMSO strength and a strikingly higher permeability of ara-A from the balance configuration when the medium of application is neat DMSO. We suspect that DMSO is more effective in eluting substance from the skin and also as a denaturant when it is placed in both compartments of the cell. In this mode there would be no dilution of the DMSO solvent at the skin's surface as the result of the diffusion of water through the skin. There are other plausible bases for this disparity between the balanced and asymmetric modes. For instance, the tendency for ara-A to partition into the cellular epidermis beneath the stratum corneum is diminished when the dermal surface is bathed in saline. Vidarabine's diffusive current across the epidermal and dermal strata might thereby be reduced to a fraction of what it is when all cellular water is exchanged for DMSO. Disruption and collapse of cell membrane structures is yet another possible contributing factor to the high permeability of ara-A when it is diffusing from neat DMSO into neat DMSO.

In their work with pilocarpine hydrochloride, Chandrasekaran and coworkers [10] showed that the side of placement of DMSO in the asymmetric configuration has an effect on permeability. It can be seen in Fig 4 that this also makes a difference for ara-A. Each way of asymmetric configuration can produce the higher permeability depending on the specific DMSO concentration, a factor not noted previously. The total picture suggests that disruptive stresses are experienced within the horny structure irrespective of which side the DMSO media are placed. At 30 and 50% DMSO, mass transfer is favored when the DMSO phase is in the receiver chamber. If the degree of damage is independent of placement, which seems a reasonable possibility, then the higher permeability at low-to-moderate DMSO concentrations seen when the ara-A is placed in a saline donor and is diffusing into a DMSO receiver reflects that the permeability change resulting from damage to the horny layer is neutralized to a degree by decreased solvation of ara-A and increased thermodynamic activity in the donor phase. Not only does the thermodynamic activity remain higher when the donor is saline, but ara-A also finds the receiver a better sink as it permeates the tissue.

The situation appears to be different when DMSO strength is greater than 50%. Here we suspect that elution of soluble matter from the stratum corneum is favored when the DMSO is in direct contact with the horny layer. This would explain the change in the order of permeability at the 75% DMSO strength. Curiously,

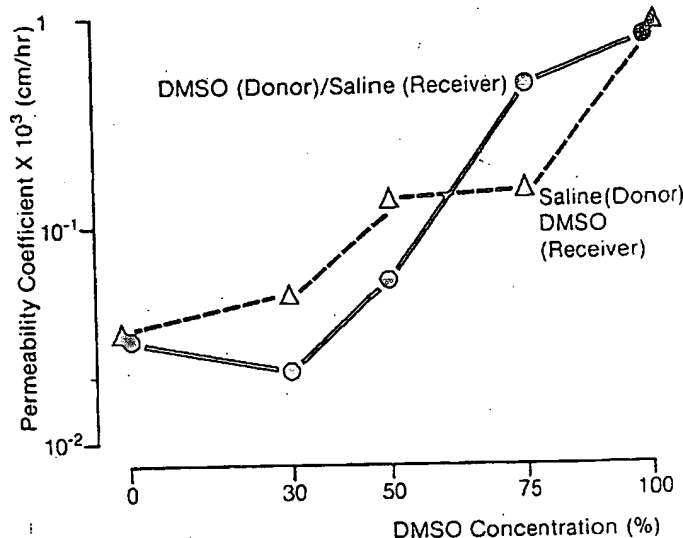


Figure 4. Comparison of permeability coefficients of ara-A through hairless mouse skin in DMSO-water (DMSO-saline). Closed circles, DMSO media were in contact with the stratum corneum; closed triangles, DMSO media were in contact with the dermis side.

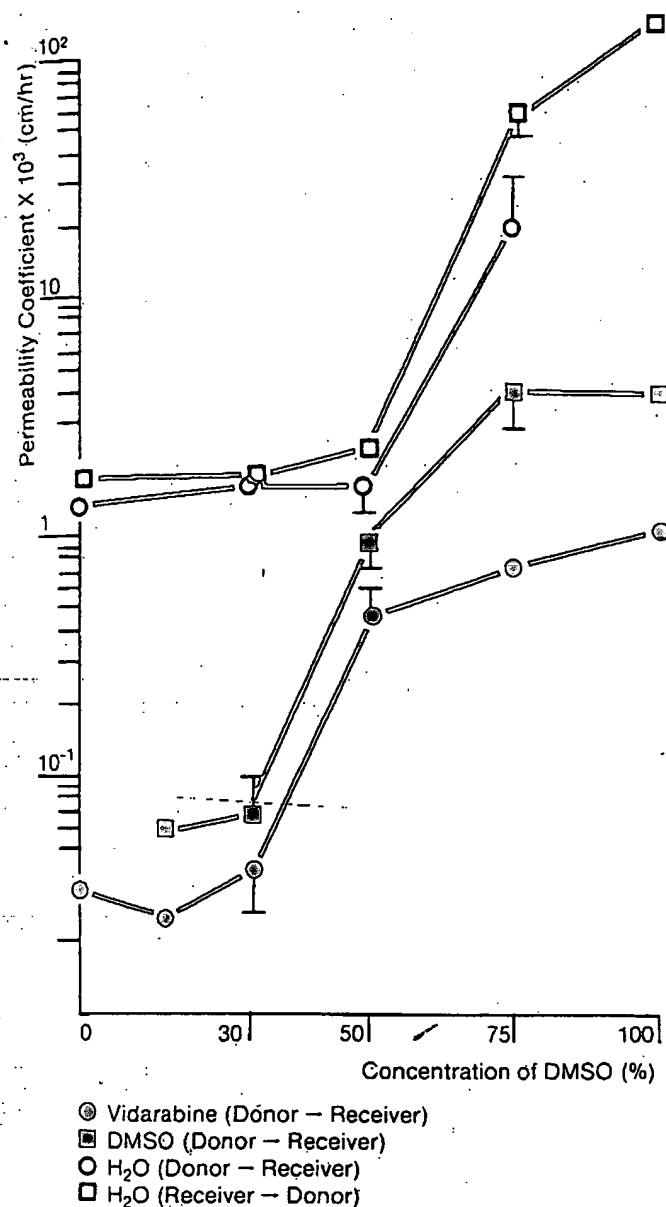


Figure 5. Concurrently determined permeability coefficients of ara-A, DMSO, and water through hairless mouse skin as a function of DMSO concentration.

the two asymmetric configuration curves come together again when the DMSO is in a neat state. Either the various contributions to barrier impairment catch up to each other at this point or there are opposing effects, which by pure chance, exactly offset each other. The latter explanation seems more plausible as it appears to us that the permeability retarding thermodynamic influence of DMSO when it is in the donor chamber is sufficient to offset the presumed differential in impairment of the horny layer in the same solvent configuration.

In either asymmetric configuration solvent cross-flows have been indicated as important to the mechanism of penetration enhancement. Additional support for this premise is given in Fig 5 for the specific asymmetric configuration with the DMSO media in contact with the stratum corneum side of the skin. Permeability coefficients of tritiated water into and out of the skin are displayed. Once concentration is taken into account, as it is in the calculation of such concentration normalized mass transfer coefficients, there appears to be little directionality to the permeability of this species. The permeability coefficients displayed for DMSO are for a net flux concurrent with and in the same direction as ara-A's.

Notably, no matter the DMSO concentration, there is, in every instance, a manifold greater backflow of water out of the skin than the diffusive flow of DMSO into it. If there were a "carrier effect," it would work against ara-A's permeation. In other words, ara-A molecules are not being drawn through the skin on a stream of solvent, the implication of the phase "carrier effect," but rather the chemical species are independently diffusing through the skin field variously altered by DMSO-water interactions with the tissue. Moreover, although the permeabilities of all 3 species, water, DMSO, and ara-A, fit well with the broader expectations of permeability as a function of DMSO concentration, it appears water's quantitative sensitivities to DMSO are unique. It will be noted that there is a large increase in the permeability coefficient at 50% DMSO for both DMSO and ara-A. Water's permeability coefficient on the other hand seems unaffected by DMSO until much higher DMSO concentrations are reached. This lack of DMSO sensitivity for water at intermediate DMSO strengths seems to have also been seen by Sweeney et al [13]. This strongly suggests that the delamination of the stratum corneum thought responsible for the increased permeability of ara-A does not of itself favor the diffusion of water. Thus, it appears that different mechanisms control the rates of diffusion of these very different molecular species within the horny structure.

Overall, it is shown that the manner in which DMSO produces permeability-enhancing effects on skin is influenced by the manner of application of DMSO and the concentration of DMSO. Partitioning factors are one determinant of permeability and in the simplest instances these alone control permeation rates. There is also clear evidence that several types of stratum corneum impairment are involved. All of these factors together lead to very complex DMSO concentration dependencies for its skin permeability enhancing effects, as revealed in standard diffusion cell experiments.

#### REFERENCES

- Schwartz PM, Shipman C Jr, Drach JC: Antiviral activity of arabinosyladenine and arabinosylhypoxanthine in herpes simplex virus-infected KB cells: selective inhibition of viral deoxyribonucleic acid synthesis in the presence of an adenosine deaminase inhibitor. *Antimicrob Agents Chemother* 10:64-74, 1976
- Whitley RJ, Soong S, Dolin R, Galasso GJ, Chien LT, Alford CA: Adenine arabinoside therapy of biopsy-proved herpes simplex encephalitis. *N Engl J Med* 297:289-294, 1977
- Ando HY, Ho NFH, Higuchi WI: Skin as an active metabolizing barrier. I. Theoretical analysis of topical bioavailability. *J Pharm Sci* 66:1525-1527, 1977
- Ando HY, Higuchi WI: In vitro estimates of topical bioavailability. *J Pharm Sci* 66:755-757, 1977
- Allenby AC, Creasey NH, Edginton JAG, Fletcher JA, Schock C: Mechanism of action of accelerants on skin permeation. *Br J Dermatol* 81(suppl 4):47-55, 1969
- Stoughton RB: Dimethyl sulfoxide induction of a steroid reservoir in human skin. *Arch Dermatol* 91:657-660, 1965
- Stoughton RB, Fritsche W: Influence of dimethyl sulfoxide on human percutaneous absorption. *Arch Dermatol* 90:512-517, 1964
- Ritschel WA: Sorption promoters in biopharmaceutics. *Angew Chem Int Ed Eng* 8:99-703, 1969
- Durrheim HH, Flynn GL, Higuchi WI, Behl CR: Permeation of hairless mouse skin. I. Experimental methods and comparison with human epidermal permeation by alkanols. *J Pharm Sci* 69:781-786, 1980
- Chandrasekaran SK, Campbell PS, Michaels AS: Effect of dimethyl sulfoxide on drug permeation through human skin. *American Institute of Chemical Engineers Journal* 23:810-816, 1977
- Kurihara-Bergstrom T, Flynn GL, Higuchi WI: Physicochemical study of percutaneous absorption enhancement by dimethyl sulfoxide: kinetic and thermodynamic determinants of dimethyl sulfoxide mediated mass transfer of alkanols. *J Pharm Sci* 75:479-486, 1986
- Kligman AM: Topical pharmacology and toxicology of dimethyl sulfoxide—part 1. *JAMA* 193:796-804, 1965

13. Sweeney TM, Downes AM, Matoltsy AG: The effect of dimethyl sulfoxide on the epidermal water barrier. *J Invest Dermatol* 461: 300-302, 1966.
14. Elfbbaum SG, Laden K: The effect of dimethyl sulfoxide on percutaneous absorption: a mechanistic study, part 1. *J Soc Cosmet Chemists* 19:119-127, 1968
15. Elfbbaum SG, Laden K: The effect of dimethyl sulfoxide on percutaneous absorption: a mechanistic study, part II. *J Soc Cosmet Chemists* 19:163-172, 1968
16. Sulzberger MB, Cortese TA Jr, Fishman L, Wiley HS, Peyakovich PS: Some effects of dimethyl sulfoxide on human skin in vivo. *Ann NY Acad Sci* 141:437-450, 1967

# Physicochemical Study of Percutaneous Absorption Enhancement by Dimethyl Sulfoxide: Kinetic and Thermodynamic Determinants of Dimethyl Sulfoxide Mediated Mass Transfer of Alkanols

KURIHARA-BERGSTROM\*, GORDON L. FLYNN\*, AND WILLIAM I. HIGUCHI†

Received May 20, 1985, from the College of Pharmacy, The University of Michigan, Ann Arbor, MI 48109-1065. Accepted for publication January 19, 1986. Present addresses: \*Basic Pharmaceuticals Research, Ciba-Geigy Corporation, Ardsley, NY 10502, and the †Department of Pharmaceutics, College of Pharmacy, The University of Utah, Salt Lake City, Utah 84112.

By first determining the thermodynamic activities and activity coefficients of methanol, 1-butanol and 1-octanol in binary dimethyl sulfoxide:water media, it has been possible to separate solubility (thermodynamic) effects of dimethyl sulfoxide from its kinetic influence as they relate to the skin permeation of these small, electrolyte alkanols. This was done by normalizing the experimental permeability coefficients found with full-thickness hairless mouse skin membranes to unit activity in the vehicle. When the dimethyl sulfoxide were placed on both sides of the skin sections in a two compartment diffusion cell, activity-adjusted permeability coefficients of permeants were invariant to dimethyl sulfoxide concentrations of strength. Thus, up to this concentration and in the absence of net solvent crosscurrents, the permeabilities of methanol, 1-butanol, and 1-octanol appear to be strictly determined by partitioning into the stratum corneum. However, when the dimethyl sulfoxide percentage strength increased to  $\geq 75\%$ , activity-adjusted permeability increased systematically and profoundly, indicating severe barrier impairment with increased diffusion across the horny layer (kinetic effect). When neat dimethyl sulfoxide was placed on both sides of the skin, the experimental permeability coefficients of the three alcohols were maximal and of similar magnitude, suggesting total functional impairment of the stratum corneum. When the dimethyl sulfoxide media were placed in contact with the stratum corneum surface of the skin membranes only, separating effects were noted at dimethyl sulfoxide concentrations  $\geq 75\%$  further supporting the idea that solvent cross flows themselves alter the horny structure. The degree of impairment was quantified under all experimental circumstances. Analysis of extracts of the stratum corneum indicated that barrier impairment is due in part to denaturation of the horny layer and denaturation of its proteins appeared to play roles in enhancement of diffusion.

Methanol, 1-butanol and 1-octanol possess widely different lipophilic properties. In studies of the effect of polarity (lipophilicity) on a specific phenomenon or process, they make a useful set of prototype compounds because of their predictable and systematically varying physicochemical properties. They have been useful in studying mass transfer mechanisms through skin and have helped define the relationship of skin permeation on lipophilic character.<sup>1-6</sup> Extensive studies from these labs<sup>1-4</sup> suggest that methanol, 1-butanol, and 1-octanol pass through hairless mouse skin by different pathways and with different rate-controlling mechanisms. These three alcohols were therefore chosen for the present study involving assessment of dimethyl sulfoxide mediation of permeation because their permeabilities through this skin from strictly aqueous solution are known and because they provided a unique opportunity to study solvent influences as a function of permeant lipophilicity.

## Theoretical Section

For the simplest possible membrane situation in which a constant, isotropic membrane separates well-stirred exter-

nal phases, the permeability coefficient,  $P$ , is expressed by:

$$P = \frac{DK_{m/v}}{h} \quad (1)$$

where  $D$ ,  $K_{m/v}$ , and  $h$  are the diffusivity (diffusion coefficient), partition coefficient between the membrane ( $m$ ) and medium ( $v$ , vehicle), and membrane thickness, respectively.

Normally in studies involving the use of diffusion cells, the membrane thickness is fixed and is little affected by medium changes. Even when this is not so as, for example, when solvents such as water and dimethyl sulfoxide act on the stratum corneum, rarely is the thickness of a membrane expanded by more than a factor of two or three. It appears, then, that varying the solvent composition of the external (vehicle) phases primarily influences the permeability coefficient by altering diffusivity, the kinetic aspect of mass transfer, and by altering partitioning, the thermodynamic determinant, and only marginally by changing the thickness. The permeability coefficient will vary as the product of the proportional changes in each varies. In order to determine kinetic and thermodynamic influences on mass transfer associated with systematic changes in the composition of phases applied to the membrane, an independent determination of the changes taking place in either the diffusion. The unexplained change in permeability which remains can then be assigned to the alternative factor.

In principle, one should be able to separate vehicle driven thermodynamic influences from other mass transfer influences, including vehicle mediated changes in the membrane solvency, by independent assessment. It is reasonable to assume that equilibrium exists across the molecular interface between the membrane and the medium, so that:

$$\begin{aligned} \mu_{2, \text{medium}} &= \mu_{2, \text{membrane}} \\ &= \mu_2^0 + RT \ln a_{2,v} \\ &= \mu_2^0 + RT \ln a_{2,m} \end{aligned} \quad (2)$$

where  $\mu_2^0$  is the chemical potential of the standard state,  $a$  is the activity, and the subscripts  $m$  and  $v$  refer to the membrane and the vehicle, respectively. It thus follows that the thermodynamic activity of the permeant is, for all practical purposes, the same on either side of the interface; that is:

$$a_{2,v} = a_{2,m} \quad (3)$$

The activity on either side of the membrane interface with the medium can be expressed in a general form as:

$$a_2 = \gamma_2 C_2 \quad (4)$$

where  $\gamma_2$  is an "activity coefficient," a factor which normalizes a prevailing concentration,  $C$ , to the respective activity.

It follows that:

$$\gamma_{2,v}C_{2,v} = \gamma_{2,m}C_{2,m} \quad (5)$$

At the medium-membrane interface:

$$K_{m/v} = \frac{C_{2,m}}{C_{2,v}} = \frac{\gamma_{2,v}}{\gamma_{2,m}} \quad (6)$$

Combining eqs. 1 and 6 gives the following form of the mass transfer coefficient:

$$P = \frac{D}{h} \frac{\gamma_{2,v}}{\gamma_{2,m}} \quad (7)$$

Once the flux of a permeant has attained a steady or quasi-steady state, the mass current can be expressed generally as:

$$\left(\frac{dm}{dt}\right)_{ss} = AP(\Delta C) \quad (8)$$

where  $(dm/dt)_{ss}$  is the steady or quasi-steady state flux taken directly from the slope of the mass penetrated ( $m$ ) versus time ( $t$ ) profile,  $A$  is the area of permeation ( $\text{cm}^2$ ), and  $\Delta C$  is the difference in concentration across the membrane as measured in the phases external to the membrane. When diffusion is into a sink (zero concentration at all times on the downstream side of the membrane),  $\Delta C$  is the applied concentration. It follows from eqs. 7 and 8 that:

$$\left(\frac{dm}{dt}\right)_{ss} = A \frac{D}{h} \frac{\gamma_{2,v}}{\gamma_{2,m}} \Delta C \quad (9)$$

Equation 9 indicates that the total flux through an isotropic, resistant barrier is proportional to the activity coefficient in the external medium and inversely proportional to the activity coefficient in the membrane, in addition to its other well established dependencies.

When the medium external to a membrane is varied by systematically varying the proportions of two miscible solvents, three variables in eq. 9 are subject to change, i.e.,  $D$ ,  $\gamma_{2,m}$ , and especially  $\gamma_{2,v}$ . For present purposes,  $h$  is presumed constant. There is no way to predict in advance how  $D$  and  $\gamma_{2,m}$  will be affected, but a systematic change in the magnitude of  $\gamma_{2,v}$ , which relates to the different solvencies of the two solvents for a given solute, is anticipated. Therefore, the sensitivity of  $\gamma_{2,v}$  is subject to independent assessment. Changes in  $D$  and  $\gamma_{2,m}$ , on the other hand, are only expected if at some point the binary solvents alter the physicochemical properties of the membrane. Changes in  $D$  and  $\gamma_{2,m}$  appear as a composite change and are not readily separable. Of considerable importance is the case where  $D$  and  $\gamma_{2,m}$  remain unchanged as the vehicle composition is varied. For this situation, the product of  $P$  times  $1/\gamma_{2,v}$  is predicted to be constant, i.e.:

$$P \frac{1}{\gamma_{2,v}} = \frac{D}{h} \frac{1}{\gamma_{2,m}} \quad (10)$$

Thus, if  $\gamma_{2,v}$  is independently known, one has a stringent test to determine whether membrane properties are changing with the change in the composition of the applied phase. For solutes like the volatile alkanols,  $\gamma_{2,v}$  can be independently assessed from vapor pressure measurements. The concept of activity coefficient determined flux is developed above for the simple isotropic membranes; the underlying principles are general, however, and can be applied to complex membranes such as the skin.

## Experimental Section

**Materials**— $[^{14}\text{C}]$ Methanol (30 mCi/mmol),  $[^{14}\text{C}]$ 1-butanol (10 mCi/mmol),  $[^{14}\text{C}]$ 1-octanol (5 mCi/mmol) (ICN Chemical and Radioisotope Division, Irvine, CA) were used as supplied. These were diluted into neat, high purity methanol (Baker Chemical Co., Phillipsburg, NJ), 1-butanol (Matheson, Coleman and Bell Manufacturing Chemists, Norwood, OH), and 1-octanol (Fisher Scientific Co., Fairlawn, NJ), respectively, for the vapor pressure measurements. Dimethyl sulfoxide (Fisher Scientific Co., Fairlawn, NJ) was used as received, and the water used in the studies was double distilled.

**Permeation Procedure**—Membranes for the study were abdominal sections obtained from the hairless mouse (Skin Cancer Hospital, Temple University, Philadelphia, PA) SKH-hr(-1) strain. In all instances the skin was taken from freshly sacrificed animals (spinal cord dislocation) and immediately mounted in the diffusion cell housing. The full-thickness skin was used.

The general assembly and operation of the diffusion cells have been detailed previously.<sup>1-4</sup> Briefly, small glass diffusion cells with  $\sim 0.6 \text{ cm}^2$  of diffusional area and with half cell volumes of  $\sim 1.5 \text{ mL}$  were used. These parameters were determined accurately for each cell. The cells were assembled with a fresh section of skin between the chambers. After rinsing, a permeant containing solution was placed on the stratum corneum side of the skin section, and a collecting medium was placed on the dermal side. Then, the media were stirred (150 rpm). Tests were begun as soon as the cell assembly was complete.

Initial and final samples were taken from the donor (permeant-containing) compartment. Aliquots of 100  $\mu\text{L}$  were taken from the receiver chamber at 1000-s intervals for up to 10,000 s (usually 7,000 s), providing 8-11 data points including one for time zero. Fresh solvent was added to the compartment following sampling to maintain constant volume in the receiver chamber. Corrections were made for the dilutions involved. The 100- $\mu\text{L}$  aliquots were placed directly into 10 mL of scintillation cocktail (AquaSol, New England Nuclear, Boston, MA). Experiments at each set of conditions were done three or more times and the results were averaged.

An aspect of experimental design unique to these studies was that the permeation was followed in media ranging from dimethyl sulfoxide:water (0, 30, 50, 70, 90, and 100% dimethyl sulfoxide with normal saline) to normal saline in one set of experiments and to dimethyl sulfoxide of the same strength in a second set. In the following discussion the first of these solvent configurations is referred to as asymmetric and the second as balanced. In the asymmetric modality the alkanols permeated in the presence of a net flux of dimethyl sulfoxide in the same direction as that of the permeant and against a net flux of water. In the balanced configuration there is no net diffusive exchange of solvent between the compartments. The dimethyl sulfoxide and water fluxes involved in the asymmetric situation were measured and are being reported separately.<sup>5</sup>

**Analysis of Permeation Data**—As in previous work<sup>1-4</sup> counts of the radiolabeled alkanols reaching the receiver chamber (corrected for dilution) were plotted against time. When the permeation process attained a quasi-steady state, as determined graphically, the permeability coefficient for the test was calculated from:

$$P = \frac{V_r}{A\Delta C} \frac{dC}{dt} \quad (11)$$

where  $P$  is the permeability coefficient ( $\text{cm/h}$ ),  $V_r$  is the receiver volume (1.4 mL),  $dC/dt$  is the quasi-steady state rate of change in radiochemical concentration in the receiver chamber (counts per 100- $\mu\text{L}$  sample per 10-min counting time),  $\Delta C$  is the initial radiochemical concentration in the donor chamber (counts per 100- $\mu\text{L}$  sample per 10-min counting time), and  $A$  is the diffusional area ( $\text{cm}^2$ ). The experiments were carried out in a manner which allowed use of the donor concentration for the concentration differential,  $\Delta C$ . The lag time tended to be too short to be estimated with any accuracy using 1000-s sampling intervals.

**Vapor Pressure Measurement**—A measured flow of nitrogen gas was passed through the system depicted in Fig. 1. The nitrogen gas stream was warmed to 37°C in a coil and then bubbled through a 37°C solution of the alkanol dissolved in one of the binary dimethyl sulfoxide:water media (0, 30, 50, 70, 90, or 100% dimethyl sulfoxide). The bubble size (frit size), gas flow rate, and solvent column height

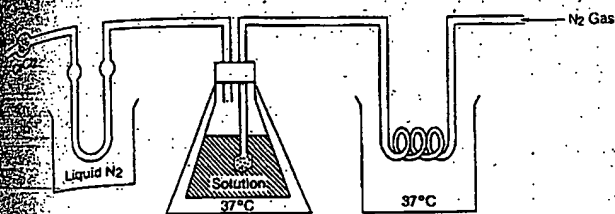


Figure 1—Measurement of vapor pressure in the gas-saturation method.

required for solution-vapor equilibrium were determined by trial and error. Conditions were selected which afforded gas saturation of the vapors of the alkanol and its solvent(s) during the passage of the gas through the liquid phase. The vapor saturated gas stream from the solution was passed into a liquid nitrogen chilled cold trap (tube) where the solvent vapors were quantitatively removed by condensation. The contents of the cold trap were rinsed directly into a scintillation cocktail for counting.

**Analysis of Vapor Pressure Data.**—The partial vapor pressures of alkanols in solution in the dimethyl sulfoxide:water media were determined from their equilibrium vapor phase concentrations in the gas phase passed through the media. If  $V_n$ , the volume of gas bubbled through a solution of one of the alkanols, is found to contain  $n$  grams of the vaporized alkanol solute (with a molecular weight,  $M_r$ ), the partial vapor pressure of the alkanol,  $P_{i, \text{gas}}$ , can be calculated approximately using the following equation based on the ideal gas law:

$$P_{i, \text{gas}} = \frac{gRT}{M_r V_n} \quad (12)$$

Assuming ideal gas behavior is appropriate at the concentrations of vapors obtained. The approximate nature of this method of vapor pressure estimation is due to the fact that the volume,  $V_n$ , assumed by the vapor is taken as the volume of the dry nitrogen gas measured before it is saturated with solution component vapor.

For more accurate estimations of partial pressure, the equation can be modified to allow for the increased volume of the gas due to the introduction of solvent vapor. The volume,  $V_b$ , of both nitrogen and the vapor through which the vapor molecules are distributed is:  $V_b(P_b - P_{i, \text{gas}})$ , where  $V_b$  is the volume of the pure, dry nitrogen before saturation,  $P_b$  is the barometric pressure, and  $P_{i, \text{gas}}$  is the partial vapor pressure of the alkanol. It follows that:

$$P_{i, \text{gas}} = \frac{g}{M_r} \frac{RT}{V_t} = \frac{g}{M_r} \frac{RT(P_b - P_{i, \text{gas}})}{V_b P_b} \quad (13)$$

which, upon solving for  $P_{i, \text{gas}}$ , yields:

$$P_{i, \text{gas}} = \frac{gRT P_b}{[M_r V_b P_b] + [gRT]} \quad (14)$$

The vapor pressure of each alkanol in each medium was calculated from eq. 14. The dimethyl sulfoxide:water media was assumed to form an ideal solution, allowing estimation of the partial pressures of each via mole fraction compositions. The partial pressures of dimethyl sulfoxide, water, and alkanol were added to get the system vapor pressure. As a critical test of the gas saturation cell, the 37°C vapor pressures of the pure liquid alkanols were determined and compared with their established vapor pressures.<sup>9</sup> It was found that 1-octanol was not fully miscible in water nor in dimethyl sulfoxide:water mixtures containing 30 and 50% dimethyl sulfoxide at the 1% total concentration used. This created difficulty as the actual concentrations of 1-octanol in the water-rich phases were experimentally determined and used to calculate activity coefficients. The measured solubilities were 0.479 mg/mL in water, 1.14 mg/mL in 30% dimethyl sulfoxide, and 2.98 mg/mL in 50% dimethyl sulfoxide.

The vapor pressures of methanol and 1-butanol were measured five times at each condition. The low vapor pressure of 1-octanol proved difficult to measure, and a longer period of gas collection was

used. Experiments on neat 1-octanol were only run in triplicate. The activity of an alkanol in a given medium was calculated from:

$$a_{2,i} = \frac{P_{i, \text{gas}}}{P_{i, \text{gas}}^0} \quad (15)$$

where  $P_{i, \text{gas}}^0$  was the experimentally determined vapor pressure of the pure alcohol. Activity coefficients were in turn calculated from the activities by:

$$\gamma_{2,i} = \frac{a_{2,i}}{X_{2,i}} \quad (16)$$

where  $X_{2,i}$  is the computed mole fraction alkanol concentration at a given solvent composition. Mole fraction was chosen as the unit of concentration because of its fundamental place in solubility theory. The different molecular weights of water and dimethyl sulfoxide caused the mole fraction composition to be curvilinear with increasing dimethyl sulfoxide concentrations.

**Extraction of Lipids and Other Dimethyl Sulfoxide Soluble Materials from the Stratum Corneum.**—The stratum corneum was isolated by immersing sections of excised skin in 0.25% w/v trypsin (Aldrich Chemical Co., Milwaukee, WI) in saline for 22 h at 37°C and then lifting off the horny layer with a spatula. Samples were rinsed, placed on a piece of aluminum foil, and dried for 1 d in a desiccator under reduced pressure. These were stored over calcium chloride in a desiccator.

Each stratum corneum sample (~100 mg) was placed in a petri dish and weighed accurately. Two milliliters of dimethyl sulfoxide:water media at one of the aforementioned percentage compositions was slowly added to the petri dish. The entire chamber was kept in a water bath at 37°C for 2 h, about the length of the permeation experiments. The tissue was then gently lifted from the petri dish with the suction of a pipette and again dried, this time for 7 d in a desiccator under reduced pressure. The sample was again weighed and the percentage change in weight was recorded.

## Results

Permeability coefficients for methanol, 1-butanol, and 1-octanol as a function of dimethyl sulfoxide concentration and

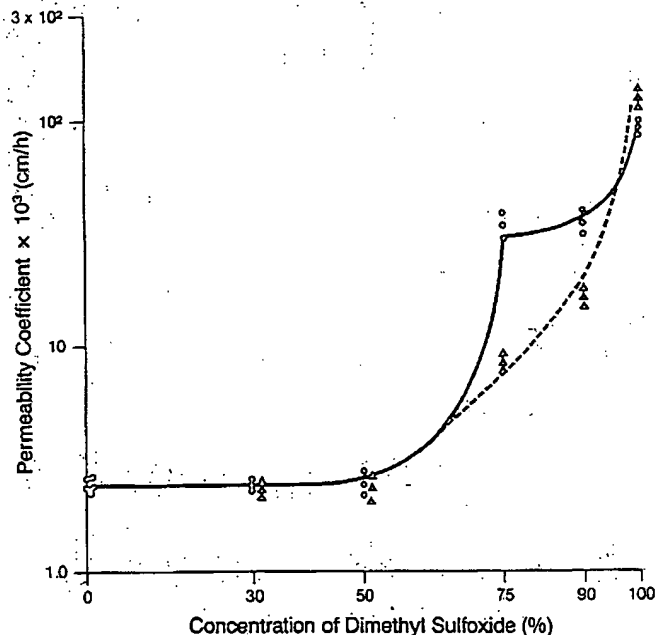
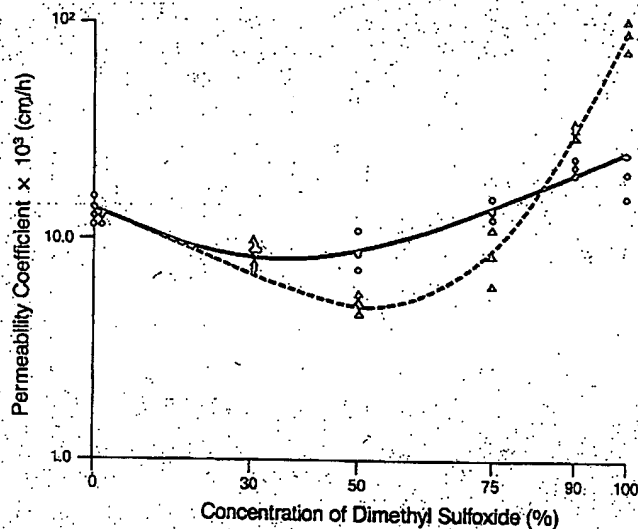


Figure 2—Permeability coefficients of methanol through fresh hairless mouse skin in dimethyl sulfoxide-water mixture. Key: (O) dimethyl sulfoxide (donor)/saline (receiver); (Δ) dimethyl sulfoxide (donor)/dimethyl sulfoxide (receiver).





**Figure 3**—Permeability coefficients of 1-butanol through fresh hairless mouse skin in dimethyl sulfoxide-water mixture. Key: (O) dimethyl sulfoxide (donor)/saline (receiver); (Δ) dimethyl sulfoxide (donor)/dimethyl sulfoxide (receiver).

cell configuration, asymmetric or balanced, are given in Figs. 2, 3, and 4. A high level of reproducibility of results at a given condition is seen.

The partial vapor pressures of these alkanols above the dimethyl sulfoxide-water mixtures are given in Table I, along with computed activities and activity coefficients. The activity coefficient profiles are important and therefore are pictorially illustrated in Figs. 5, 6, and 7 for methanol, 1-butanol, and 1-octanol, respectively. The experimentally determined vapor pressures of the neat liquid alkanols are given in Table II, where they are compared with established literature values.<sup>9</sup>

Figure 8 shows the loss in stratum corneum weight, due to

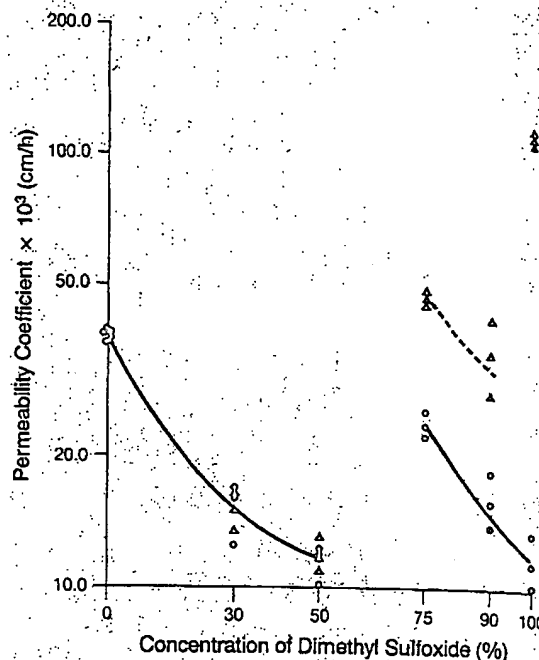


**Figure 4**—Permeability coefficients of 1-octanol through fresh hairless mouse skin in dimethyl sulfoxide-water mixture. Key: (O) dimethyl sulfoxide (donor)/saline (receiver); (Δ) dimethyl sulfoxide (donor)/dimethyl sulfoxide (receiver).

extraction of soluble materials, as a function of dimethyl sulfoxide concentration.

## Discussion

The permeability coefficients of the alkanols displayed in Figs. 2, 3, and 4 clearly are affected by dimethyl sulfoxide and the manner in which it is administered to the skin. In the profiles for all three alkanols there are notable differences in

**Table I**—Partial Vapor Pressures, Activities, and Activity Coefficients of Methanol, 1-Butanol, and 1-Octanol in Binary Dimethyl Sulfoxide-Water Media When Incorporated at 1% Concentration in the Pure and Mixed Solvents

Compound	Conc. of Dimethyl Sulfoxide	Partial Vapor Pressure, mmHg <sup>a</sup>	Activity ( $P/P^0$ )	Activity Coefficient ( $\gamma_2$ )
Methanol	0%	$2.10 (\pm 0.17) \times 10^{-1}$	$1.00 (\pm 0.08) \times 10^{-3}$	$2.26 (\pm 0.19) \times 10^{-1}$
1-Butanol		$1.71 (\pm 0.04)$	$1.13 (\pm 0.03) \times 10^{-1}$	$5.74 (\pm 0.14) \times 10^{-1}$
1-Octanol		$7.74 (\pm 2.01) \times 10^{-2b}$	$7.76 (\pm 2.00) \times 10^{-1}$	$2.56 (\pm 0.67) \times 10^{-1}$
Methanol	30%	$2.61 (\pm 0.21) \times 10^{-1}$	$1.25 (\pm 0.10) \times 10^{-3}$	$2.19 (\pm 0.17) \times 10^{-1}$
1-Butanol		$1.51 (\pm 0.17)$	$1.00 (\pm 1.14) \times 10^{-1}$	$3.94 (\pm 0.45) \times 10^{-1}$
1-Octanol		$6.00 (\pm 1.06) \times 10^{-2b}$	$5.94 (\pm 1.04) \times 10^{-1}$	$1.16 (\pm 0.20) \times 10^{-1}$
Methanol	50%	$3.35 (\pm 0.51) \times 10^{-1}$	$1.60 (\pm 0.24) \times 10^{-3}$	$2.27 (\pm 0.36) \times 10^{-1}$
1-Butanol		$1.10 (\pm 0.03)$	$7.31 (\pm 0.20) \times 10^{-2}$	$2.34 (\pm 0.06) \times 10^{-1}$
1-Octanol		$4.85 (\pm 0.22) \times 10^{-2b}$	$4.80 (\pm 0.22) \times 10^{-1}$	$7.30 (\pm 0.33) \times 10^{-1}$
Methanol	75%	$3.62 (\pm 0.26) \times 10^{-1}$	$1.73 (\pm 0.12) \times 10^{-3}$	$1.73 (\pm 0.12) \times 10^{-1}$
1-Butanol		$5.40 (\pm 0.88) \times 10^{-1}$	$3.58 (\pm 0.58) \times 10^{-2}$	$8.04 (\pm 1.31)$
1-Octanol		$2.69 (\pm 0.53) \times 10^{-2}$	$2.66 (\pm 0.53) \times 10^{-1}$	$1.03 (\pm 0.53) \times 10^{-1}$
Methanol	90%	$4.62 (\pm 0.43) \times 10^{-1}$	$2.20 (\pm 0.20) \times 10^{-3}$	$1.66 (\pm 0.15) \times 10^{-1}$
1-Butanol		$1.20 (\pm 0.21) \times 10^{-1}$	$7.94 (\pm 1.45) \times 10^{-3}$	$1.33 (\pm 0.24)$
1-Octanol		$8.10 (\pm 1.81) \times 10^{-3}$	$8.02 (\pm 1.82) \times 10^{-2}$	$2.32 (\pm 0.53) \times 10^{-1}$
Methanol	100%	$1.13 (\pm 0.31)$	$5.38 (\pm 1.50) \times 10^{-3}$	$3.13 (\pm 0.88) \times 10^{-1}$
1-Butanol		$2.81 (\pm 0.23) \times 10^{-2}$	$1.86 (\pm 0.15) \times 10^{-3}$	$2.42 (\pm 0.19) \times 10^{-1}$
1-Octanol		$1.60 (\pm 0.37) \times 10^{-4}$	$1.59 (\pm 0.37) \times 10^{-3}$	$3.56 (\pm 0.83) \times 10^{-1}$

<sup>a</sup> The values represent averages of five results for methanol and 1-butanol and averages of three results for 1-octanol. Standard deviations are given in brackets. <sup>b</sup> These data were obtained in saturated (two phase) solutions. See text for experimental concentrations in the aqueous phase.

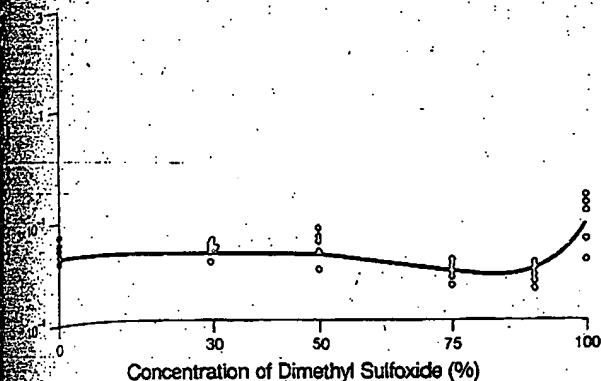


Figure 5—Activity coefficients of methanol in dimethyl sulfoxide–water mixture at 37°C.

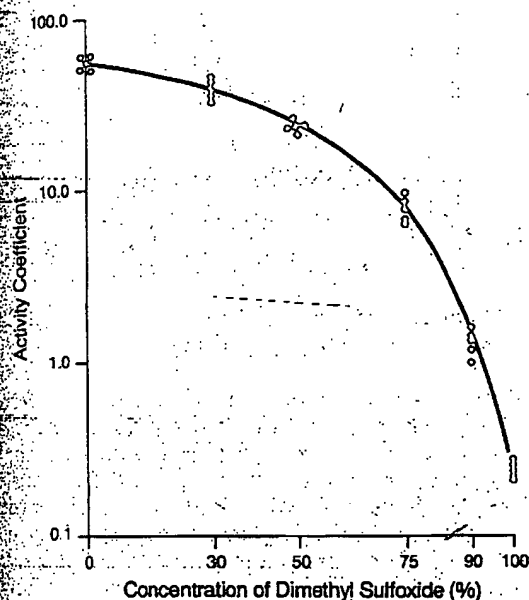


Figure 6—Activity coefficients of 1-butanol in dimethyl sulfoxide–water mixture at 37°C.

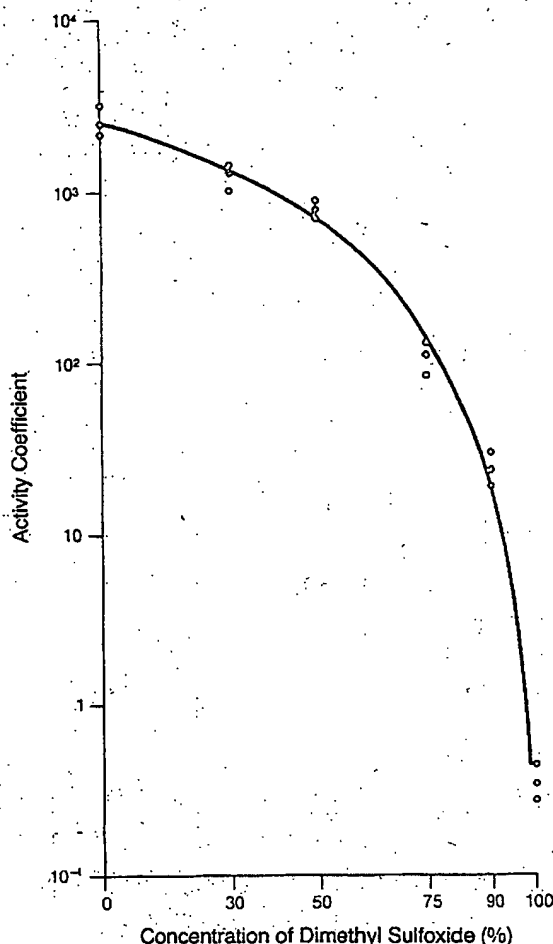


Figure 7—Activity coefficients of 1-octanol in dimethyl sulfoxide–water mixture at 37°C.

Table II—Vapor Pressures of Pure Alkanols at 37°C.

Compound	Vapor Pressure, mmHg <sup>a</sup>	
	Exp. values	Lit. values <sup>b</sup>
Methanol	209 (± 8.66)	211
1-Butanol	15.1 (± 0.88)	15
1-Octanol	0.101 (± 0.016)	0.37 <sup>c</sup>

<sup>a</sup>These values are the average of three results. The standard deviation is in brackets. <sup>b</sup>These data are taken from ref. 9. <sup>c</sup>This value involves extrapolation of data obtained from >100 to 37°C. Apparently, no 37°C estimate exists in the literature. Under these circumstances, the agreement is considered satisfactory.

In an attempt to factor out the causes of the overall permeability behavior, thermodynamic activities and mole fraction based activity coefficients of the respective alkanols were determined as a function of solvent composition. It can be seen from the data in Table I that the activities of each of the alkanols were affected differently as dimethyl sulfoxide was titrated into the solvent medium. For methanol, the activity was systematically increased and, in pure dimethyl sulfoxide, was 5.4 times greater than in water. This simply means water is the better solvent for methanol. In contrast, activities of both 1-butanol and 1-octanol decreased as the dimethyl sulfoxide percentage was raised. Over the solvent range the thermodynamic activity of 1-butanol dropped over 60-fold, while that of 1-octanol dropped almost 500-fold. Thus, as hydrophobicity is increased, solvation of the higher alkanols in dimethyl sulfoxide is markedly favored.

As patterns of behavior for the asymmetric and balanced solvent configurations. For methanol, the skin is more permeable in the asymmetric mode at 70 and 90% dimethyl sulfoxide concentrations but, if anything, there is a crossover in the curves at or before 100% dimethyl sulfoxide. With 1-butanol, the trends are clearly separated at 50% dimethyl sulfoxide and the crossover comes between 75% and 90% dimethyl sulfoxide. Both asymmetric and balanced configuration patterns for 1-octanol are extraordinary and break abruptly between 50 and 75% dimethyl sulfoxide. It is obvious that the permeation of 1-octanol is favored in the balanced configuration above 50% dimethyl sulfoxide. With the exception of 1-butanol, the permeability profiles for the alkanols in the two solvent configurations are identical for up to 50% dimethyl sulfoxide. Based on simple *t* tests of averages at individual dimethyl sulfoxide concentrations, the differences in values for 1-butanol apparent at 50 and 75% are not statistically significant at an acceptable level of confidence. Overall, the solvent configuration does not appear to make much difference with 0–50% dimethyl sulfoxide concentrations. At the higher dimethyl sulfoxide concentrations, however, profound differences in behavior between the two solvent configurations are noted.



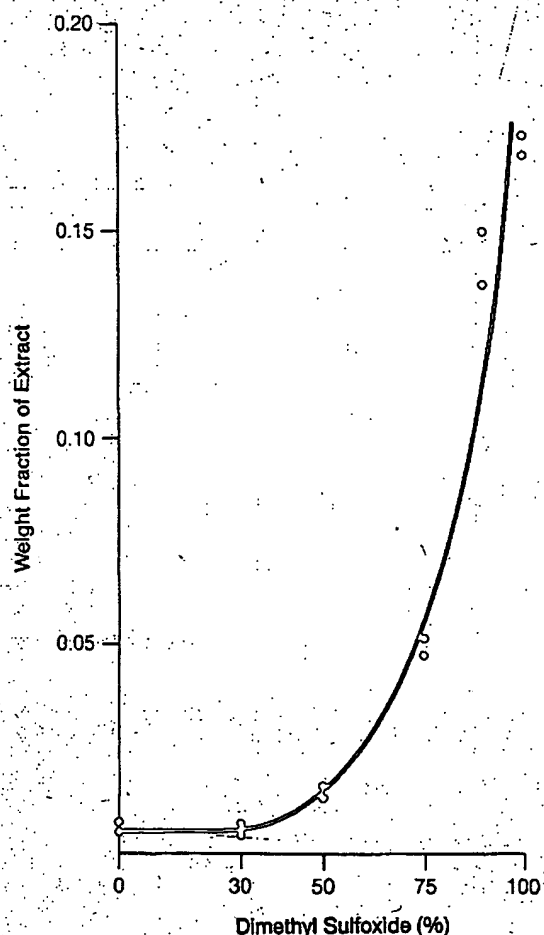


Figure 8—Solvent extraction from stratum corneum in the presence of dimethyl sulfoxide.

Patterns in mole fraction based activity coefficients are displayed in Figs. 5, 6, and 7 for methanol, 1-butanol, and 1-octanol, respectively. The choice of mole fraction as the unit of solute concentration results in a surprisingly flat curve for methanol. The trend for 1-butanol from pure water to pure dimethyl sulfoxide is continuously downward. The sensitivity of 1-butanol to increasing dimethyl sulfoxide composition lies between that of methanol and 1-octanol. The activity coefficient of 1-octanol dropped precipitously. Its activity coefficient of 0.34 in pure dimethyl sulfoxide was 7500 times less than that found in pure water ( $2.56 \times 10^3$ ). In part, the choice of mole fraction concentration to compute activity coefficients magnifies the difference in the activity coefficients seen across the solvent composition span due to the difference in molecular weights and liquid densities of water and dimethyl sulfoxide. The choice of mole fraction itself leads to a fourfold change in the activity coefficient in pure water compared with that in pure dimethyl sulfoxide. Another factor in the case of 1-octanol is that the octanol added was not completely solubilized in the 0, 30, and 50% dimethyl sulfoxide. Therefore, the measured concentrations of 1-octanol in the aqueous phases of these mixtures (0.479, 1.14, and 2.98 mg/mL, respectively) were used in the calculations. Because the 1-octanol was not completely solubilized in this range, the thermodynamic activity itself varied only slightly, as expected.

According to eq. 10, when changes in the thermodynamic activity of a permeant in the vehicle alone decide the relative rate of the permeation process, permeability coefficients can be normalized to a constant value by dividing the experimental values by the respective activity coefficients in the solvents of application. When applied to the data for methanol,

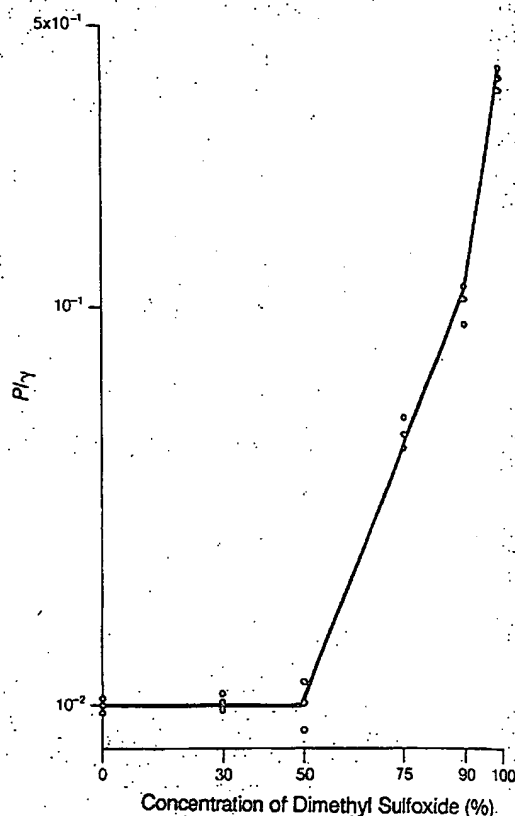


Figure 9—The ratio of permeability coefficient and activity coefficient of methanol in the presence of dimethyl sulfoxide.

1-butanol, and 1-octanol permeating the skin, this normalizing procedure produces the interesting results seen in Figs. 9, 10, and 11. These figures are produced from data for the alkanols administered in the balanced solvent configuration. For all three alkanols, the permeability is invariant within the boundaries of expected experimental variability up to and including the 50% strength of dimethyl sulfoxide. Considering that this is true for three permeants of wide ranging polarity, these results prove unequivocally that partitioning changes due to altered solvency in the vehicle phase are the overwhelmingly important factor in the data trends. It might be noted that  $D$  and  $\gamma_{2,m}$ , which relate here to the stratum corneum, are both expected to vary in the same upward direction and, therefore, should not offset each other. At dimethyl sulfoxide concentrations up to 50%, normalized permeability coefficients obtained in the asymmetric solvent configuration exhibit essentially identical features.

Concentrations of dimethyl sulfoxide above 50% show an absolute departure in the permeability patterns for the two methods used to configure the donor and receiver media. As seen in the activity coefficient normalized data, there is also a departure from the simple partitioning-determined trend. In either configuration, the  $P/\gamma_{2,v}$  values for each of the alkanols takes a dramatic upward turn. This indicates general and profound changes in membrane permeability, which in this study means substantial impairment of the stratum corneum. Imbibition of dimethyl sulfoxide and altered solvency in the critical horny phase of the skin membrane (change in  $\gamma_{2,m}$ ) is one possible general cause. Increasing diffusivity due to solvent alteration of the molecular structure or organization of the stratum corneum (i.e., a change in  $D$ ) is the second possibility. Both might be associated with the opening of new pathways through the horny layer and a change in the permeation mechanism. The increases at high dimethyl sulfoxide concentrations are so large that a change in mechanism is highly probable. In this regard, the nearly

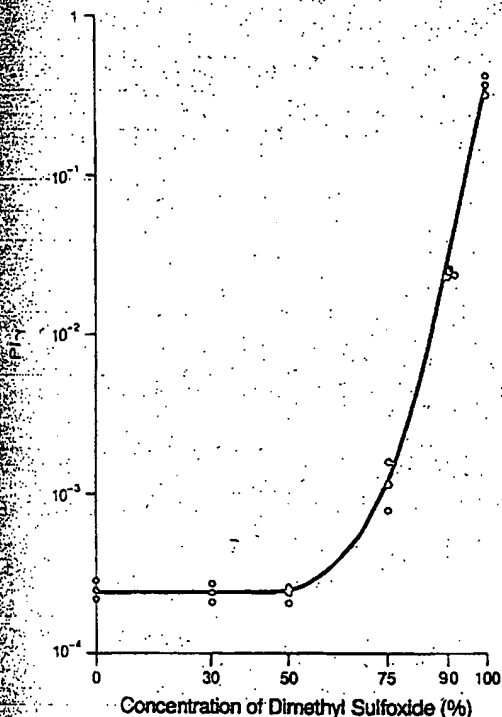


Figure 10—The ratio of permeability coefficient and activity coefficient of 1-butanol in the presence of dimethyl sulfoxide.

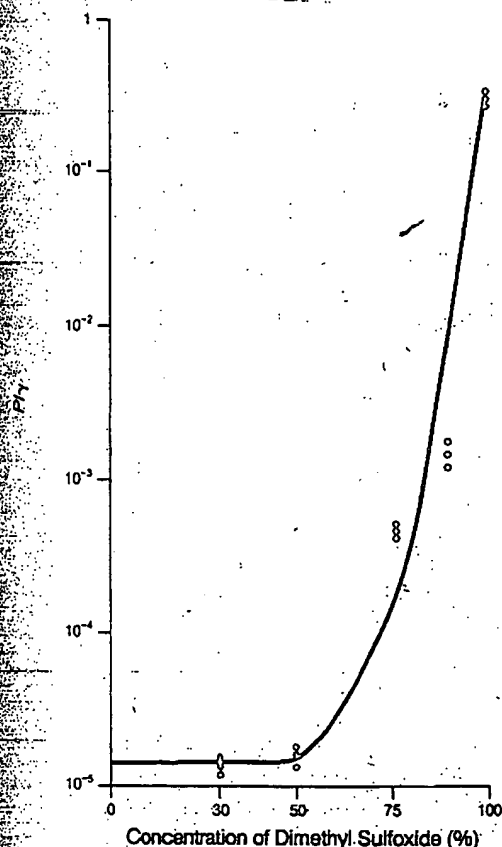


Figure 11—The ratio of permeability coefficient and activity coefficient of 1-octanol in the presence of dimethyl sulfoxide.

Identical permeability coefficients (absolute values) for methanol, 1-butanol, and 1-octanol in neat dimethyl sulfoxide in the balanced solvent configuration is an indicating factor. Such behavior would only be seen under circumstances

where diffusion is structurally insensitive, as would occur through a continuous solvent medium. This suggests that a dimethyl sulfoxide rich pathway is established through the stratum corneum and other skin structures. The average of all permeability coefficients of these alkanols is  $\sim 3 \times 10^{-5}$  cm/s (0.11 cm/h). Assuming a partition coefficient of unity for the presumed dimethyl sulfoxide regime in the skin structure, and taking into account the 400- $\mu$ m thickness of the full-skin sections, a diffusion coefficient estimate of  $1.2 \times 10^{-6}$  cm<sup>2</sup>/s is produced. This is in good agreement with a previous estimate of the diffusivity of vidarabine in the water-filled dermal matrix of  $1.3 \times 10^{-6}$  cm<sup>2</sup>/s.<sup>10</sup> The slightly lower magnitude for the smaller alkanols is reasonable in this instance because the viscosity and density of dimethyl sulfoxide are larger than those found for water.

Several mechanisms have been advanced for the enhancement of dimethyl sulfoxide on skin permeability, including elution of stratum corneum lipids,<sup>11,12</sup> denaturation of stratum corneum structural proteins (keratin),<sup>13-15</sup> and delamination of the horny layer by stress resulting from crosscurrents of highly water interactive dimethyl sulfoxide and water.<sup>16</sup> We believe the data patterns in these studies support all three mechanisms; the effect which dominates in a particular situation seems to be a result of the concentration of dimethyl sulfoxide and its method and duration of application to the skin. First, Fig. 8 shows that neither water nor binary dimethyl sulfoxide:water mixtures with up to 50% dimethyl sulfoxide have much ability to elute material from the stratum corneum. This ability increases dramatically as the dimethyl sulfoxide concentration is further increased, resulting in an 18% weight loss in the stratum corneum mass in neat dimethyl sulfoxide. These studies were done with a ratio of dimethyl sulfoxide to stratum corneum that was virtually the same as the ratio in the permeability experiments; the contact time was also similar. The striking parallel in tissue weight loss and in lost barrier integrity for three compounds as physicochemically different as methanol, 1-butanol, and 1-octanol (as seen in Figs. 9, 10, and 11) can hardly be an accident. Second, the higher permeability of methanol (and possibly 1-butanol) from binary dimethyl sulfoxide:water solutions of high dimethyl sulfoxide concentration and into water (asymmetric solvent configuration) and similar, even more profound effects seen with vidarabine<sup>9</sup> add to the already convincing evidence of Chandrasekaran et al.<sup>16</sup> which supports the idea that the horny structure is physically disrupted by the cross flows of the two solvents in question. Finally, the permeation of these model permeants out of a pure phase of dimethyl sulfoxide and into a pure dimethyl sulfoxide phase (balanced configuration) has an irregularity most notable in the profile for 1-octanol (Fig. 4). Here, the permeability is high. As mentioned, the barrier property left is about that expected if the solvent (dimethyl sulfoxide) itself were the conducting medium in the membrane. We suspect this exaggeratedly impaired state of the membrane is in part caused by denaturation of the keratin structure, a phenomenon which can be demonstrated in dimethyl sulfoxide soaked pieces of stratum corneum by several techniques, including X-ray diffraction.<sup>13-15</sup> Taking all data into account it appears that maximum impairment of the stratum corneum may be approached in the 100% dimethyl sulfoxide balanced configuration and possibly even in the 100% dimethyl sulfoxide to saline system. Transport would then be solely controlled by the cellular epidermis and the dermis, much as it is when the skin is stripped. With 100% dimethyl sulfoxide:saline, it is likely the epidermis/dermis is relatively water rich. This would not greatly affect the P value for methanol because it is so evenly soluble in water and dimethyl sulfoxide, as reflected in its activity coefficients. Thus, the values for the balanced and asymmetric configurations are similar at  $118 \times 10^{-3}$  cm/h versus 91.8

$\times 10^{-3}$  cm/h, respectively. However, the permeability coefficient for octanol should be influenced by media configuration and it was, as seen in the  $113 \times 10^{-3}$  cm/h value for the balanced configuration and the  $11 \times 10^{-3}$  cm/h value for the 100% dimethyl sulfoxide to saline case. Alternatively, the exaggerated degree of denaturation seen when pure dimethyl sulfoxide was placed on both sides of the skin may not occur in the asymmetric solvent situation due to a relatively rapid flow of water out of the horny surface, a factor which we believe could keep the dimethyl sulfoxide concentration in the horny layer below the critical level for full denaturation of its protein mass.

### References and Notes

1. Durrheim, H. H.; Flynn, G. L.; Higuchi, W. I.; Behl, C. R. *J. Pharm. Sci.* 1980, 69, 781-786.
2. Flynn, G. L.; Durrheim, H. H.; Higuchi, W. I. *J. Pharm. Sci.* 1981, 70, 52-65.
3. Behl, C. R.; Flynn, G. L.; Kurihara, T.; Harper, N.; Smith, W.;

- Higuchi, W. I.; Ho, N. F. H.; Pierson, C. L. *J. Invest. Dermatol.* 1980, 75, 346-352.
4. Behl, C. R.; Flynn, G. L.; Kurihara, T.; Smith, W.; Gatmaitan, O.; Higuchi, W. I.; Ho, N. F. H.; Pierson, C. L. *J. Invest. Dermatol.* 1980, 75, 340-345.
5. Scheuplein, R. J. *J. Invest. Dermatol.* 1967, 48, 79-88.
6. Scheuplein, R. J.; Blank, I. H. *J. Invest. Dermatol.* 1973, 60, 286-296.
7. Higuchi, T. *J. Soc. Cosmet. Chem.* 1960, 11, 85-97.
8. Kurihara, T., Ph.D. Thesis; University of Michigan, Ann Arbor, MI, 1983.
9. Jordan, T. E. "Vapor Pressure of Organic Compounds"; Interscience: New York, 1954; pp 65, 69, and 76.
10. Yu, C. D.; Higuchi, W. I.; Ho, N. F. H.; Fox, J. L.; Flynn, G. L. *J. Pharm. Sci.* 1980, 69, 770-772.
11. Allenby, A. C.; Creasey, N. H.; Edington, J. A. G.; Fletcher, J. A.; Schock, C. *Br. J. Dermatol.* 1969, 81, 47-55.
12. Embery, G.; Dugard, P. H. *J. Invest. Dermatol.* 1971, 57, 308-312.
13. Elftbaum, S. E.; Laden, K. *J. Soc. Cosmet. Chem.* March 1968, 19, 163-172.
14. Montes, L. F.; Day, J. L.; Wand, C. J.; Kennedy, L. *J. Invest. Dermatol.* 1967, 48, 184-196.
15. Scheuplein, R. J.; Ross, L. *J. Soc. Cosmet. Chem.* 1970, 21, 853-873.
16. Chandrasekaran, S. K.; Campbell, P. S.; Michaels, A. S. *AIChE J.* 1977, 23, 810-815.

**This Page is Inserted by IFW Indexing and Scanning  
Operations and is not part of the Official Record**

**BEST AVAILABLE IMAGES**

Defective images within this document are accurate representations of the original documents submitted by the applicant.

Defects in the images include but are not limited to the items checked:

- ☐ **BLACK BORDERS**
- ☐ **IMAGE CUT OFF AT TOP, BOTTOM OR SIDES**
- ☐ **FADED TEXT OR DRAWING**
- ☐ **BLURRED OR ILLEGIBLE TEXT OR DRAWING**
- ☐ **SKEWED/SLANTED IMAGES**
- ☐ **COLOR OR BLACK AND WHITE PHOTOGRAPHS**
- ☐ **GRAY SCALE DOCUMENTS**
- ☐ **LINES OR MARKS ON ORIGINAL DOCUMENT**
- ☐ **REFERENCE(S) OR EXHIBIT(S) SUBMITTED ARE POOR QUALITY**
- ☐ **OTHER:** \_\_\_\_\_

**IMAGES ARE BEST AVAILABLE COPY.**

**As rescanning these documents will not correct the image problems checked, please do not report these problems to the IFW Image Problem Mailbox.**